20S PROTEASOME ASSEMBLY: ALTERNATIVE PATHWAYS AND COMPLEXES

by

Lindsay J. Hammack

A Dissertation

Submitted to the Faculty of Purdue University

In Partial Fulfillment of the Requirements for the degree of

Doctor of Philosophy

Department of Biology

Indianapolis, Indiana

December 2017

THE PURDUE UNIVERSITY GRADUATE SCHOOL
STATEMENT OF COMMITTEE APPROVAL

Dr. Andrew R. Kusmierczyk
Department of Biology
Dr. Amber L. Mosley
Indiana University School of Medicine
Dr. Stephen Randall
Department of Biology
Dr. AJ Baucum
Department of Biology

Approved by:

Dr. Theodore Cummins
Head of the Graduate Program

ACKNOWLEDGMENTS

First, I would like to express my sincere gratitude to Dr. Andrew Kusmierczyk who provided me the opportunity to pursue a PhD in his laboratory. His guidance from the start of my first project to the completion of this dissertation has been insightful and encouraging. I could not have asked for a better mentor.

I would also like to thank my family for their unconditional support during this journey.

TABLE OF CONTENTS

LIST OF TABLES

LIST OF FIGURES

LIST OF ABBREVIATIONS

ARC – AAA ATPase ring-shaped complex

Bpa – bacterial proteasome activator

CC – crosslinkable cystiens

CP – core particle

Dop – deaminase of Pup

HbYX – hydrophobic, tyrosine, and amino acid

HMWC – high molecular weight complex

HP – holoproteasome

Hsp – heat shock protein

ICAR – immobilized cobalt affinity resin

iCP – immunoproteasome

IFNγ – interferon gamma

IP – immunoprecipitation

Mpa – mycobacterium proteasome ATPase

PA# – proteasome activator

PAC – proteasome assembly chaperone

PafE – proteasome accessory factor E

PAGE – polyacrylamide gel electrophoresis

PAN – proteasome activating nucleotidase

Pba – proteasome biogenesis-associated

PHP – pre-holoproteasome

POMP – proteasome maturation protein

PPS – Pup-proteasome system

Pup – prokaryotic ubiquitin-like protein

REG – regulatory

RP – regulatory particle

Rpn – regulatory particle non-AAA-ATPase

Rpt – regulatory particle AAA-ATPase

SAMP – small archaeal modifier protein

Ssa – stress sensitivity subfamily A

TB – tuberculosis

tCP – thymoproteasome

TNF – tumor necrosis factor

UbaA - ubiquitin-like activating protein

Ump1 – ubiquitin-mediated proteolysis 1

UPS – ubiquitin proteasome system

WT – wild type

ZPAC – zygote proteasome assembly chaperone

ABSTRACT

Author: Hammack, Lindsay, J. PhD
Institution: Purdue University
Degree Received: December 2017
Title: 20S Proteasome Assembly: Alternative Pathways and Complexes
Committee Chair: Andrew Kusmierczyk

The ubiquitin-proteasome system is responsible for the targeted degradation of proteins within the cell. The 26S proteasome, which is the protease of this system, is a high molecular weight complex consisting of 33 subunits that arrange to form two smaller complexes the 19S regulatory particle (RP) and the 20S core particle (CP). The 19S RP can bind one or both ends of the 20S CP and is responsible for recognizing the ubiquitinated substrates. After recognition, the 19S RP will subsequently deubiquitinate, unfold, and translocate the substrates into the proteolytic 20S CP. The 20S CP consists of seven unique α and seven unique β subunits that arrange into four stacked rings, with two α rings capping two β rings. Assembly of the $\alpha_{1-7}\beta_{1-7}\beta_{1-7}\alpha_{1-7}$ structure begins with the formation of an α ring and proceeds through specific assembly intermediates. This process is assisted by assembly chaperone proteins that promote on pathway interactions to efficiently construct the 20S CP. In this dissertation, three new findings are described which further characterize the proteasome assembly pathway. First, novel non-canonical complexes comprised of proteasome subunit α4 were identified *in vivo*, revealing proteasome subunits can assemble into complexes outside of the proteasome. Second, Hsp70 proteins, Ssa1/2, were shown to assist in the assembly of 20S CPs, adding to the growing list of proteins guiding proteasome assembly. Third, a novel complex was identified which is believed to represent a new proteasome assembly intermediate.

CHAPTER 1. INTRODUCTION

1.1 Ubiquitin-Proteasome System Overview

Proteasomes are proteases that help maintain protein homeostasis, which is essential for cellular function. Proteasomes are found throughout the eukaryotic and archaeal domains and within a few bacterial lineages. In eukaryotes, the proteasome is an essential component of the ubiquitin-proteasome system. This well characterized system is responsible for the targeted degradation of proteins. Proteins destined for degradation are first ubiquitinated through an enzymatic cascade consisting of three enzymes E1 (ubiquitin activating enzyme), E2 (ubiquitin conjugating enzyme), and E3 (ubiquitin ligase) (reviewed by (Hershko & Ciechanover, 1998; Hochstrasser, 1996; Jentsch, 1992). In this cascade, the 76 amino acid protein, ubiquitin, is initially activated by the E1 enzyme in an ATP dependent manner where ubiquitin's C-terminus is covalently attached to a cysteine residue within the active site of E1, forming an E1-ubiquitin thioester. Next, ubiquitin is transferred to a cysteine on E2. Then by E2 alone or in combination with E3, the ubiquitin is transferred to a lysine on the substrate forming an isopeptide bond. Ubiquitin has seven endogenous lysines that may undergo ubiquitination. Several subsequent rounds of ubiquitination results in the formation of a polyubiquitin chain. These chains are characterized according to the lysine residues chosen for polyubiquitination. Proteins tagged with K48 and K11 specific chains are deubiquitinated, unfolded, and degraded by the proteasome (Chau et al., 1989; Lu, Lee, King, Finley, & Kirschner, 2015; Meyer & Rape, 2014; Xu et al., 2009).

The 26S proteasome is a large multi-subunit complex that consists of a 20S core particle (CP; also known as the 20S proteasome), which is the protease of the complex, and a 19S regulatory particle (RP) that may cap one or both ends of the 20S CP (DeMartino & Slaughter, 1999). The 19S RP recognizes, deubiquitinates, unfolds, and feeds substrates into the proteolytic 20S CP. The 26S proteasome and the 20S CP are the best characterized of the proteasome complexes; however, several proteasome sub-types exist. These sub-types appear to house unique functions. Some sub-types are formed by the capping of alternative activator complexes. Other sub-types are composed of specialized 20S CP subunits or an alternative arrangement of canonical subunits. Despite considerable progress in elucidating the structure and function of the

proteasome, how this intricate structure is assembled is not completely understood. Proper and efficient assembly of proteasomes is vital for cellular homeostasis. By better understanding the proteasome assembly pathway, therapies can be designed to target the pathway. This dissertation will focus on 20S CP assembly. Work over the last decade has supported the idea of a canonical linear assembly pathway for the 20S CP. Growing evidence suggests that 20S CP assembly is not simply a linear process, but likely occurs through multiple pathways and through a variety of intermediates.

1.2 26S Proteasome Structure

The eukaryotic 26S is approximately 2.5 MDa. It contains two main sub-complexes, a 20S core particle (CP) and a 19S regulatory particle (RP). The 19S RP can cap one or both ends of the 20S CP (DeMartino & Slaughter, 1999). The 20S CP (~730 kDa) is the proteolytic center of the 26S proteasome and consists of 14 unique subunits, seven distinct α and β subunits, that assemble into four stacked hetero-heptameric rings: $\alpha_{1\text{-}7}\beta_{1\text{-}7}\beta_{1\text{-}7}\alpha_{1\text{-}7}$ (Groll et al., 1997). The proteolytic activity is sequestered within the central hollow chamber formed by the stacked rings. Three of the seven β subunits (β1, β2, and β5) contain propeptides that are cleaved upon 20S CP assembly, exposing a catalytically active threonine residue (Thr1) (Groll et al., 1997). This catalytic activity is shielded from the cellular environment by α subunit N-terminal tails covering the opening to the central pore. To allow for substrate entry, these gating N-terminal tails are displaced by activator proteins, such as the 19S RP (Groll et al., 1997).

The 19S RP (~700 kDa) is made up of 19 subunits that are classified as Rpt (Regulatory Particle AAA-ATPase) or Rpn (Regulatory Particle non-AAA-ATPase) subunits. These subunits assemble into two sub-components, a base and a lid (Glickman et al., 1998). The terms lid and the base are still used, but are quite misleading in light of published 26S cryo-EM structures (X. Huang, Luan, Wu, & Shi, 2016b; Lander et al., 2012; Schweitzer et al., 2016). The base of the 19S RP is made up of six homologous AAA-ATPase subunits (Rpt1-6) (Tomko, Funakoshi, Schneider, Wang, & Hochstrasser, 2010) and four non-ATPase subunits Rpn1, Rpn2, Rpn10, and Rpn13. Rpn1 binds UBL (ubiquitin-like) domains, while Rpn10 and Rpn13 bind ubiquitin directly (Elsasser et al., 2002; Husnjak et al., 2008; Saeki, Sone, Toh-e, & Yokosawa, 2002). The Rpt subunits form a hexameric ring that is responsible for unfolding substrates in an ATP

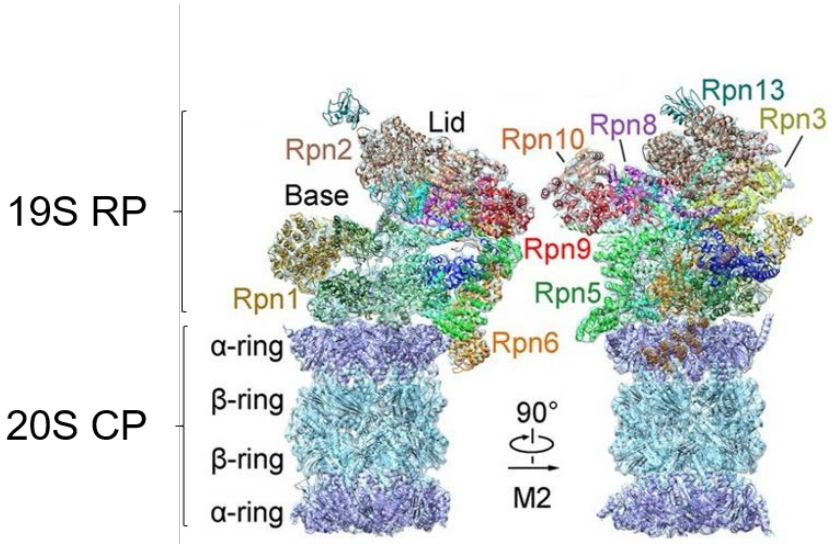

Figure 1.1 Cryo-EM 26S proteasome yeast
The 19S RP and 20S CP components of the 26S proteasome are indicated. Image modified from Bai Luan et al 2016.

dependent manner, opening the α ring gate, and feeding substrate into the 20S CP (Rabl et al., 2008; Smith et al., 2007). The Rpt ring opens the α ring gate through the C-terminal extensions of Rpt2, 3, and 5. These three Rpt subunits contain a C-terminal HbYX motif, which is a tri-peptide motif consisting of a hydrophobic (Hb) residue followed by a tyrosine (Y), then any amino acid (X). These C-terminal extensions will bind to the intersubunit pockets of the α ring. The carboxylate group on the 'X' residue of these Rpt subunits will form a salt bridge with a conserved lysine found at the base of 6 of the 7 α intersubunit pockets (Rabl et al., 2008; Smith et al., 2007).

The lid is made of nine non-ATPase subunits, one of which, Rpn11, is essential in deubiquitination of substrates (Verma et al., 2002; T. Yao & Cohen, 2002). Both the 20S CP and the 19S RP have been shown to assemble in distinct pathways that involve specific chaperone proteins (Funakoshi, Tomko, Kobayashi, & Hochstrasser, 2009; Hirano et al., 2005; Kusmierczyk, Kunjappu, Funakoshi, & Hochstrasser, 2008; Kusmierczyk, Kunjappu, Kim, & Hochstrasser, 2011; Le Tallec et al., 2007; Le Tallec, Barrault, Guerois, Carre, & Peyroche, 2009; X. Li, Kusmierczyk, Wong, Emili, & Hochstrasser, 2007; Roelofs et al., 2009; Saeki, Toh, Kudo, Kawamura, & Tanaka, 2009; Yashiroda et al., 2008). A detailed review of 26S assembly can be found here (Howell, Tomko, & Kusmierczyk, 2017).

1.3 20S Conservation

Proteasomes are found throughout the archaeal and eukaryotic domains; however, in the bacteria it is only found in the Actinomycete (De Mot, Nagy, Walz, & Baumeister, 1999) and Nitrospirales lineages (De Mot, Schoofs, & Nagy, 2007). These bacterial proteasomes are thought to have been acquired through a lateral gene transfer event (Lupas et al., 1997; Volker & Lupas, 2002). Regardless of origin, all 20S CPs have the same barrel like structure with a catalytically active central hollow chamber gated by α subunit N-terminal tails. While this dissertation is focused on proteasomes, it is worth noting that bacteria contain a variety of proteases that appear to maintain cellular homeostasis, and several bacterial species use a combination of proteases: Lon, ClpAP, HslV, and proteasome (Gille et al., 2003). The HslV protease in particular has striking similarities to the 20S CP (Bochtler, Ditzel, Groll, & Huber, 1997).

HslV is considered a distant relative to the proteasome. HslV's protease component shares some sequence and structural similarity to the catalytically active β subunits of the 20S proteasome (Bochtler et al., 1997; Chuang, Burland, Plunkett, Daniels, & Blattner, 1993; Gille et al., 2003). Moreover, like the proteasome, HslV is a multi-subunit complex consisting of rings and employs an N-terminal threonine nucleophile for catalytic activity (Bochtler et al., 1997; Bochtler, Song, Hartmann, Ramachandran, & Huber, 2001; Groll et al., 1997). In addition to HslV, a bioinformatic study in 2008 identified two other new groups of ancient hypothetical bacterial proteasomes (Valas & Bourne, 2008). One group, Anbu (ancestral beta subunit), is found in some cyanobacteria, and the other group, BPH (β-proteobacteria proteasome homologue), is found exclusively within a few β-proteobacteria (Valas & Bourne, 2008). Since that initial bioinformatic study, Anbu was crystalized and shown to form a dodecameric open ring complex (Fuchs et al., 2017). The authors' bioinformatic analysis of Anbu places it at the early stages of proteasome evolution and suggests that Anbu's open rings might have descended from an evolutionary precursor stage in the development of a closed ring, self-compartmentalizing, protease (Fuchs et al., 2017). This same study tested several substrates, but unfortunately no substrates for Anbu were identified; to date no catalytic activity has been described for Anbu (Fuchs et al., 2017).

1.4 Proteasome Tagging Systems and Activators

In all domains of life, the essential function of the proteasome is to degrade proteins. Both archaea and bacteria employ tagging systems and activators with proteasomes that are reminiscent of the ubiquitin-proteasome system.

1.4.1 Bacteria: Modifier Pup and Activators ARC, Mpa and PafE/Bpa

Bacterial proteasomes utilize a modifier protein called Pup (prokaryotic ubiquitin-like protein) that functions as a part of the Pup-proteasome system (PPS) (Pearce, Mintseris, Ferreyra, Gygi, & Darwin, 2008). This modifier protein attaches to substrates in a unique manner called pupylation. The C-terminus of the Pup protein contains a glutamine. In the first step of pupylation, this glutamine is deamidated by an enzyme called Dop (deamidase of Pup) to form a glutamate (Pearce et al., 2008; Striebel et al., 2009). Through the action of another enzyme, Pup ligase PafA, the glutamate side chain on Pup is covalently linked to a lysine on the target protein (Guth, Thommen, & Weber-Ban, 2011). There are exceptions to this method of tagging. For instance, in *Streptomyces coelicolor*, Pup is synthesized with a glutamate, and oddly still contains the Dop enzyme, even though Pup does not require deamidation (Bentley et al., 2002; Compton, Fernandopulle, Nagari, & Sello, 2015). One explanation for this is that Dop has an additional function besides deamidation. Two different groups described this new enzymatic activity for Dop, depupylation (Burns et al., 2010; Imkamp et al., 2010). Depupylation is the removal of Pup from substrates which is analogous to deubiquitination observed in eukaryotes (Burns et al., 2010; Imkamp et al., 2010).

In addition to having a tagging system, bacterial species containing proteasomes also have activator proteins that bind to the α ring of 20S CPs and stimulate degradation. Two types of activators have been identified in bacteria. The first activator was identified in *Rhodococcus erythropolis* and is referred to as ARC (AAA ATPase Ring-shaped Complex) (Wolf et al., 1998). A homologue of ARC was identified in *Mycobacterium tuberculosis*, Mpa (mycobacterium proteasome ATPase) (Darwin, Ehrt, Gutierrez-Ramos, Weich, & Nathan, 2003; Darwin, Lin, Chen, Li, & Nathan, 2005; Striebel, Hunkeler, Summer, & Weber-Ban, 2010). The second type activator was identified by two different groups at around the same time. One group called the activator Bpa (bacterial proteasome activator), and the other group referred to it as PafE (proteasome accessory factor E) (Delley et al., 2014; Jastrab et al., 2015). Both of these

activators contain a penultimate tyrosine and are suspected to use a similar gate opening mechanism as the eukaryotic 19S RP (Delley et al., 2014; Imkamp, Ziemski, & Weber-Ban, 2015; Jastrab et al., 2015; Striebel et al., 2010) Mpa/ARC is an ATP dependent activator that unfolds and degrades puplylated substrates (Striebel et al., 2010). Bpa/PafE is an ATP independent activator, and a recent Cryo-EM analysis of Bpa-20S suggests that this activator is structurally similar to the eukaryotic 11S (PA28 activators) (Bolten et al., 2016).

1.4.2 Archaea: Modifier SAMP and Activators PAN, Cdc48, and AMA

Ubiquitin like proteins, SAMP1, SAMP2, and SAMP3 (small archaeal modifier protein 1, 2, and 3) and an E1 like enzyme, UbaA (ubiquitin-like activating protein of Archaea) were described in archaeal species *Haloferax volcanii* (Humbard et al., 2010; Miranda et al., 2014; Miranda et al., 2011). UbaA activates the SAMP proteins through an E1-like mechanism (Miranda et al., 2011). All three SAMPs can form isopeptide bonds via their C-terminal glycine residues and lysine residues on the target proteins (Hepowit et al., 2012; Humbard et al., 2010; Miranda et al., 2014; Miranda et al., 2011). SAMP2, but not SAMP1, was shown to form a SAMP2 chain, by forming an isopeptide bond to itself (Humbard et al., 2010). SAMP3 was shown to form chains of SAMP3, but whether these chains are attached to substrates still needs to be determined (Miranda et al., 2014).

Archaeal 20S CP contains a closed α ring gate (Benaroudj, Zwickl, Seemuller, Baumeister, & Goldberg, 2003; Smith et al., 2005; H. Zhang et al., 2009). By in vitro methods, three proteasome activators have been identified in archaea PAN, proteasome activating nucleotidase (Wilson, Ou, Aldrich, & Maupin-Furlow, 2000; Zwickl, Ng, Woo, Klenk, & Goldberg, 1999), Cdc48 (Barthelme & Sauer, 2012; Forouzan et al., 2012), and AMA (Archaeoglobus and methanogenic archaea) (Djuranovic, Rockel, Lupas, & Martin, 2006; Summer, Bruderer, & Weber-Ban, 2006). All three activators are AAA ATPases (Forouzan et al., 2012). PAN is an archaeal homologue of eukaryotic 19S RP AAA ATPase (Wilson et al., 2000; Zwickl, Voges, & Baumeister, 1999). PAN is found sporadically throughout archaea, and of the PAN proteins identified, only some contain a HbYX motif (Reuter, Kaczowka, & Maupin-Furlow, 2004; Yu et al., 2010). Despite lacking a HbYX motif or PAN all together, all archaeal genomes sequenced encode 20S CP α and β subunits (Maupin-Furlow, 2013).

The archaeal species lacking PAN may employ Cdc48 and/or AMA as proteasome activators. Cdc48 from *Thermoplasma acidophilim* can interact with 20S CPs in an ATP-dependent manner to stimulate degradation (Barthelme & Sauer, 2012). AMA is only found in Archaeoglobus and methanogenic archaea (Djuranovic et al., 2006; Summer et al., 2006). It was first shown to have unfoldase activity (Djuranovic et al., 2006), and was later shown to stimulate 20S CP activity (Forouzan et al., 2012); however, the AMA-20S complex has not been isolated in vivo or in vitro.

1.5 Canonical 20S CP Assembly

While the overall structure of the 20S proteasome is highly conserved. The paths by which these proteasomes assemble are distinct between the three domains. The assembly pathway in eukaryotes is much more complicated than archaeal or bacterial pathways due to the fact it is made up of seven unique α and β subunits that occupy specific locations within the assembled structure. Data collected from several studies has shed light on what is likely the canonical or preferred assembly pathway in eukaryotes.

The current view of eukaryotic assembly begins with the formation of an α ring. This α ring acts as a scaffold for incoming β subunits (Hirano et al., 2005), and its formation appears to be essential for assembly. The β subunits bind to the α ring in the following order: β2, β3, β4, β5, β6, β1, and β7 (Hirano et al., 2008). To date three α/β subunit intermediates have been characterized in eukaryotes: the 13S complex, containing one α ring with β2, β3, and β4; the 15S (also known as the -β7 half-mer), consisting of a full α ring plus all of the β subunits, except β7; and the half-proteasome, which is one full α ring and one full β ring. Once two half-proteasomes are assembled, they will dimerize to form a pre-holoproteasome (PHP)(X. Li et al., 2007). At the PHP stage in assembly, the propeptides on β1, β2, and β5 are auto-catalytically cleaved, exposing a catalytically active threonine residue (Thr1), creating the degradation component of the 26S proteasome, the holoproteasome (HP) (Figure 1.2) (Chen & Hochstrasser, 1995; Heinemeyer, Fischer, Krimmer, Stachon, & Wolf, 1997).

Initial reports of eukaryotic assembly demonstrated that it mimicked archaeal assembly (Frankenberg, Hsu, Yakota, Kim, & Clark, 2001; Groll, Brandstetter, Bartunik, Bourenkow, & Huber, 2003; Zwickl, Kleinz, & Baumeister, 1994). Archaeal proteasomes also appear to

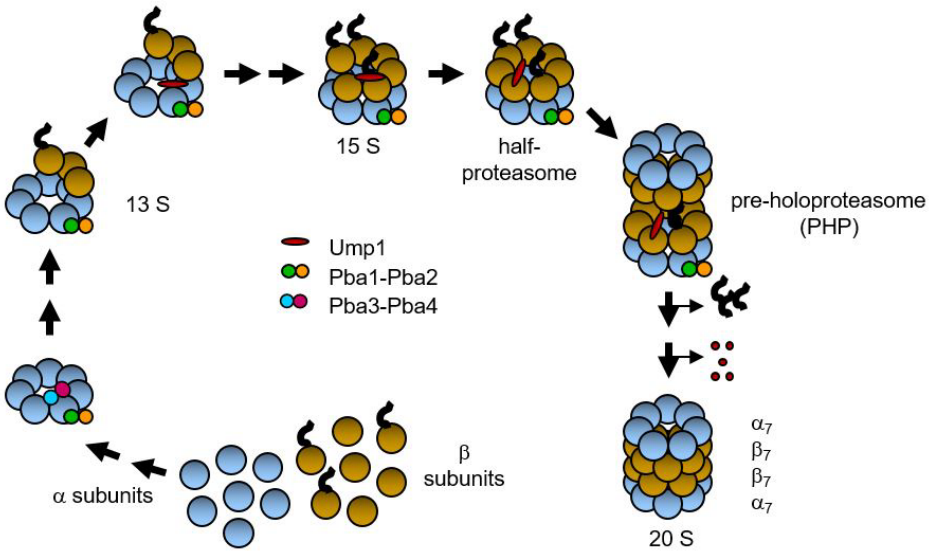

Figure 1.2 Canonical 20S CP assembly pathway
α and β subunits assemble to form the 20S CP. At least four assembly intermediates have been isolated: 13S, 15S, half proteasome, and pre-holoproteasome. Assembly is aided by assembly chaperones Ump1, Pba1-Pba2, Pba3-Pba4.

assemble via an α ring dependent pathway, with α ring formation being an essential first step for assembly. However, a study looking at recombinantly expressed archaeal subunits demonstrated that an alternative α ring independent pathway is also possible. Mutations were made to the α subunits to disrupt α ring formation. When these non-ring forming α subunits where mixed with β subunits, proteasomes still assembled, indicating that proteasomes can assemble through the initiation of α/β subunit interactions. This alternative pathway is redolent of the bacterial pathway (discussed below), where fully formed α rings are not a necessary first step to initiate assembly (Panfair, Ramamurthy, & Kusmierczyk, 2015).

Bacterial 20S subunits, like eukaryotic and archaeal subunits, arrange into four heptameric rings $\alpha_7\beta_7\beta_7\alpha_7$ (Tamura et al., 1995; Voges, Zwickl, & Baumeister, 1999). One major difference between eukaryotic and bacterial assembly occurs at the first step. Eukaryotic assembly initiates through α ring formation (Hirano et al., 2005). Bacterial assembly initiates through the interaction of α and β subunits, possibly α/β dimers. These dimers were suggested to arrange into a half-proteasome intermediate, which consists of one α ring and one β ring (Sharon, Witt, Glasmacher, Baumeister, & Robinson, 2007; Zuhl, Seemuller, Golbik, &

Baumeister, 1997). Two half-proteasomes will dimerize forming a pre-holoproteasome. Upon maturation, like in eukaryotes, the β subunit propeptide will autocatalytically cleave producing a catalytically active 20S proteasome (Zuhl et al., 1997).

1.5.1 Chaperoned 20S CP Assembly

Each subunit of the eukaryotic 20S CP occupies a specific position in the final quaternary structure. To achieve proper assembly, this process must be well regulated within the cell. Assembly chaperone proteins function to ensure proper 20S CP assembly by preventing off pathway interactions and aiding in assembly kinetics. Chaperones can be either extrinsic or intrinsic. Extrinsic chaperones are proteins that participate in assembly but are independent from the 20S CP components and do not take part in the assembled 20S CP. There are five dedicated eukaryotic 20S CP assembly chaperone proteins Ump1, Pba1, Pba2, Pba3 and Pba4. There is also evidence to suggest that Blm10, a 20S CP activator, may also participate in 20S CP assembly. Intrinsic chaperones include features of specific subunits, such as N-terminal or C-terminal extensions, that help guide assembly. While bacterial and archaeal proteasomes are less complex than their eukaryotic counterpart, some of these regulatory features appear to be evolutionarily conserved.

1.5.2 Pba1-Pba2 (PAC1-PAC2)

Pba1 and Pba2 (PAC1 and PAC2 in mammals) form a heterodimer associated with early proteasomal intermediates in both yeast (X. Li et al., 2007) and mammals (Hirano et al., 2005). While yeast lacking Pba1-Pba2 are still viable (Kusmierczyk et al., 2011), knockout of PAC1, the mammalian homolog of Pba1, in mice results in embryonic lethality (Sasaki et al., 2010). This heterodimer participates throughout entire assembly process. It likely has several functions; some of the functions described for this chaperone include, preventing premature 19S RP binding (Wani, Rowland, Ondracek, Deeds, & Roelofs, 2015) and stabilizing the formation of α rings (Hirano et al., 2005; Kusmierczyk & Hochstrasser, 2008; Le Tallec et al., 2007; Wani et al., 2015). Furthermore, these proteins were crystalized with mature 20S, which may also suggest a role outside of assembly (Stadtmueller et al., 2012).

Pba1 and Pba2 have functional C-terminal HbYX motifs (Kusmierczyk et al., 2011). The exact binding pockets were identified through a crosslinking strategy (Tian et al., 2011) and

confirmed in the 20S-Pba1-Pba2 crystal structure (Stadtmueller et al., 2012). The Pba1 C-terminus binds to the α5-α6 intersubunit pocket, while the Pba2 C-terminus binds to the α6-α7 intersubunit pocket (Stadtmueller et al., 2012). This heterodimer interacts with the same α ring surface as 20S CP activators, such as the 19S RP, but has a higher affinity for α rings containing intermediates than α rings that are associated with mature 20S CPs (Wani et al., 2015).

Recently, single particle electron microscopy (EM) in combination with crosslinking mass spectrometry (CX-MS) were used to determine the structure of Pba1-Pba2 bound to a 15S intermediate (Kock et al., 2015). This analysis demonstrated that the α rings in intermediates are much broader than the mature 20S CP. Pba1-Pba2 sit within this broad opening making substantial contacts with several α subunits. Upon maturation, the Pba1-Pba2 heterodimer is squeezed out the pore opening and sits on top of the α ring (Kock et al., 2015). Pba1-Pba2 stay bound to the α ring until the β subunits are processed. It has been hypothesized that Pba1-Pba2 binding is regulated by allosteric signaling between the maturing β subunits and the Pba1-Pba2 binding sites. This hypothesis was initially formed by the observation that archaeal orthologs of Pba1-Pba2, PbaA and PbaB (discussed below) in *Methaoncoccus maripaludis*, bound exclusively to the archaeal 20S that contained β propeptides but not to mature 20S CP (Kusmierczyk et al., 2011). Again this mechanism was suggested by Wani et al., (2015) who pointed out that β7 makes direct contact with α6 and α7, which are the α subunits that Pba1-Pba2 bind (Stadtmueller et al., 2012), and this direct interaction could be used to induce a conformational change to the α ring during maturation (Wani et al., 2015).

In contrast to the above hypotheses, Stadmueller et al indicated through binding kinetics that the Pba1-Pba2 heterodimer can bind to the mature 20S CP, suggesting that the Pba1-Pba2 heterodimer may also have a functional role with mature 20S CP (Stadtmueller et al., 2012). However, it is important to note that this binding was observed under non-physiological (low) salt conditions. When the salt concentration was increased Pba1-Pba2 binding affinity decreased, therefore it is unclear if the binding observed is functionally relevant.

1.5.2.1 Archaeal Orthologs PbaA and PbaB

Archaeal orthologs of Pba1 and Pba2, PbaA and PbaB, were first identified in *Methanococcus maripaludis* (Kusmierczyk et al., 2011). These two proteins contain C-terminal

HbYX motifs and interact with proteasomal precursors. PbaA's HbYX motif, but not PbaB's, is essential for binding to proteasome intermediates (Kusmierczyk et al., 2011).

Another group looking at archaeal homologs PbaA and PbaB in *Pyrococcus furiosus*, revealed PbaB forms a homotetramer, binds preferentially to the mature 20S, and can act as a proteasomal activator (Kumoi et al., 2013). This same study noted that PbaA in *Pyrococcus furiosus* has a C-terminal HbYX motif, but does not bind 20S CP (Kumoi et al., 2013). To elucidate its function this same group crystalized PbaA (Sikdar, Satoh, Kawasaki, & Kato, 2014). PbaA forms a homopentamer, where the C-terminus is buried within the structure (Sikdar et al., 2014).

There is still much to learn regarding the functional roles of PbaA and PbaB. In *Methanococcus maripaludis* PbaA appears to be functionally related to the eukaryotic proteasome assembly chaperone Pba1-Pba2, while PbaB's function is not clear (Kusmierczyk et al., 2011). In *Pyrococcus furiosus* PbaB acts as an activator, while PbaA's function is still unknown (Kumoi et al., 2013; Sikdar et al., 2014).

1.5.2.2 Bacterial Orthologs

A bioinformatic study in 2008 revealed that *Mycobacterium tuberculosis* contained two orthologs to PAC2, Rv2125 and Rv2714 (Iyer, Burroughs, & Aravind, 2008). Both proteins crystalized as trimers (L. Bai et al., 2017; Grana et al., 2009). Structural features of Rv2714 hint that it may function in a biosynthetic pathway (Grana et al., 2009). A recent study examined Rv2125 and Rv2724 in relationship to proteasomes. Immunoprecipitation studies revealed that neither ortholog interacted with open gate *M. tuberculosis* 20S CP (L. Bai et al., 2017). Furthermore, disruption of the Rv2125 in *M. tuberculosis* had no obvious phenotype (L. Bai et al., 2017), and proteomic analysis of the mutant strain showed no major differences in protein expression levels when compared to wild type (L. Bai et al., 2017). The authors of this study concluded that Rv2125 and Rv2714 are not proteasome assembly chaperones and likely do not participate in proteasome biology (L. Bai et al., 2017).

Rv2125 and Rv2714 lack a C-terminal HbYX motif, which is the mechanism by which Pba1 and Pba2 bind to eukaryotic 20S CPs (Kusmierczyk et al., 2011; Stadtmueller et al., 2012; Tian et al., 2011); and one of the primary roles described for Pba1-Pba2 is stabilization of α rings (Hirano et al., 2005; Wani et al., 2015) which prokaryotic proteasomes do not form.

However, there is considerable evidence demonstrating this class of chaperones also has non-HbYX mediated interactions with assembling 20S proteasomes (Howell et al., 2017). For instance, Pba1-Pba2 interact with a subset of α subunits in yeast (Kusmierczyk et al., 2008; Le Tallec et al., 2007) and mammalian cells (Hirano et al., 2005). Furthermore, Pba1-Pba2 were shown to make substantial contacts with several α subunits while sitting within the α ring of a 15S intermediate (Kock et al., 2015); it is possible that these Pba2 homologues may have non-HbYX interactions with proteasome intermediates. Disrupting Rv2125 in *M. tuberculosis* had no obvious growth defects (L. Bai et al., 2017), yet similar observations were made in yeast: *pba1Δ*, *pba2Δ*, and *pba1Δpba2Δ* had no obvious growth defects (X. Li et al., 2007). Rv2125 did not bind to mature 20S proteasomes (L. Bai et al., 2017), but whether Rv2125 or Rv2714 interact with assembling proteasomes remains to be elucidated.

1.5.3 Pba3-Pba4 (PAC3-PAC4)

Pba3 and Pba4 were identified and characterized by several different groups at roughly the same time. The mammalian homolog of Pba3, PAC3, was initially identified bound to proteasomal intermediates in mammalian cells. PAC3 was shown to form a dimer and bind exclusively to one α subunit, α2, and to several β subunits (Hirano et al., 2006). Knockdown experiments suggested that PAC3 is involved in α ring formation (Hirano et al., 2006). Shortly after the characterization of PAC3, its yeast ortholog (Poc3) was discovered and found to form a 40 kDa heterodimer with Poc4, the ortholog of mammalian PAC4 (Le Tallec et al., 2007). Two other groups independently described the functionality of this heterodimer. These groups identified these proteins as Dmp1-Dmp2 (Yashiroda et al., 2008) and Pba3-Pba4 (Kusmierczyk et al., 2008); for simplicity these chaperones will be referred to as Pba3-Pba4. The Pba3-Pba4 heterodimer ensures that the α3 subunit is incorporated in the α ring in-between α2 and α4 (Kusmierczyk et al., 2008). It has also been suggested that this heterodimer ensures the incorporation of α4 into the α ring (Takagi et al., 2014). One study which looked at *pba4*Δ cells identified an off pathway complex in which α2 had replaced α4 in the α ring (Takagi et al., 2014). Pull down experiments done independently by two different labs indicated that this heterodimer associates with α5 (Kusmierczyk et al., 2008; Yashiroda et al., 2008), and a crystal structure of Pba3-Pba4-α5 was solved (Yashiroda et al., 2008). Furthermore, Pba3 and Pba4

were shown to interact with α6 (Yashiroda et al., 2008) and somewhat with α1 (Kusmierczyk et al., 2008).

1.5.4 Ump1 (POMP)

Ump1was the first proteasome assembly chaperone to be characterized (Ramos, Hockendorff, Johnson, Varshavsky, & Dohmen, 1998). Ump1 is intrinsically disordered (Sa-Moura, Simoes, et al., 2013; Uekusa et al., 2013) and is found bound to one of the earliest 20S CP intermediates, the 13S complex (X. Li et al., 2007). This chaperone stays associated with the assembling 20S CP until two half-proteasomes dimerize. This results in Ump1 being encapsulated in the newly formed PHP, and once the β subunits are processed Ump1 becomes the first proteasomal substrate (X. Li et al., 2007; Ramos et al., 1998).

When *UMP1* is deleted in yeast cells there are fewer 20S CPs and 26S proteasomes; additionally, there is a buildup of proteasomal precursors. Oddly, these precursors contained chymotrypsin-like activity, which is normally associated with processed β5, suggesting that Ump1 may normally inhibit the autocatalytic activity of β5 (Ramos et al., 1998). Another hypothesis proposed that the role of Ump1 is to ensure that β7 is in place before the two half-proteasomes dimerize (X. Li et al., 2007). It has been suggested that both hypotheses are likely to be correct. Ump1's N-termini and C-termini may each be fulfilling one of these functions (Howell et al., 2017). A recent study looking at electron microscopy with crosslinking and mass spectrometry argued that Ump1 interacts within the interior α/β subunit interface of the 15S intermediate (Kock et al., 2015). The C-terminus is likely important for these contacts, (Burri et al., 2000; Howell et al., 2017), and may be responsible stabilizing incoming β subunits (Howell et al., 2017), including β5. The N-terminus of Ump1 is near β6 and is likely extending outside of the β ring (Kock et al., 2015). Thus, the N-terminus is probably well positioned to block premature dimerization and also to detect β7 incorporation, which would then presumably relieve the Ump1-dependent block (Howell et al., 2017).

1.5.5 Blm10

A sixth possible assembly chaperone, Blm10, was first described as a proteasomal activator (Schmidt et al., 2005). Blm10 can bind to the 20S CP α ring and stimulate peptide hydrolysis in an ATP independent manner (Schmidt et al., 2005; Ustrell, Hoffman, Pratt, &

Rechsteiner, 2002). However, unlike the 19S RP which uses multiple C-termini to bind the α intersubunit pockets, Blm10 is a large protein (~250 kDa) that folds to form a dome over the α ring, binding to the α5-α6 intersubunit pocket via a single C-terminus (Sadre-Bazzaz, Whitby, Robinson, Formosa, & Hill, 2010). Blm10 binds to this pocket via a C-terminal HbYX motif (Dange et al., 2011). Blm10 localizes to the nucleus and has been implicated in DNA repair (Blickwedehl et al., 2008; Blickwedehl et al., 2007; Doherty et al., 2012; Ustrell et al., 2002), mitochondrial function (Sadre-Bazzaz et al., 2010), and spermatogenesis (L. Huang, Haratake, Miyahara, & Chiba, 2016; Khor et al., 2006; Qian et al., 2013).

Shortly after its original characterization, Blm10 was identified associating with proteasomal precursors in a yeast strain over expressing β7. The amount of precursors associated with Blm10 increased when the propeptide of β5 was deleted (X. Li et al., 2007). While a *BLM10* deletion had only a modest effect on proteasome assembly at low temperatures, a *BLM10* deletion combined with a truncation of the β7 C-terminal extension (β7ΔC19) had a severe growth defect that was not observed in the single β7ΔC19 (Marques, Glanemann, Ramos, & Dohmen, 2007). This double mutant accumulated proteasomal precursors, had reduced peptidase activity, and contained unprocessed β2 in the 20S and 26S proteasomes (Marques et al., 2007). These results strongly advocate that Blm10 contributes to the stabilization and maturation of 20S CP, although the mechanism of this interaction is unknown.

1.5.6 β Subunit Propeptides

Subunits β1, β2, β5, β6, and β7 are synthesized with cleavable propeptides. The proteolytic subunits β1, β2, and β5 undergo autocatalytic processing of their propeptides, exposing a N-terminal threonine nucleophile (Huber et al., 2016). These propeptides protect Thr1 from deactivation by N-terminal acetylation (Arendt & Hochstrasser, 1999; Groll et al., 1999; Jager, Groll, Huber, Wolf, & Heinemeyer, 1999).

Deletion of the β5 propeptide in yeast, β5Δ*pro*, is lethal (Chen & Hochstrasser, 1996). To further characterize assembly events, Li et al. carried out a high copy suppressor screen with β5Δ*pro* and with β5 propeptide mutants that have an assembly defect. They discovered that high copy expression of β7 ($\beta7^{HC}$) suppressed the assembly defect observed in the β5 propeptide mutants. Moreover, the $\beta7^{HC}$ suppressed the lethal phenotype of the β5Δ*pro* . When a β5Δ*pro*

subunit variant is co-expressed with wild type β5, the β5Δ*pro* is incorporated into the 20S poorly. However, if β7 is overexpressed at the same time, the β5Δ*pro* variant incorporates into the assembling 20S more readily (X. Li et al., 2007). The authors suggest that the β5 propeptide and β7 likely assist a common step in assembly after 15S formation (X. Li et al., 2007). Furthermore, the $\beta7^{HC}$ suppression of β5Δ*pro* was shown to be dependent on the β7 C-terminal tail (see below). When the last 15 residues of the β7 C-terminal tail were deleted, the high copy suppression of β5Δ*pro* was abolished (X. Li et al., 2007). β7's C-terminus and the β5 propeptide have overlapping functions (X. Li et al., 2007; X. Li, Li, Arendt, & Hochstrasser, 2016). The function of the β5 propeptide has also been linked to Ump1 because an *UMP1* deletion can also suppress the lethality of β5Δ*pro* (Ramos et al., 1998). In addition to elucidating the roles of β5pro and β7, proteasomes purified and analyzed from the strain containing β5Δ*pro* with β7 (β^{7HC}) over expression accumulated 15S intermediates and an unidentified low molecular weight species (below the 15S) (X. Li et al., 2007).

Unlike β5 the propeptide, β1 and β2 propeptides are not essential for viability in yeast; however, deletion of β2's propeptide, or mutating the threonine nucleophile to an alanine, results in a growth defect (Arendt & Hochstrasser, 1997; Jager et al., 1999). When both β1 and β2's propeptides are deleted a more severe growth defect is seen than in the β2Δ*pro* alone (Arendt & Hochstrasser, 1999). Very little is known about β7's propeptide besides that it is not essential in yeast and is partially processed by β2 during assembly (Groll et al., 1999). β6's propeptide appears to have a functional role in assembly. Comparable to the β5 propeptide, deletion of the β6 propeptide is lethal and may be rescued by an *UMP1* deletion (X. Li et al., 2007).

1.5.6.1 β Propeptide Function in Bacterial 20S

While no proteasome chaperones have been identified in bacterial species to date, intrinsic features of the subunits themselves are important for assembly. Depending on the bacterial species, the same intrinsic features appear to have different roles. In *Rhodococcus erythropolis* the β subunit propeptide is important for promoting assembly, but it is not essential for viability (Kwon, Nagy, Adams, Baumeister, & Jap, 2004; Zuhl et al., 1997). In contrast, the *M. tuberculosis* proteasome β subunit propeptide has an inhibitory effect on assembly and maturation (D. Li et al., 2010).

1.5.7 C-terminal Tails of β subunits

In addition to propeptides, the C-terminal extensions of β7 and β2 are important for 20S assembly. The β7 extension extends from one half-proteasome and inserts into the other half-proteasome upon dimerization. The β2 extension wraps around the β3 subunit within the same β ring (Groll et al., 1997). When the last 19 residues of β7 are truncated (β7ΔC19), there is an accumulation of half-proteasome complexes, implicating the last 19 residues of β7 as an essential component for efficient half-proteasome dimerization (Ramos, Marques, London, & Dohmen, 2004). When the last 30 residues of the yeast β2 C-terminal tail were truncated, the yeast were no longer viable (Ramos et al., 2004).

1.5.8 Intrinsic Features of α Subunits

α subunits and β subunits share similar tertiary structures (Lowe et al., 1995); however, α subunits have N-terminal extensions. These extensions serve as a gating mechanism for the fully assembled 20S (Rabl et al., 2008; Saeki & Tanaka, 2007; Smith et al., 2007), and they contain a conserved α-helix (H0) which is important for assembly (Zwickl et al., 1994). This feature of α subunits allows them to form stable rings, whereas β subunits lack an H0 helix and do not form stable rings on their own (Zwickl et al., 1994). In addition to the H0 helix there are likely unique α subunit functions in regard to assembly. The Fub1 (function of boundary 1) protein has been shown to interact with 20S CP subunits (Hatanaka et al., 2011). Double deletion of *FUB1* and *PBA4* in yeast results in lethality, which can be suppressed by the additional deletion of α3 (Yashiroda et al., 2015). Interestingly, N-terminal deletion of α7 also suppressed this lethality, but not the N-terminal deletion of α3 (Yashiroda et al., 2015). While the focus of this study was on Fub1, it does shed light on the possibility that the α7 subunit's N-terminus has a functional role outside of 20S CP gating (Yashiroda et al., 2015).

1.6 General Chaperones Involved in Assembly

The TRC/GET protein pathway (transmembrane recognition complex (TRC)/guided entry of tail-anchored (GET)) has been implicated in 20S CP assembly. The TRC (mammals)/GET (yeast) pathway mediates the insertion of tail-anchored (TA) proteins into the ER. Its involvement in proteasome assembly was initially determined through a genetic screen for

mutants that showed synthetic growth defects with *nas6Δ* in yeast (Nas6 is an RP assembly factor) (Akahane, Sahara, Yashiroda, Tanaka, & Murata, 2013). The *nas6Δ* screen identified a growth defect in strains lacking *GET3*. Further examination of *GET1*, *GET2*, and *GET3* deletions in combination with deletions involved in proteasome assembly (*UMP1*, *NAS6*, or *HSM3*) each yielded a synthetic growth defect (Akahane et al., 2013).

In addition to studies done in yeast, the mammalian homolog of GET3, TRC40, was examined. TRC40 knockdown in HEK293T cells resulted in an accumulation of ubiquitinated proteins, and a reduction in proteasomal peptidase activity, which suggested that the TRC pathway (similar to GET), may also be involved in proteasome assembly (Akahane et al., 2013). Furthermore, a deletion of the most upstream component of the TRC pathway, Bag6, a multifunctional chaperone, was shown to hinder proteasome assembly. Specifically, the Bag6 knockdown induced an accumulation of proteasomal intermediates and caused a defect in RP assembly (Akahane et al., 2013). These results suggested that membrane insertion of some unknown TA protein, along with Ump1 and the propeptides of the β subunits, might be responsible for efficient assembly of β subunits on α rings (Akahane et al., 2013). These results are consistent with a previous study done in mammals which demonstrated that early 20S CP assembly intermediates bound by POMP (mammalian homolog of Ump1) are associated with the ER membrane (Fricke, Heink, Steffen, Kloetzel, & Kruger, 2007).

Heat shock proteins (Hsps) of the Hsp70 family have been routinely detected in high throughput mass spectrometry studies looking at purified proteasomes (Gong et al., 2009; Guerrero, Milenkovic, Przulj, Kaiser, & Huang, 2008; Verma et al., 2000). Interpreting this data is difficult because on the one hand, Hsp70 proteins are very abundant and frequently represented in collections of non-specific proteins routinely detected by mass spectrometry (Mellacheruvu et al., 2013). On the other hand, Hsp70 proteins have well established roles in the ubiquitin-proteasome system, which include enhancing substrate ubiquitination and delivery of substrates to the proteasome (Arndt, Rogon, & Hohfeld, 2007; Huyer et al., 2004; Kettern, Dreiseidler, Tawo, & Hohfeld, 2010; Metzger, Maurer, Dancy, & Michaelis, 2008; Plemper, Bohmler, Bordallo, Sommer, & Wolf, 1997; Shiber & Ravid, 2014). However, no role in proteasome assembly has been ascribed to these proteins. Recently a study that examined both 20S intermediates and intact 20S CP in yeast via native PAGE and subsequent mass spectrometry, revealed that the yeast Hsp70 proteins, Ssa1/2, associated with early 20S CP

intermediates, but not the fully assembled 20 CP (Hammack, Firestone, Chang, & Kusmierczyk, 2017). When these proteins were deleted in yeast cells the intermediates they associated with were greatly reduced, suggesting Ssa1/2 are important for stabilizing these intermediates. Other Hsp proteins have been identified interacting specifically with assembling proteasomes. Hsp90 was shown to be important for 26S assembly (Yamano et al., 2008).

1.7 Alternative Proteasomes

In eukaryotes the canonical 20S CP is ubiquitous. Variations of this structure allow for cellular adaptation or tissue specific function. The alternative assemblies identified to date include the α4-α4 proteasome, described in yeast and in mammalian cells, the immunoproteasome and thymoproteasome, found in vertebrates, and the testis specific 20S CP represented in *Drosophila* and in mammals.

1.7.1 α4-α4 Proteasomes

The α4-α4 proteasome was first described by Velichutina et al (2004). In yeast, α3 is the only non-essential 20S CP subunit, and through a crosslinking strategy it was determined that when α3 is deleted, α4 readily takes its place on the α ring (Velichutina, Connerly, Arendt, Li, & Hochstrasser, 2004). The deletion of Pba3-Pba4 chaperone also induces the formation of these alternative proteasomes (Kusmierczyk et al., 2008) The Pba3-Pba4 chaperone is important for α ring assembly, ensuring α3 is incorporated in-between α2 and α4. Furthermore, yeast expressing these alternative proteasomes can tolerate heavy metal stress better than wild type yeast cells (Kusmierczyk et al., 2008). This might be due to the alternative α ring gate formed in the absence of α3. Deletion of α3's N-terminus results in an opening of the 20S CP α ring gate (Groll et al., 2000). Recently this alternative proteasome was described in mammalian cells, and the levels of this alternative proteasome are regulated by PAC3-PAC4, the mammalian homologs of Pba3-Pba4 (Padmanabhan, Vuong, & Hochstrasser, 2016).

1.7.2 Immunoproteasome and Thymoproteasome

The immunoproteasome (iCP), iCP sub-types, and thymoproteasome (tCP) are 20S CP variants that work as part of the immune system in vertebrates. The iCP was first characterized by Aki et al (1994) when they examined the effect of interferon-γ (IFNγ) on proteasomes. In the

iCP, instead of the β1, β2, and β5 subunits, these proteasomes contain paralogs β1i, β2i, and β5i. In addition to being induced by IFNγ, they are also induced by tumor necrosis factor (TNF) (Aki et al., 1994; Tanaka, 1994). These proteasomes are important for adaptive immunity, since they produce peptides that bind to the major histocompatibility complex (MHC), which is important for antigen presentation (Gaczynska, Rock, & Goldberg, 1993; Kincaid et al., 2011; Rock & Goldberg, 1999).

Sub-types of iCPs have been described in HeLa cells exposed to INFγ (Klare, Seeger, Janek, Jungblut, & Dahlmann, 2007), cancer cell lines, and in human tissues (Guillaume et al., 2010). Guillaume et al (2010) identified two iCP sub-types, one where β5i was the only immuno-subunit and another where only β5i and β1i were present. These were identified in cancer cell lines not exposed to INFγ and in some normal human tissues including liver, small bowel, colon, and monocyte-derived dendritic cells (Guillaume et al., 2010). The levels of sub-type iCPs were highly variable between individual tissue samples, and the authors suggested that this may be due to the variability in an individual's inflammatory response (Guillaume et al., 2010). The tCP, like the iCP contains β1i and β2i, but instead of β5i it has a specialized β5t subunit. β5t is only expressed in thymic epithelial cells. This alternative proteasome is important for the development of CD8 T cells in the thymus (Murata et al., 2007).

1.7.3 Assembly of the Immunoproteasome and Thymoproteasome

The immuno-subunits assemble into CPs more readily than β1, β2, and β5 (Griffin et al., 1998). This is likely due to alternative assembly pathway(s) employed by the immuno-proteasome subunits. During iCP assembly β1i and β2i are the first two subunits to bind to the α ring, with β1i binding first (M. Bai et al., 2014; Griffin et al., 1998; Groettrup, Standera, Stohwasser, & Kloetzel, 1997; Nandi, Woodward, Ginsburg, & Monaco, 1997), which differs from canonical assembly where β2, β3, and β4 bind first to the α ring (Hirano et al., 2008). Furthermore, β5i will bind immediately after β3, which again deviates from the normal CP assembly, which requires β4 to incorporate before β5 (M. Bai et al., 2014). The assembly mechanisms of the immunoproteasome sub-types β5i and β5i β1i have not been elucidated.

While the assembly roles of β5 with Ump1 have been well established (X. Li et al., 2007; Ramos et al., 1998), there are conflicting reports regarding β5i's role in iCP biogenesis (M. Bai

et al., 2014; Heink, Ludwig, Kloetzel, & Kruger, 2005; Jayarapu & Griffin, 2004; Witt et al., 2000). Bai et al suggested the mature portion of β5i is responsible for early incorporation during iCP assembly. This was concluded by testing the incorporation of β5 modified with the β5t propeptide and the β5i propeptide. The construct with the β5t propeptide incorporated more rapidly than wild type β5, whereas the construct with the β5i propeptide assembled in to CPs at the same rate as wild type (M. Bai et al., 2014). Regarding β5i, Witt et al similarly suggested that while β5i's propeptide promoted correct incorporation and maturation it was not essential for iCP incorporation, since β5iΔ*pro* incorporated into iCPs (Witt et al., 2000). A report by Heink et al argued that β5i and its propeptide are important for iCP biogenesis. Through yeast two-hybrid screens and pull down assays, β5i and UMP1 interactions were illustrated as being essential for the rapid biogenesis of iCPs (Heink et al., 2005). UMP1 contacted both β5i's propeptide and mature form, but had a higher affinity for the proform for β5 (Heink et al., 2005). Another yeast two-hybrid screen detected UMP1 interactions with β1i, β1, β5, β6, and β7, but not β5i (Jayarapu & Griffin, 2004).

The tCP follows a similar assembly pathway to the iCP, except β5t incorporates instead of β5i. Even though both β5t and β5i are transcriptionally expressed in thymo epithelial cortical cells, nearly all CP species are tCP. Bai et al's work described the importance of β5t's propeptide for early incorporation on to the tCP.

A recent study revealed that the β5i, β1i, and β5t were highly enriched for variation amongst the public human genome sequence databases. β5t appeared to be the most enriched for predicted damaging variations (Nitta et al., 2017). Some of these β5t variations were examined in mice and showed impaired CD8 T cell development in vivo, suggesting that β5t polymorphisms influence T cell development which may contribute to an individual's predisposition to autoimmunity (Nitta et al., 2017).

Even though these proteasomes are specialized, the canonical 20S CP assembly chaperones and activators participate in the biogenesis and function of these proteasomes. Assembly chaperones, UMP1, PAC1-PAC2, and PAC3-PAC4, function during iCP and tCP biogenesis (M. Bai et al., 2014; Heink et al., 2005). The presence of UMP1 appears to be critical for the early incorporation β1i and β2i on to the α ring (M. Bai et al., 2014), while UMP1 β5i interactions are important for accelerated immunoproteasome biogenesis (Heink et al., 2005).

1.7.4 Immunoproteasome Activators

Activators that bind the iCP include the 19S regulatory particle (PA700), Blm10 (PA200), and 11S (PA28/REG αβ, and γ) . Both the 19S and Blm10 were discussed in previous sections 1.2 and 1.5.5, respectively. The 19S RP can bind the iCP making a 26S immunoproteasome; *in vitro* this iCP has the highest rate of degradation (Cascio, Hilton, Kisselev, Rock, & Goldberg, 2001; Raule, Cerruti, & Cascio, 2014) and has the most potential for generating peptides that are the appropriate size for MHC presentation directly or after trimming (Cascio, 2014). While Blm10 has been shown to increase the peptidase activity of the iCP (Pickering & Davies, 2012), so far there is no evidence of Blm10 producing peptides for antigen presentation. The PA28αβ activator (Dubiel, Pratt, Ferrell, & Rechsteiner, 1992; Ma, Slaughter, & DeMartino, 1992) is induced by IFNγ (Ahn et al., 1995; Realini, Dubiel, Pratt, Ferrell, & Rechsteiner, 1994), and is found throughout the cytoplasm of jawed vertebrates (Fort, Kajava, Delsuc, & Coux, 2015). PA28αβ is made up of two subunits, PA28α and PA28β, that form a heteroheptameric ring, $PA28\alpha_4\beta_3$ (Huber & Groll, 2017; Z. Zhang et al., 1999). This activator is presumed to promote antigen presentation (Groettrup et al., 1996).

PA28α and PA28β form homo-heptameric complexes when expressed recombinantly (Huber & Groll, 2017; Knowlton et al., 1997; Wilk, Chen, & Magnusson, 2000). $PA28\alpha_7$, $PA28\beta_7$, and $PA28\alpha_4\beta_3$ can each stimulate peptide hydrolysis of proteasomes (Huber & Groll, 2017). $PA28\alpha_7$ and $PA28\alpha_4\beta_3$ can bind both 20S CP and iCP, but in vivo binding has only been demonstrated for iCP (Ahn et al., 1995; J. Li & Rechsteiner, 2001; Pickering & Davies, 2012). Since $PA28\alpha_4\beta_3$ is the most stable and active of the PA28 species identified, it is likely the relevant species *in vivo* (Huber & Groll, 2017).

There are conflicting reports surrounding PA28αβ and iCP formation. One study looking at mouse knockouts for PA28α and PA28β, saw less iCP and concluded that PA28αβ is necessary for efficient iCP assembly (Preckel et al., 1999). Another study looking at PA28αβ deficient mice indicated that PA28αβ is not required for iCP assembly or antigen processing, but appears to be important for the processing of specific antigens (Murata et al., 2001). Interestingly, both PA28αβ and 19S can simultaneously bind a 20S CP creating a PA28αβ-20S CP-19S proteasome hybrid (Hendil, Khan, & Tanaka, 1998; Tanahashi et al., 2000). PA28αβ appears to modify the catalytic activity of the 26S proteasome such that it

enhances the variability of epitopes produced (Cascio, Call, Petre, Walz, & Goldberg, 2002). This activator reduces the size of peptides produced by the iCP. Other studies tested activator binding and activity under oxidative stress in mammalian cells, and showed that PA28αβ is induced under oxidative stress and in vitro stimulates both immunoproteasome and 20 CP degradation of oxidized substrates (Pickering & Davies, 2012).

Another activator that can bind immunoproteasomes is PA28γ, which is a homolog of PA28αβ. This activator is not induced by INFγ, forms a homohepatmeric ring, and is localized to the nucleus (Masson, Andersson, Petersen, & Young, 2001; Rechsteiner, Realini, & Ustrell, 2000). PA28γ is found throughout metazoans, but is not present in yeast and plants (Masson et al., 2001).

The precise function of PA28γ is still under investigation. Mice deficient for PA28γ show mild phenotypes, such as slow growth and a ~10% reduction in size compared to wild type (Murata et al., 1999; Z. Zhang & Zhang, 2008). A study in *Drosophila* revealed that PA28γ increases the trypsin-like activity of the proteasome (Masson et al., 2001). Studies in mammalian cells have suggested roles that include regulating apoptosis (Barton et al., 2004; Z. Zhang & Zhang, 2008), cell proliferation (Z. Zhang & Zhang, 2008), immunity (Barton et al., 2004), oxidative stress (Pickering & Davies, 2012) and possibly spermatogenesis (L. Huang et al., 2016).

1.7.4.1 PA28γ homologue in *Trypanosoma brucei*

Proteasomes were identified and purified from *Trypanosoma brucei* which is a parasitic protozoan that causes African sleeping sickness (Hua, To, Nguyen, Wong, & Wang, 1996). Shortly after its identification, a 26kDa protein (PA26) was found associating with active 20S (To & Wang, 1997). Further analysis showed that PA26 readily forms a hexameric ring when expressed recombinantly, and PA26 can bind rat 20S CP and stimulate peptide hydrolysis activity while recombinant human PA28α did not affect 20S from *T. brucei* (Y. Yao, Huang, et al., 1999). Yeast lack a PA28 homologue, yet the recombinantly expressed *T. brucei* PA26 can bind yeast 20S and stimulate peptide hydrolysis, as can recombinantly expressed human PA28αβ (Masters, Pratt, Forster, & Hill, 2005).

1.7.5 Testis Specific Proteasome

Very little is known about testis specific proteasomes. They were first identified in *Drosophila melanogaster* and were characterized as having a unique α type subunit, the testis specific isoform Prosα6T, that is important for male fertility (Zhong & Belote, 2007). A testis specific proteasome ("spermatoproteasome") was later described in mammals (Qian et al., 2013; Uechi, Hamazaki, & Murata, 2014). This proteasome contains a unique α4 subunit called α4s (Qian et al., 2013). This novel α4s has ~82-85% amino acid sequence identity with wild type α4 and is only expressed in the testis, where the α4s CP is the predominant proteasome species (Qian et al., 2013; Uechi et al., 2014). Between the two studies that have characterized the α4s CP, there is some disagreement as to whether the immuno-β subunits are part of α4 CP. Qian et al., (2013) indicated that the immuno-β subunits are part of the α4s CP, while Uechi et al (2014) carried out IPs with α4s and did not pull down any immuno-β subunits. The activator PA200 (Blm10) was associated with α4s CP more so than any other activator, suggesting α4s CP preferentially interacts with Blm10. Deletion of *BLM10* in mice disrupted spermatogenesis (Qian et al., 2013).

In addition to spermatoproteasomes, a 20S CP assembly chaperone ZPAC (zygote proteasome assembly chaperone), was described in mouse gonads and zygotes (Shin et al., 2013). ZPAC was discovered when researchers were looking into the maternal-to-zygote transition during which maternal proteins are degraded by proteasomes and new proteins are transcribed and translated from the zygote's genome. Further characterization of ZPAC revealed that it forms a complex with Ump1 that associates with 20S CP intermediates, and knockdown of ZPAC in embryos caused abnormal development (Shin et al., 2013). Another group looked at ZPAC's role in mouse spermatogenesis. ZPAC was argued to be involved in germline survival and apoptosis (Shimizu et al., 2014). More work still needs to be done to elucidate the functional roles of ZPAC.

1.8 Non-canonical Structures Formed by Proteasome Subunits

Some proteasomal α subunits can readily form high molecular weight complexes. Gerards et al demonstrated that when human α7 is expressed recombinantly in *E.coli*, it forms a high molecular weight complex. This complex is a double ring structure with each ring consisting of

seven subunits (Gerards et al., 1997). This double ring structure was reminiscent of a complex observed with recombinantly expressed α subunits form archaea. When archaeal α and β subunits are recombinantly coexpressed they readily form proteasomes; however, when human α7 was coexpressed with β7, or β1 (both are the immediate neighbors of α7 within the adjacent β ring), no proteasome-like structures were formed (Gerards et al., 1997). When α7 was coexpressed with its α ring neighbors, α1 or α6, the α subunits assembled into heterogeneous complexes (Gerards, de Jong, Bloemendal, & Boelens, 1998). Recently, Ishii et al crystalized the α7 double ring structure. Consistent with the work done by Gerards and colleagues, this group demonstrated that the presence of α6 disrupts the formation of the α7 tetradecamer by forming smaller complexes consisting of α7 and α6 (Ishii et al., 2015).

To date no high molecular weight complexes of α7, α7-α1, or α7-α6 have been identified in vivo. We recently identified a non-canonical complex in yeast that consists of proteasome subunit α4 and Ssa1/2 (Hammack & Kusmierczyk, 2017). While no structural studies have been performed on this complex, our crosslinking strategy argues that this complex forms oligomers that we hypothesize to be α4 rings. The formation of this complex opens the door toward the possibility of extra-proteasomal roles for proteasome subunits. Experiments are currently underway to further characterize this complex.

1.9 Proteasomes as Therapeutic Targets

The proteasome degrades regulatory proteins within the cell. Proteasome inhibition has been shown to accumulate regulatory proteins such as cell cycle progression proteins (Cusack et al., 2001; S. A. Shah et al., 2001) and oncoproteins (Dietrich, Bartsch, Schanz, Oesch, & Wieser, 1996). This accumulation sensitizes cells to apoptosis (reviewed by (Adams, 2004)). This apoptotic sensitivity is greater in malignant cells which makes proteasome inhibition a promising target for cancer therapy (Hideshima et al., 2001). There are three proteasome inhibitors currently on the market, and several others are in clinical trials (Manasanch & Orlowski, 2017). A recent study has suggested that miRNA may also be advantageous for proteasome inhibition (Zhang et al 2015).

In addition to cancer therapy, targeting bacterial proteasomes may have therapeutic applications. Zeroing in on *Mycobacterium tuberculosis* proteasomes may be an effective

strategy for treating tuberculosis. Also, understanding the Pup-proteasome's role in producing different types of metabolites, including antibiotic and antifungal compounds, in actinomycete *Streptomyces coelicolor* may be a useful in isolating new antibiotic and antifungal compounds.

1.9.1 Proteasome Inhibitors

Three proteasome inhibitors Velcade (brotezomib), Kyprolis (carfilzomib), and Ninlaro (ixazomib) have been approved for the treatment multiple myeloma (Kane, Bross, Farrell, & Pazdur, 2003; Kubiczkova, Pour, Sedlarikova, Hajek, & Sevcikova, 2014; Kuhn et al., 2007; Moreau et al., 2016; L. A. Raedler, 2016; Richardson & Anderson, 2003; Siegel, 2012). Brotezomib has also been approved to treat mantle-cell lymphoma (Holkova & Grant, 2012; L. Raedler, 2015). These inhibitors work by inhibiting the chymotrypsin activity of β5. Brotezomib was the first proteasome inhibitor used to treat multiple myeloma (Kane et al., 2003). It is a reversible dipeptide boronate inhibitor that targets both β5 and β5i and also interacts with β1 to a lesser extent (Demo et al., 2007). In addition to treating multiple myeloma and mantle-cell lymphoma, bortezomib shows promise in the treatment of atopic dermatitis (Kim, Cho, Cheon, & Kim, 2017). A study in mice showed brotezomib to increase the expression levels of claudin 1 and ameliorate the symptoms of atopic dermatitis (Kim et al., 2017).

Carfilzomib entered the market in 2012 (Thompson, 2013). It is an irreversible inhibitor belonging to the epoxyketone family and is based on the natural product epoxomicin (Groll, Koguchi, Huber, & Kohno, 2001; Harshbarger, Miller, Diedrich, & Sacchettini, 2015). Opozomib, an oral analogue of carfilzomib, is being tested in clinical trials and shows anti-myeloma activity and is well tolerated (Hari et al., 2014; J. Shah et al., 2015). Ixazomib was approved by the FDA as the first orally administered proteasome inhibitor for the treatment of multiple myeloma (Moreau et al., 2016; L. A. Raedler, 2016). While the development of each new drug has improved patient outcomes, severe side effects are still observed and resistance can eventually develop.

1.9.2 Endogenous Inhibitor MicroRNA-101

MicroRNAs regulate gene expression by binding to target mRNA molecules. This binding suppresses translation of the mRNA transcript. Early studies looking at MicroRNA-101 (miR-101) demonstrated that it was downregulated in cancer cell lines, and ectopic expression of

miR-101 suppressed tumor growth (Su et al., 2009; Varambally et al., 2008). Zhang et al 2015 demonstrated that miR-101 acts as an endogenous proteasome inhibitor by targeting and down regulating the expression of proteasome assembly chaperone POMP (mammalian UMP1). Unlike the aforementioned inhibitors, miR-101 works by disrupting proteasome assembly (X. Zhang et al., 2015). Moreover, POMP suppression, by either miR-101 or by POMP siRNA, was able to re-sensitize cells resistant to bortezomib (X. Zhang et al., 2015). This work sheds light on how the assembly machinery may be targeted for cancer pharmacotherapy.

1.9.3 Targeting Bacterial Proteasomes for Human Therapeutics

In addition to targeting proteasomes for cancer therapy, bacterial proteasomes also serve as useful targets for the development of antibiotics and treatment of tuberculosis (TB). TB is a major global health problem. Per the World Health Organization, in 2015 there were 10.4 million new cases of TB; 1.4 million of those cases resulted in death (*Global Tuberculosis Report*, 2016). The proteasome in *M. tuberculosis* appears to be a promising target for the development of therapeutic agents (Bibo-Verdugo, Jiang, Caffrey, & O'Donoghue, 2017; Samanovic & Darwin, 2016). One hypothesis is that nitric oxide (NO) is important for controlling bacterial growth, such as *M. tuberculosis* in humans (Choi, Rai, Chu, Cool, & Chan, 2002; Nicholson et al., 1996; Wang et al., 1998). A 2003 study screened 10,100 transposon mutants in *M. tuberculosis* for sensitivity to nitric oxide and other reactive nitrogen intermediates. Five mutants that displayed sensitivity were proteasome associated genes (Darwin et al., 2003). Furthermore, they demonstrated that treating wild type *M. tuberculosis* with proteasome inhibitor sensitizes it to reactive nitrogen intermediates (Darwin et al., 2003). Proteasomes inhibitors that target *M. tuberculosis* may prove to be useful treatments (Bibo-Verdugo et al., 2017), but targeting other unique aspects of the bacterial proteasome system, such as pupylation (Samanovic & Darwin, 2016) or assembly may also be worthwhile.

Another actinomycete, *S. coelicolor*, has potential implications for human therapeutics. This group of actinomycetes produces several different types of metabolites including antibiotic and antifungal compounds (Chater, Biro, Lee, Palmer, & Schrempf, 2010; Chater & Chandra, 2008; Flardh & Buttner, 2009). Understanding how this actinomycete regulates its metabolism and maintains protein homeostasis is important for understanding the development of these compounds. A few groups have looked at the Pup-proteasome system in relationship to *S.*

coelicolor's protein homeostasis and secondary metabolite production. Disruption or deletion of the Pup-ligase or the Pup-proteasome system results in sensitivity to cumene hyperoxide (Compton et al., 2015). Strains with a Pup deletion were also shown to be sensitive to hydrogen peroxide, have impaired spore formation, and produce less secondary metabolites (Boubakri et al., 2015; Mao et al., 2014). Furthermore, Boubarki and colleagues identified two Pup targets that are involved in antibiotic production, OsaA (Bishop, Fielding, Dyson, & Herron, 2004) and FtsI (Bennett et al., 2009). While this is the first published evidence of Pup being involved in *S. coelicolor's* antibiotic production, another group suggested this role for Pup previously (Liu, Chater, Chandra, Niu, & Tan, 2013).

CHAPTER 2. NON-CANONICAL COMPLEXES

Chapter 2 along with Appendix A were originally published in Biochemical and Biophysical Research Communications (BBRC).

Hammack, L. J., & Kusmierczyk, A. R. (2017). Assembly of proteasome subunits into non-canonical complexes in vivo. *Biochem Biophys Res Commun, 482*(1), 164-169. doi:10.1016/j.bbrc.2016.11.024

2.1 Abstract

Proteasomes exist in all domains of life. In general, they are comprised of a compartmentalized protease whose activity is modulated by one or more regulatory complexes with which it interacts. The quaternary structure of this compartmentalized protease, called the 20S proteasome, is absolutely conserved and consists of four heptameric rings stacked coaxially. The rings are made of structurally related α and β subunits. In eukaryotes, assembly factors chaperone the α and β subunits during 20S biogenesis. Here we demonstrate that proteasome subunits can assemble into structures other than the canonical 20S proteasome in vivo. Specifically, the yeast α4 subunit forms high molecular weight complexes whose abundance increases when proteasome function is compromised. Results from a disulfide crosslinking approach are consistent with these complexes being ring-shaped. Though several eukaryotic α subunits can form rings when expressed recombinantly in bacteria, this is the first evidence that such noncanonical complexes exist *in vivo*.

2.2 Introduction

The 26S proteasome comprises two major sub assemblies: the 20S proteasome, also known as the core particle (CP), and a 19S regulatory particle (RP) (Beck et al., 2012; da Fonseca, He, & Morris, 2012). The CP consists of four heptameric rings built up from two structurally related subunits, α and β, in an $\alpha_7\beta_7\beta_7\alpha_7$ arrangement (Groll et al., 1997; Hu et al., 2006; Lowe et al., 1995). In eukaryotes, the α and β rings contain seven different subunits, and peptide hydrolysis activity resides within the β1, β2, and β5 subunits. Assembly of the CP is guided by structural features intrinsic to the CP subunits and by extrinsic factors in the form of dedicated assembly

factors (reviewed in (Kunjappu & Hochstrasser, 2014)). There are five such factors in eukaryotes, Ump1 and Pba1–4 (called PAC1–4 in mammals).

Assembly of the CP begins with the formation of α rings which serve as a platform for the subsequent entry of β subunits until a half-proteasome (i.e. $\alpha_7\beta_7$) intermediate is formed (Hirano et al., 2008). Two half-proteasomes dimerize to give rise to the CP, a process that coincides with the autocatalytic removal of propeptides on the enzymatically active β subunits (Chen & Hochstrasser, 1996). The assembly factors perform several functions, including: ensuring the correct placement of subunits within the rings (Kusmierczyk et al., 2008), performing key checkpoint functions (X. Li et al., 2007), preventing non-desirable interactions between CP subunits themselves (Hirano et al., 2005; Takagi et al., 2014) and preventing binding of RP to immature CP species (Wani et al., 2015). The end result is a fully functional CP with all subunits occupying a defined position. However, evidence has been mounting that the structure of the CP need not be considered fixed.

In the yeast *Saccharomyces cerevisiae*, the α3 subunit is not essential for viability; in α3Δ yeast cells, an alternative CP is formed in which a second copy of α4 occupies the position normally held by α3 (Velichutina et al., 2004). These "α4–α4 proteasomes", so-called because their α rings now contain two neighboring α4 subunits, also arise in yeast when the Pba3-Pba4 assembly factor is absent (Kusmierczyk et al., 2008) even though α3 is still present. Recently, α4–α4 proteasomes were shown to exist in mammalian cells, arguing that formation of this alternative CP is evolutionarily conserved (Padmanabhan et al., 2016).

Here we present additional evidence that the CP structure need not be considered immutable. In addition to enabling the formation of α4–α4 proteasomes, we find that α4 assembles into high molecular weight complexes (HMWCs) that are most likely rings of α4 subunits. Some eukaryotic α subunits can form non-canonical rings when expressed recombinantly in bacteria but the relevance of these structures was not clear (Gerards et al., 1998; Gerards et al., 1997; Ishii et al., 2015; Y. Yao, Toth, et al., 1999). This is the first report of such structures existing in wild type cells *in vivo*, raising the possibility of functional significance.

2.3 Materials and Methods

2.3.1 Strains and Yeast Culture

Yeast strains are listed in Supplementary Table 1. The α2HF strain (MATa) was generated by backcrossing to the wild type the α2HF strain (MATα) kindly provided by Mark Hochstrasser. The crosslinkable α4 (α4CC) was engineered as described (Velichutina et al., 2004), except we employed a C-terminal Flag tag. One liter yeast cultures were grown in YPD at 30 °C to mid-log phase. Yeast cells were harvested by centrifugation at 4,000 x *g* and the pellets washed with 40 ml of H_2O prior to storage at –80 °C.

2.3.2 Yeast Lysis and Flag Purification

Yeast cell pellets were thawed in cold water and gently resuspended in 48 ml of Buffer A (40 mM Hepes-NaOH pH 7.5, 10% (v/v) glycerol, 350 mM NaCl, 0.1% (v/v) Tween-20 supplemented with yeast protease inhibitors (Sigma) according to manufacturer's instructions). The suspension was transferred to a 50 ml bead beater lysis chamber along with 0.5 mm glass beads (BioSpec). The yeast cells were lysed via bead beating with cycles of 1 minute bead beating followed by one minute of rest/cooling for a total of 15 cycles. Total lysates were centrifuged at 11,000 rpm for 1 hour at 4 °C in a Beckman J2-21M centrifuge using a JA-20 rotor. The supernatant (soluble lysate) was transferred to a fresh 50 ml conical tube and the protein concentration was measured via Bradford Assay (ThermoScientific) or BCA Protein Assay Kit (ThermoScientific). When processing parallel samples, equal amounts of protein from the soluble lysate were incubated with 200 µl of anti-Flag agarose resin (Sigma) overnight at 4 °C. The anti-Flag agarose resin was collected in a 30 ml gravity column (Bio-Rad) and washed with 60 ml of Buffer A. The resin was then transferred to a fresh microcentrifuge tube and centrifuged for 30 seconds at 4,000 × *g*. Excess Buffer A was aspirated, and the Flag-tagged proteins were eluted with 300 µl of Flag peptide (Sigma), at a concentration of 5 µg/µl in Tris-buffered saline (TBS), for 30 minutes at 4 °C. The eluted proteins were collected by transferring the resin mixture to a Pierce Micro-spin column (ThermoScientific) and centrifuging at 10,000 × *g* for 3 minutes.

2.3.3 Electrophoresis

Samples were subjected to SDS-PAGE and native PAGE as previously described (Kusmierczyk et al., 2011) except 4–15% non-denaturing polyacrylamide gradient gels, as well as 10%, 12% and 11–15% step gradient SDS-PAGE gels were used as indicated. For all gels, the migration of molecular size standards is indicated to the left of each gel image in the figures. The 4–15 % gradient gels were precast Mini-PROTEAN TGX (Bio-Rad) while all others were poured in lab. For native PAGE, purified protein (20 μg) was mixed with 5× non-denaturing sample buffer (0.5 M Tris-HCl, pH 8.8, 50% (v/v) glycerol, traces of bromophenol blue). Non-denaturing gels were run at 60 V for 10 hours at 4 °C. Substrate overlay assay was carried out as described (Kusmierczyk et al., 2011). The native gels were stained with Imperial Protein Stain (ThermoScientific). Loading control samples were run on reducing 12% SDS-PAGE. All SDS-PAGE gels were stained with GelCode blue (ThermoScientific).

For Western blotting, samples were run on 10% SDS-PAGE gels and transferred to PVDF membrane for 1 hour at 15 V using a GENIE Electrophoretic Transfer (Idea Scientific). The membrane was blocked overnight with 5% (w/v) non-fat milk in TBS. The membrane was incubated with primary anti-Flag antibody (Sigma), diluted 1:2000 in 5% (w/v) non-fat milk in TBS, for 1 hour at room temperature with gentle rocking. The membrane was washed 3 times with TT Buffer (0.1 % (v/v) Tween-20 in TBS) for 5 minutes and then incubated for 1 hour at room temperature with gentle rocking in TT buffer containing secondary goat anti-mouse IgG_1 antibody (SouthernBiotech) diluted 1:5000. The membrane was again washed 3 times as above before adding ECL substrate (ThermoFisher) and exposing to film.

2.3.4 Disulfide Crosslinking

Disulfide crosslinking was performed as described (Kusmierczyk et al., 2011). Crosslinked and noncrosslinked samples were mixed with 2 x SDS sample buffer without DTT and loaded onto 11-15% SDS PAGE step gradient gels. Where indicated, a 25 μl aliquot of each sample was reduced with 2 μl of 1M DTT at room temperature for 15 minutes.

2.3.5 Depletion Assay

Yeast cell pellets were lysed and CP purified with anti-Flag agarose resin as above. Aliquots of the Flag eluates were subjected to depletion via immobilized-cobalt affinity resin

(ICAR) as described (Panfair et al., 2015),with the following modifications. The samples were applied to 150 μl of resin (TALON resin; Clontech) for 1 hour at 4 °C with gentle rocking. The flow through from the first ICAR purification was subjected to a second round of ICAR using a fresh 150 μl of resin.

2.3.6 Mass Spectrometry Analysis

Slices were cut from indicated gels and submitted to the Indiana University School of Medicine Proteomics Core Facility (IUSM-PCF) to identify proteins by LC-MS/MS. Summarized and annotated data describing the identified proteins are presented in table format throughout the manuscript and supplementary information. The data analysis files provided by IUSM-PCF in Microsoft Excel format, can be found in the accompanying Data In Brief article (L. Hammack & A. R. Kusmierczyk, 2016).

2.4 Results

Initially, we set out to study the formation and function of α4–α4 proteasomes in yeast. We employed a crosslinking strategy (Velichutina et al., 2004) using an engineered α4 subunit (α4CC) with a C-terminal Flag epitope (Figure 2.1A). When α4–α4 proteasomes are present, the α4CC subunit gives rise to a diagnostic α4 dimer on non-reducing SDS-PAGE under mildly oxidizing conditions. This dimer was readily observed when CP was purified from α3Δ yeast. However, the α4 dimer was not observed in the wild type sample (lane 2) consistent with previous observations that α4-α4 proteasomes are not detectable (at least using this approach) in wild type yeast cells (Kusmierczyk et al., 2008; Velichutina et al., 2004).

Interestingly, additional bands appeared near the top of the SDS-PAGE gel under non-reducing conditions. Like the α4 dimer, these species required the presence of α4CC and disappeared under reducing conditions (Figure 2.1B); they also failed to form in the absence of added oxidant (Figure 2.1C). This argues that these slowly migrating species were the result of the engineered disulfide crosslink. However, unlike the α4 dimer, these species were also present in wild type cells, albeit at lower levels compared to α3Δ cells (Figure 2.1B, lanes 2 versus 4). LC-MS/MS which confirmed the presence of α4 (not shown) consistent with the slowly migrating species being a multimer (or multimers) of α4 crosslinked to itself.

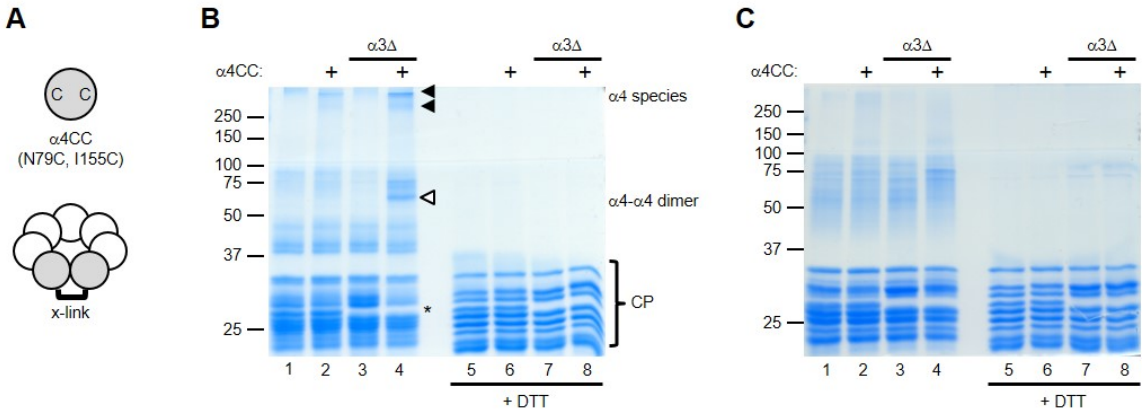

Figure 2.1 Detection of novel α4-containing species
(A) Schematic of crosslinkable α4 subunit (α4CC) and the resulting crosslink from adjacent α4's with an α ring. (B) Flag-purified CP from the indicated yeast strains were treated with $CuCl_2$ to initiate crosslinking. Samples were subjected to SDS-PAGE under non-reducing (lanes 1 to 4), or reducing (lanes 5 to 8) conditions. White arrowhead denotes position of α4–α4 dimer. Black arrowheads denote slow-migrating novel α4 species. Asterisk denotes migration of the α3 subunit, or its absence in α3Δ strains. Bracket denotes subunits of the CP. Migration of molecular size standards is indicated on the left. (C) Analysis as in (B) except the samples were not crosslinked.

To determine if the slowly migrating species represented actual α4-containing high molecular weight complexes (HMWCs), we analyzed Flag-purified CP samples by native PAGE. The major complex in each sample, migrating near the 670 kDa size standard, was the CP (Appendix A, Supplementary Figure 1). Species migrating slower than the CP were likely complexes of CP and Blm10; these were more abundant in the α3Δ samples because CP lacking α3 are constitutively open and Blm10 preferentially binds to CP with an open (or disordered) gate (Lehmann, Jechow, & Enenkel, 2008). Species migrating faster than the CP were also observed, some of which were likely CP assembly intermediates (Appendix A, Supplementary Figure 1, bracket); if α4 HMWCs were present, they would likely be found among them. To better visualize these faster migrating species, all of our subsequent native PAGE gels were loaded with an excess of protein (Figure 2.2A).

We excised several of these faster migrating species and submitted them for analysis by LC-MS/MS (Appendix A, Supplementary Figures 2 to 7, and see also (L. Hammack & A. R. Kusmierczyk, 2016)). As expected, all six bands analyzed suggested the presence of CP assembly intermediates. For example, band 1 contained all α subunits, all β subunits except β7, as well as the assembly factors Ump1, and Pba1-Pba2 (Figure 2.2A and Appendix A,

Supplementary Figure 2). This is consistent with band 1 containing the 15S assembly intermediate of the CP (Kunjappu & Hochstrasser, 2014) (alternatively known as the "–β7 half-mer" (X. Li et al., 2007)). Interestingly, the composition of band 3 argued it too contained the 15S (Appendix A, Supplementary Figure 4). Yet band 3 migrated slightly slower than that band 1, and was also more intense.

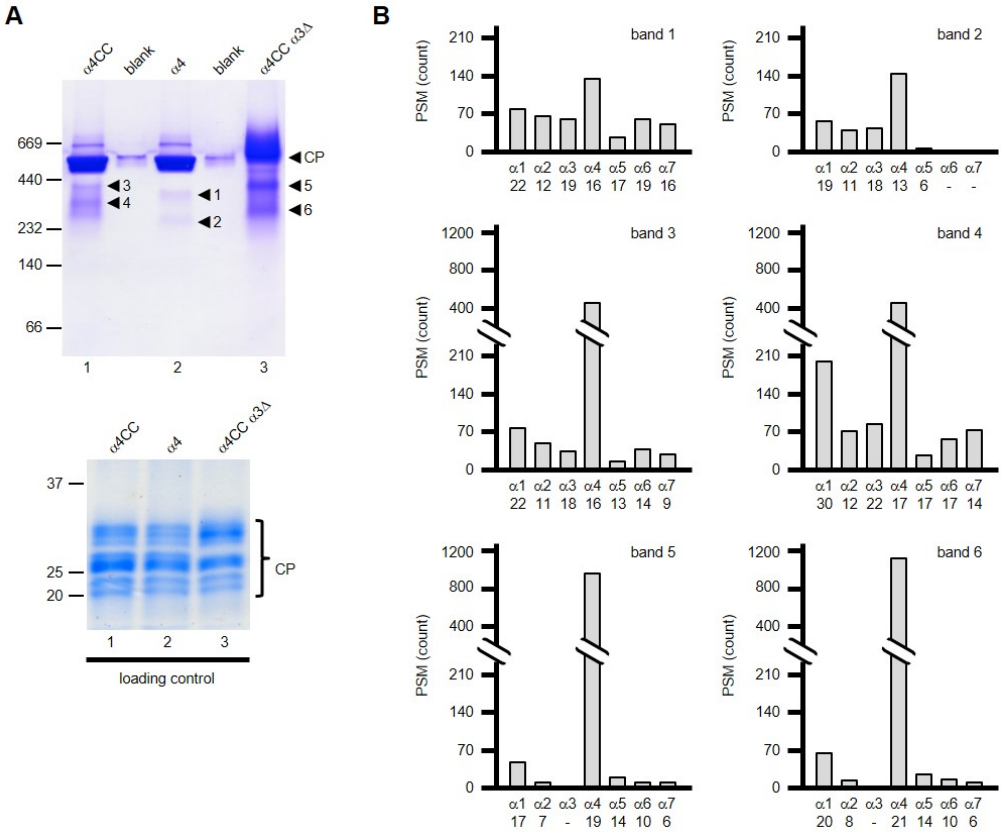

Figure 2.2 Analysis of putative α4-containing HMWCs by native PAGE
(A) Native PAGE of Flag-purified CP from the indicated yeast strains (top panel). Arrowheads denote migration of CP and of CP assembly intermediates (1-6). No protein was loaded in lanes labeled "blank" to minimize effect of spillover between samples. To verify equal loading of proteins, aliquots of the Flag-purified material were subjected to SDS-PAGE (bottom panel). (B) Contents of bands 1-6 in (A) were analyzed by LC-MS/MS. Graphs indicate the total count of PSMs (peptide spectral matches) for peptides derived from individual α subunits. Numbers below each subunit represent the actual number of peptides identified by LC-MS/MS for that subunit.

Band 3 was derived from a wild type yeast strain containing α4CC whereas band 1 was derived from an isogenic strain containing (non-crosslinkable) α4. Hence, the difference in their

electrophoretic mobility can be accounted for in two, not mutually exclusive, ways. On the one hand, to generate α4CC, two amino acids with non-ionizable sidechains were replaced by cysteines, which can be appreciably ionized at the pH of the resolving gel; this could affect the charge of α4CC-containing species and hence contribute to a migration difference of 15S in

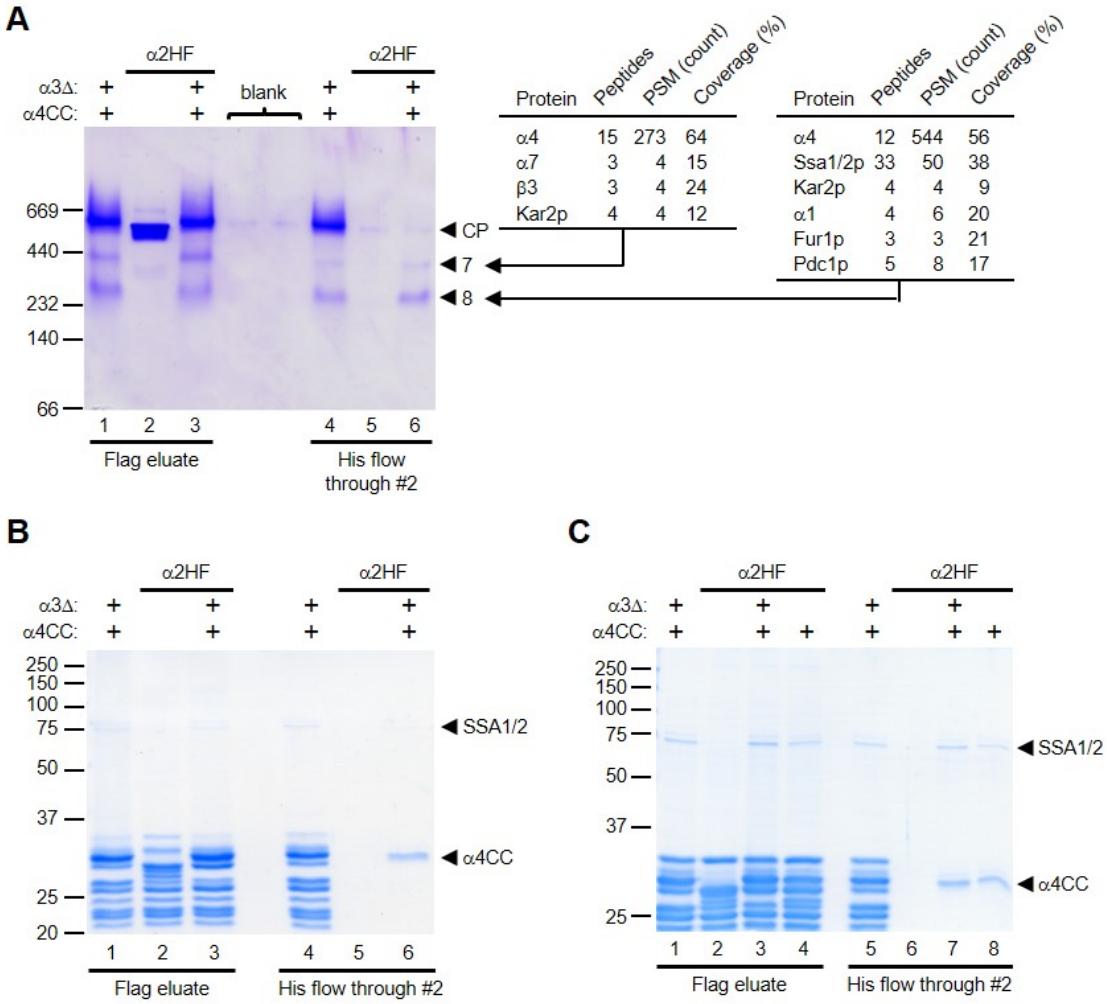

Figure 2.3 Depletion analysis confirms novel α4 complexes
(A) Aliquots of Flag-purified CP from the indicated yeast strains were subjected to native PAGE (lanes 1 to 3). The remainder of the Flag-purified material was depleted of his-tagged proteins via two rounds of binding to immobilized-cobalt affinity resin (ICAR). Aliquots of the flow through from the second binding to ICAR were loaded on the same native PAGE gel (lanes 4-6). Arrowheads denote the position of CP and two faster migrating species (7 and 8) that remain following depletion. Contents of bands 7 are shown at right. (B) Aliquots of samples in (A) were also analyzed by SDS-PAGE. (C) Depletion analysis was repeated to demonstrate that wild type yeast strains also possess the novel α4 complexes.

band 1 versus band 3. On the other hand, the increased intensity of band 3 could represent a novel species not found in band 1 i.e. the sought-after α4 HMWCs. Consistent with the later scenario, we observed an excess of spectral counts for peptides derived from the α4 subunit, compared to those derived from other α subunits, in band 3 (Figure 2.2B). This vast excess was observed for all bands from samples containing α4CC (bands 3-6) and argued that these bands contained considerably more α4 than the other subunits. The simplest explanation was that bands 3 through 6 included, not only CP assembly intermediates but also comparably sized HMWCs consisting of α4CC (Appendix A, Supplementary Figures 2 to 7). The subunit composition of bands 1 through 6, including the excess of α4 in bands 3 to 6, was reproducible (Appendix A, Supplementary Figure 8).

To confirm the existence of these novel α4-containing HMWCs as independent species, we pursued a depletion approach (Appendix A, Supplementary Figure 9). Initially, we chose to do this in an α3Δ background because our data suggested these HMWCs are more abundant when α3 is deleted (Figures 2.1B and 2.2). We employed a strain in which α2 was C-terminally tagged with a tandem epitope consisting of a hexahistidine tag (his tag) and a Flag tag (α2HF). We crossed α2HF and α4CC α3Δ yeast to generate the α4CC α3Δ α2HF experimental depletion strain. We prepared lysates from cultures of the experimental depletion strain, and its two parental strains as controls (α4CC α3Δ and α2HF), and isolated all Flag-tagged species. We subjected the Flag eluates to both native and SDS-PAGE (Figures 2.3A and 2.3B, lanes 1 to 3). The CP was the major species in all the samples and faster migrating species were also observed. The faster migrating species in the two α4CC containing strains (Figure 2.3A, lanes 1 and 3) were the equivalent of bands 5 and 6 in Figure 2.2A. As expected, these two bands were absent in the α2HF strain (Figure 2.3A, lane 2) because this strain did not contain Flag-tagged α4; it is not possible to isolate any α4 HMWCs from this strain. The Flag eluates were depleted of any his-tagged proteins via two rounds of binding to immobilized cobalt affinity resin (ICAR) (Appendix A, Supplementary Figures 9 and 10). Protein complexes not containing his-tagged components would remain in the second “flow through” (Figures 2.3A and 2.3B, lanes 4 to 6).

The his flow through of the sample from the α4CC α3Δ parental control looked like its corresponding Flag eluate; since no α2HF was present, none of the species were retained on the ICAR (Figures 2.3A and 2.3B, lane 4; Appendix A, Supplementary Figure 10, lane 1). The his

flow through of the α2HF parental control strain was nearly completely empty; since the only Flag tagged protein in this strain was also his-tagged, all Flag-containing species were depleted by ICAR (Figures 2.3A and 2.3B, lane 5), though a tiny amount of CP did escape depletion. In the his flow through of the experimental strain, nearly all of the CP was depleted, except for the tiny amount also present in the α2HF sample (Figure 2.3A, lane 6). Importantly, the two species migrating faster than CP were recovered in considerable amounts (bands 7 and 8), consistent with these species containing Flag-tagged α4 but not his-Flag-tagged α2. LC-MS/MS analysis confirmed the dominant species in each band was α4, though a considerable amount of the closely related Hsp70 paralogs, Ssa1p and Ssa2p, were present in band 8. The LC-MS/MS results were corroborated by SDS-PAGE showing α4 as the major species and a weaker Hsp70-containing band (Figure 2.3B, lane 6). We repeated the depletion analysis and included the wild type (i.e. non α3Δ) yeast strain for comparison, which confirmed that these α4 HMWCs are also present in wild type cells (Figure 2.3C).

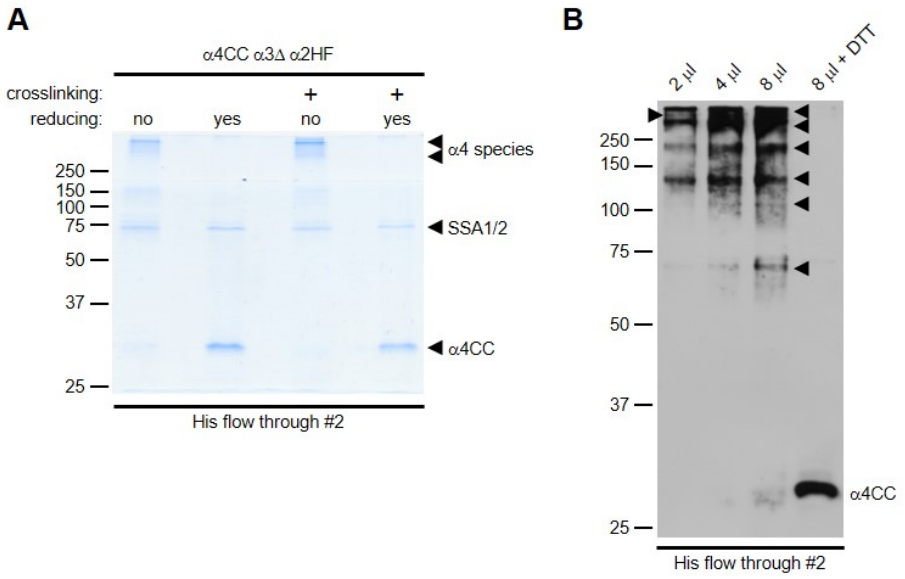

Figure 2.4 Quaternary structure of α4 HMWCs
(A) Aliquots of the α4 HMWCs isolated by depletion analysis, as in Figure 2.3, were incubated in the presence or absence of $CuCl_2$ to induce crosslinking. Samples were subjected to SDS-PAGE under non-reducing and reducing conditions. (B) Increasing amounts of α4 HMWCs were subjected to SDS-PAGE under non-reducing conditions (2, 4, and 8 µl), or reducing conditions (8 µl + DTT), followed by Western blotting with anti-Flag antibody. Arrowheads denote position of crosslinked products containing increasing copies of α4. The position of the monomer is denoted by α4CC.

Finally, we subjected aliquots of the his flow through from the α4CC α3Δ α2HF depletion strain (containing α4 HMWCs) to SDS-PAGE under reducing and non-reducing conditions; prior to electrophoresis, the samples were either treated (or not treated) with $CuCl_2$ to initiate crosslinking (Figure 2.4A). Under non-reducing conditions, all the α4 migrated as distinct species near the top of the resolving gel. This confirmed that the α4 HMWCs isolated in the depletion analysis were the same slowly migrating α4 species initially observed by non-reducing SDS-PAGE (Figure 2.1B), and consisted of α4 crosslinked to itself. This was further verified by Western blotting which demonstrated an expected α4 laddering pattern (Figure 2.4B); this occurs when some of the α4 HMWCs in the sample are not completely crosslinked. It is notable that $CuCl_2$ was not required to observe the α4 HMWCs in Figure 2.4, unlike in Figure 2.1B. We have shown before that protracted purification protocols, especially involving ICAR, are sufficiently oxidizing to allow crosslinking to occur even in the absence of exogenous oxidant (Panfair et al., 2015) (see also Appendix A, Supplementary Note).

2.5 Discussion

We provide evidence that the α4 subunit exists in high molecular weight complexes (HMWCs) outside of the CP *in vivo* (Figures 2.1B and 2.3). These non-canonical species are likely ring-shaped because their discovery was enabled by a cross-linking strategy developed to detect the placement of two α4 subunits within the same α-ring (Velichutina et al., 2004) and because we observed a distinctive α4 laddering pattern that would be expected if these were rings (Figure 2.4B). The seven crosslinked bands observed in the laddering pattern could be evidence for an octameric ring, though it is possible that two of the bands (presumably the two highest bands) each contain seven copies of α4. This would occur if one band is derived from a completely crosslinked (i.e. closed) heptameric ring and one band is derived from a heptameric ring with one crosslink missing (i.e. an open chain of 7 subunits). Circular and linear topologies of a protein can migrate differently on SDS-PAGE (Iwai & Pluckthun, 1999).

Non-canonical rings containing different combinations of α subunits have been observed before, but only when the α subunits were recombinantly produced in bacteria (Gerards et al., 1998; Gerards et al., 1997; Ishii et al., 2015; Y. Yao, Toth, et al., 1999). Thus, it was not clear if their recombinant existence was relevant physiologically. This is the first evidence that such

complexes exist *in vivo,* in wild type cells. The two species we observed on native PAGE (Figure 2.3A, bands 7 and 8) could be single and double α4 rings that exist in equilibrium. There are several reasons why these particular α4 HMWCs escaped detection until now, even though the α4–α4 crosslinking approach was used before (Kusmierczyk et al., 2008; Velichutina et al., 2004). First, the previous studies were interested in detecting α4–α4 proteasomes, specifically the characteristic α4-α4 dimers. Their analysis was not optimized to detect HMWCs, which likely failed to enter the resolving gel. Here, using a lower percentage step gradient gel, we were able to detect these HMWCs (Figure 1B) which just barely entered the resolving gel. Second, the HMWCs may not be as stable as CP, especially when analyzed by native PAGE; the presence of crosslinkable α4 was needed to clearly visualize them (Figure 2.3 and Appendix A, Supplementary Figure 8; see also Supplementary Note). Finally, these HMWCs are comparable in size to known CP intermediates (such as 13S, 15S, and half-proteasome species) and can thus be obscured by them. The excess of spectral counts for α4-derived peptides was consistent with this (Figure 2.2B) and our depletion experiments (Figure 2.3) confirmed it. We suggest increased vigilance in interpreting native PAGE data for proteasome assembly.

The purpose of these α4 HMWCs remains to be determined. Recently α4-GFP was found localized into puncta in the absence of Pba3-Pba4 chaperone (Takagi et al., 2014). It is not clear if these “aggregates” of α4 are related to the α4 HMWCs observed here, but we note that HMWCs are already observed in wild type yeast cells. The observation that levels of HMWCs can increase, such as when α3 is deleted, suggests their levels could be regulated. This regulation might involve Ssa1/Ssa2 proteins, which associate tightly with HMWCs, surviving the extended depletion protocol.

Our data are consistent with HMWCs having a physiological role, though we cannot yet rule out the possibility that these are misassembled products destined for removal by the protein quality control machinery. However, the recent study which identified α4-α4 proteasomes in mammalian cells, using the same crosslinking approach as here, also acknowledged higher molecular weight species containing α4 *in vivo* (Padmanabhan et al., 2016). Though these species were not studied further, we note with interest their observation of an α4 laddering pattern (for example, Figure 2.2E in reference (Padmanabhan et al., 2016)) similar to what we

observed here (Figure 2.4B). This raises the possibility that the formation of α4 HMWCs, like the formation of α4-α4 proteasomes, is evolutionarily conserved.

CHAPTER 3. SSA1/2 ASSIST IN 20S ASSEMBLY

Chapter 3 along with Appendix B were originally published in Biochemical and Biophysical Research Communications (BBRC).

Hammack, L. J., Firestone, K., Chang, W., & Kusmierczyk, A. R. (2017). Molecular chaperones of the Hsp70 family assist in the assembly of 20S proteasomes. *Biochem Biophys Res Commun, 486*(2), 438-443. doi:10.1016/j.bbrc.2017.03.059

3.1 Abstract

The eukaryotic 26S proteasome is a large protease comprised of two major sub assemblies, the 20S proteasome, or core particle (CP), and the 19S regulatory particle (RP). Assembly of the CP and RP is assisted by an expanding list of dedicated assembly factors. For the CP, this includes Ump1 and the heterodimeric Pba1-Pba2 and Pba3-Pba4 proteins. It is not known how many additional proteins that assist in proteasome biogenesis remain to be discovered. Here, we demonstrate that two members of the Hsp70 family in yeast, Ssa1 and Ssa2, are bona fide CP assembly factors. Ssa1 and Ssa2 interact genetically and physically with proteasomal components. Specifically, they associate tightly with known CP assembly intermediates, but not with fully assembled CP, through an extensive purification protocol. And, in yeast lacking both Ssa1 and Ssa2, specific defects in CP assembly are observed.

3.2 Introduction

Protein quality control in eukaryotes is maintained via several evolutionarily conserved machineries, including the ubiquitin-proteasome system (UPS) and the molecular chaperone network (MCN) (Amm, Sommer, & Wolf, 2014; reference; Tomko & Hochstrasser, 2013). The former provides a major route of protein degradation, removing damaged, misfolded, and no-longer-needed proteins. The latter assists in proteins attaining their native state following synthesis, and in returning misfolded proteins to the native state following stress. How the UPS and MCN interact is a topic of considerable interest.

The MCN is comprised of a number of highly conserved protein families, many of which are nucleotide-driven machines. Perhaps the best studied of these include members of the Hsp60, Hsp70, and Hsp90 protein families (Houry, 2014). One way in which the MCN can interact with

the UPS is via proteins destined for degradation (Shiber & Ravid, 2014). However, MCN proteins could also function in the biogenesis of the UPS components themselves, such as the 2.5 MDa proteasome, yet this role remains underexplored.

The 26S proteasome is an intricate assembly of 33 distinct proteins in multiple copies (X. Huang, Luan, Wu, & Shi, 2016a; Luan et al., 2016). It can be subdivided into two major sub-assemblies, the 19S regulatory particle (RP) and the 20S core particle (CP), also known as the 20S proteasome. The CP consists of four heptameric rings stacked on top of each other. Seven distinct α subunits (α1 to α7) make up each outermost ring and seven distinct β subunits (β1 to β7) make up the two inner rings (Groll et al., 1997). Proteolytic activity resides in the β1, β2 and β5 subunits which are synthesized as proproteins (Arendt & Hochstrasser, 1999; Chen & Hochstrasser, 1996). CP assembly begins with the formation of an α ring which becomes a platform for the incorporation of β subunits (Hirano et al., 2008; Zwickl et al., 1994). Addition of β subunits occurs in stages defined by a number of intermediates: the 13S intermediate (which includes β2, β3, and β4); the 15S intermediate (which includes all β subunits except β7); and the half-proteasome (which contains a completed β ring) (Hirano et al., 2008; X. Li et al., 2007; Marques et al., 2007). Two half-proteasomes dimerize to produce the preholoproteasome (PHP), a fleeting species that looks like a CP but whose β subunits retain their propeptides (X. Li et al., 2007). As the β subunits undergo autocatalytic processing to reveal their N-terminal threonine nucleophiles, the PHP matures into the fully functional CP.

CP assembly is regulated by features intrinsic to the subunits themselves and by extrinsic factors in the form of dedicated assembly chaperones. The latter include Ump1, Pba1-Pba2, and Pba3-Pba4 (also known as hUmp1, PAC1-PAC2, PAC3-PAC4 in mammals) (Tomko & Hochstrasser, 2013). Whether any additional proteins participate in CP assembly remains an open question. Using the yeast *Saccharomyces cerevisiae* as a model system, we demonstrate that members of the Hsp70 family, specifically Ssa1 and Ssa2, are directly involved in CP biogenesis.

3.3 Materials and Methods

3.3.1 Yeast Strains and Plasmids

Yeast strains used are listed in Appendix B, Supplementary Table 2. Plasmids used are listed in Appendix B Supplementary Table 3. All yeast manipulations were carried out according to established protocols (C. Guthrie, 1991). Dilution series were carried out as described (Kusmierczyk et al., 2008). Yeast strain numbers (AKY) are shown in brackets.

3.3.2 Protein Purification

The lysis of yeast pellets and subsequent Flag purification was carried out as described (Hammack & Kusmierczyk, 2017) except equal amounts of soluble lysate were bound to 150 µl of anti-Flag agarose for 3 hours then eluted. For each sample, the 300 µl Flag eluate was divided as follows: 100 µl aliquot for native PAGE; 50 µl aliquot for SDS-PAGE; and the remaining Flag eluate (150 µl) was subjected to depletion via immobilized-cobalt affinity resin (ICAR). Depletion was carried out as described (Hammack & Kusmierczyk, 2017) with the following modifications. The samples were applied to 50 µl of cobalt resin (TALON resin; Clontech) for 1h at 4 C with gentle rocking. The flow through from the first round of ICAR depletion was subjected to a second round of ICAR depletion using a fresh 50 µl aliquot of resin. The flow through from the second round of ICAR depletion was split into a 100 µl aliquot for native PAGE and a 50 µl aliquot for SDS-PAGE. The Flag eluate and the second ICAR flow through were analyzed via native PAGE (40 µl), and loading controls were analyzed by reducing SDS-PAGE (15 µl).

3.3.3 Electrophoresis and Blotting

SDS-PAGE, on 12% gels, and native PAGE, on 4–15% Mini-PROTEAN TGX precast gradient gels (Bio-Rad) were carried out as described except native gels were electrophoresed for 11 hours (Hammack & Kusmierczyk, 2017). Native gels were stained with Imperial Protein Stain (ThermoScientific) and SDS-PAGE gels were stained with GelCode blue (ThermoScientific). Prior to staining, some native gels were subjected to substrate overlay assay carried out as described (Kusmierczyk et al., 2011). The migration of size standards is indicated

to the left of each gel. Western blotting was carried out as described (Hammack & Kusmierczyk, 2017) using anti-Express antibodies (Invitrogen).

3.3.4 Proteomic Analysis

Gel slices were submitted to the Indiana University School of Medicine Proteomics Core Facility (IUSM-PCF) on a fee-for-service basis. Protein contents of the gel slices were identified by LC-MS/MS as described (L. J. Hammack & A. R. Kusmierczyk, 2016). Summarized and annotated data is presented in the main text and Appendix B. Data discussed in the main text refers only to proteins that were identified on the basis of more than one unique peptide in order to decrease the likelihood of false-positives (Carr et al., 2004). The original data provided by the core facility (Excel files) is provided in supplementary information in Appendix B.

3.4 Results

Our initial interests lay in determining whether additional extrinsic factors existed that assisted in proteasome biogenesis. We focused our search on the CP and employed a depletion scheme (Hammack & Kusmierczyk, 2017) to enrich for CP assembly intermediates. We generated a series of yeast strains: “WT”; “PHP”; and “2/3-PHP” (Appendix B Supplementary Figure 11). The PHP strain is the key experimental strain and should allow the isolation of CP assembly intermediates up until, and including, the preholoproteasome (PHP). The PHP strain expresses all three mutant β subunits β1(T1A), β2(T1A), and β5(T1A), as well as a wild type β5 to keep the strain alive (Chen & Hochstrasser, 1996). The 2/3-PHP strain expresses two mutant β subunits, β1(T1A) and β2(T1A).

We prepared soluble lysates from cultures of all three strains, isolated CP species via the Flag epitope on β4, and analyzed the purified material by native and SDS-PAGE (Figures 3.1A,B lanes 1 to 3). We’ve reported the need to overload native gels to visualize assembly intermediates (Hammack & Kusmierczyk, 2017) and did so again here. CP was the major species in each sample, migrating near the 670 kDa size standard (Figure 3.1) and Appendix B, Supplementary Figure 12). Species migrating slower than CP were Blm10-bound CP (Lehmann et al., 2008). More Blm10-bound species were present in the 2/3-PHP sample (Figures 1A,B asterisk). Species migrating faster than CP were likely assembly intermediates (Figure 3.1A, lanes 1 to 3, bands 1 and 2).

Next, the hexahistidine tag on the β5 subunit (β5-his) enabled a depletion strategy to remove CP via sequential passage of Flag-purified material over two immobilized-cobalt affinity resin (ICAR) columns (Hammack & Kusmierczyk, 2017). Aliquots of the second flow-through were analyzed by native and SDS-PAGE (Figures 3.1A,B lanes 4 to 6). A number of observations were made. First, in the WT and 2/3-PHP samples, the CP band was almost completely absent suggesting that the depletion strategy was effective. A small amount of CP remained, as judged by a faint residual CP band and weakly detectable activity on the overlay assay (Appendix B, Supplementary Figure 12). However, additional rounds of ICAR depletion

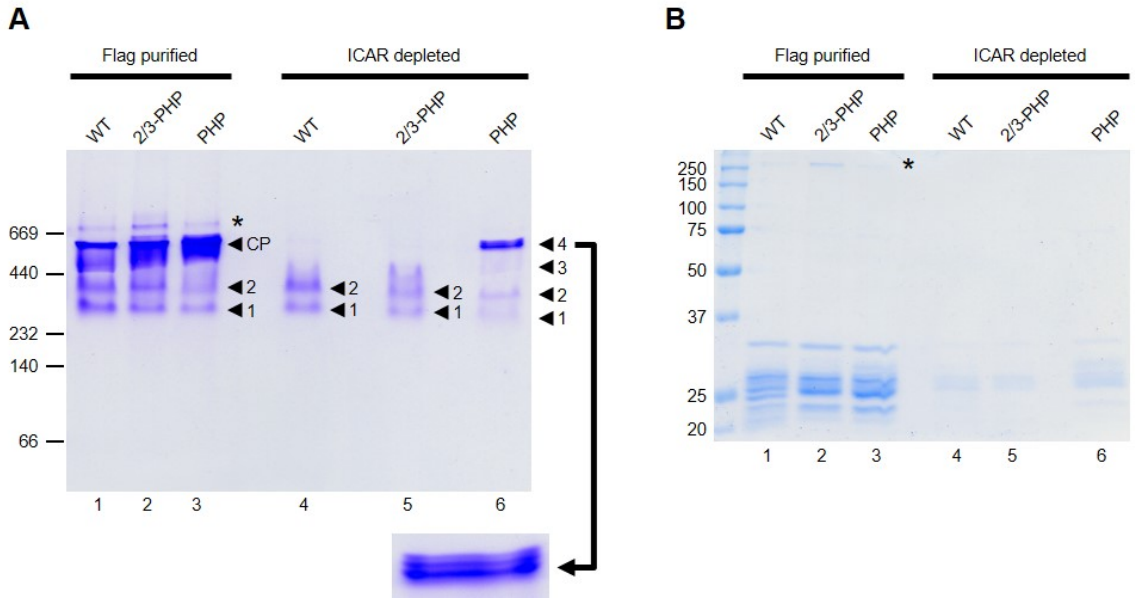

Figure 3.1 Depletion analysis to isolate CP assembly intermediates
(A) Native PAGE analysis of Flag-purified CP (β4-Flag) from the indicated yeast strains (lanes 1 to 3). The Flag-purified material was subjected to two rounds of depletion by ICAR to remove his-tagged proteins. Aliquots of the flow through from the second ICAR round were analyzed on the same native PAGE gel (lanes 4 to 6). Arrowheads denote CP and other bands of interest. Asterisk denotes position of Blm10-bound CP. (B) Aliquots in (A) analyzed by SDS-PAGE; asterisk denotes position of Blm10.

did not reduce this residual CP band further and only decreased the overall yield of protein (not shown); we suggest that the residual CP may be due to some β5 subunits losing their his-tag to proteolysis post-lysis. Second, the pair of putative assembly intermediates (bands 1 and 2) was still present following depletion. Finally, the PHP sample retained a considerable band migrating at the position of the CP (band 4). Given that β5(T1A) was not his-tagged, this suggested we

were able to isolate the PHP. A fainter band migrating below the putative PHP was also observed (band 3).

Table 3.1 Select composition of excised bands

	PHP				2/3-PHP		WT	
	4	3	2	1	2	1	2	1
α1	328	66	95	109	112	134	201	195
α2	124	28	39	36	58	60	72	78
α3	170	42	57	59	85	74	110	104
α4	223	35	72	98	92	131	558	314
α5	124	20	26	8	34	13	64	15
α6	222	40	54	6	56	12	132	5
α7	85	21	37	67	50	19	74	11
β1	109	13	4					5
β2	157	42	49	58	75	94	99	125
β3	62	24	31	37	44	54	57	51
β4	53	17	20	26	33	35	36	39
β5	253	47	6	6	5		7	6
β6	209	28						
β7	277	74	10					
Ump1	80	5	7	30	36	31	34	54
Pba1	78	19	25	7	34	9	114	9
Pba2	38	4	11		17		44	
Ssa1/2		6	63	29	56	16	40	11

Bands 1 to 4 were excised and analyzed by LC-MS/MS (Appendix B, Supplementary Figures 13 to 20). Band 4 was actually a series of three closely spaced bands (Figure 3.1A, enlarged). It was not possible cut these bands apart, thus the analysis of band 4 reflects material from all three bands. Band 4 contained all α and β subunits, as well as the assembly factors Ump1 and Pba1-Pba2 (Table 1). We also recovered peptides from the β5 propeptide (Figure 3.1C). This composition is consistent with band 4 containing PHP. Interestingly, band 4 exhibited some catalytic activity (Appendix B, Supplementary Figure 12) but the resolution was not sufficient to determine which of the three bands was active. Consequently, band 4 must also contain some species with wild type β5. We offer a plausible explanation for the three bands in Supplementary Figure 21 (Appendix B). Band 3 had identical composition to band 4 (Table 3.1), including peptides from the β5 propeptide (not shown) but it displayed no activity (Appendix B, Supplementary Figure 12). Band 3 likely represents a half-proteasome.

Band 2 migrated similarly across all three samples, as did band 1, suggesting two identical species were present. Indeed, band 2 from each sample returned considerable peptide

spectral matches (PSMs) from all α subunits plus β2, β3, β4 and the assembly factors Ump1 and Pba1-Pba2 (Table 3.1). Some peptides for other β subunits were also recovered. However, these were either not uniformly present in all bands, or were present in considerably lower PSMs, suggesting they were not stoichiometric components of band 2 which most likely contained the 13S intermediate. Band 1 was similar to band 2 except that we observed comparatively fewer PSMs for α5 and α6 in all three samples, and fewer PSMs for α7 in the 2/3-PHP and WT samples (Table 3.1). As above, this suggests that these subunits may not be stoichiometric components of the complex in band 1. Furthermore, we recovered no peptides for Pba2. We conclude that band 1 likely contains a species we refer to as "sub-13S" (i.e. a 13S intermediate lacking Pba2, α5, α6, and probably α7).

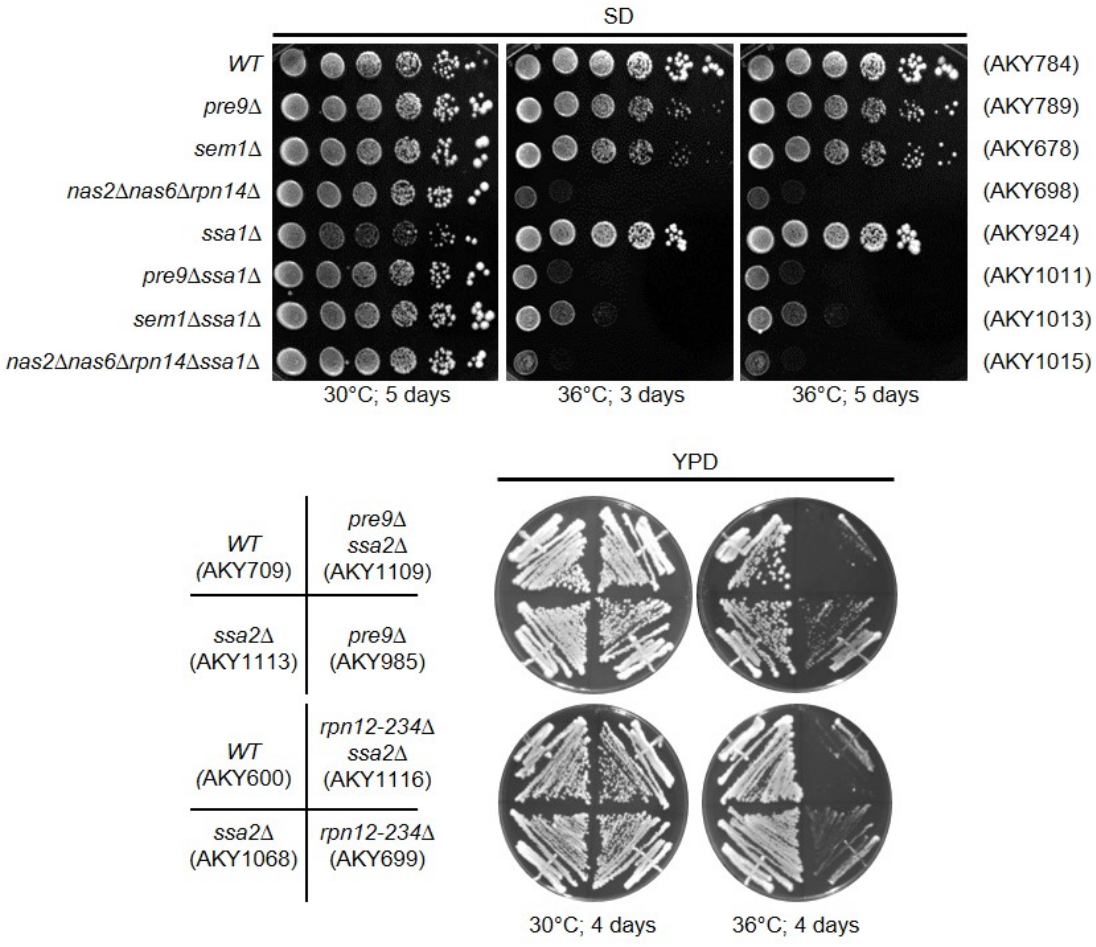

Figure 3.2 Phenotype analysis of *ssa* mutants
Dilution series were prepared and the yeast spotted onto SD plates (top). Alternatively, yeast from individual colonies were struck out onto YPD plates (bottom). The temperature and duration of plate incubation are indicated.

Each of the bands analyzed gave rise to peptides from a number of additional proteins (Appendix B, Supplementary Tables 13 to 20). Most of these were not likely candidates for assembly factors because they were recovered with only a few peptides, and/or were derived from highly abundant metabolic enzymes (e.g. Eno2, Pfk26, Adh1) which are likely contaminants. However, two proteins from the Hsp70 family, Ssa1 and Ssa2, emerged as possible candidates. We shall refer to these proteins as Ssa1/2 because they share 97% amino acid identity, making it difficult to definitively assign all observed peptides to either isoform. Ssa1/2 were identified with considerable PSMs in bands 1 and 2 from all three strains, but not in the more highly abundant band 4, arguing that they were not just non-specifically binding to CP subunits.

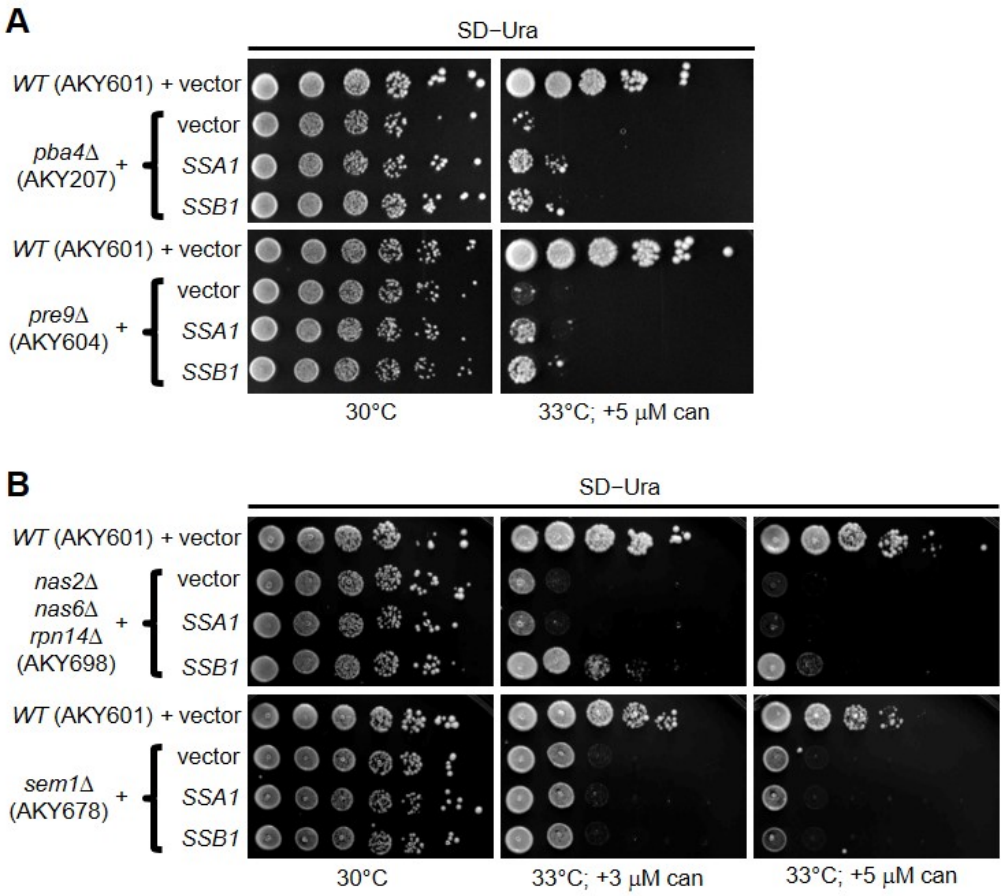

Figure 3.3 Suppressor analysis
Dilution series of CP mutants (A), and RP mutants (B), transformed with Hsp70-containing plasmids, or vector-only controls. Plates were incubated for 3 days.

Physical association of Hsp70 proteins with proteasomes has been observed (Gong et al., 2009; Guerrero et al., 2008; Verma et al., 2000) But these high-throughput studies only considered chaperone binding to intact proteasomes (see also Appendix B, Supplementary Notes). To strengthen the case for a role in assembly, we first carried out a series of genetic experiments. When yeast were grown at 36º C (Figure 3.2), we observed synthetic sick interactions between deletion of *SSA1*, or *SSA2*, and proteasome mutants that affect assembly of CP (*pre9*Δ) and the lid subcomplex of the RP (*sem1*Δ or *rpn12-234*Δ) (Funakoshi, Li, Velichutina, Hochstrasser, & Kobayashi, 2004; Kusmierczyk et al., 2008; Tomko & Hochstrasser, 2011) . This was not due to a general decrease in cytoplasmic Hsp70 activity because no effects were observed when another Hsp70 gene, *SSB1*, was deleted (Appendix B, Supplementary Figure 22A). No obvious synthetic sick interaction was seen with a mutant affecting assembly of the base subcomplex of the RP (*nas2*Δ*nas6*Δ*rpn14*Δ) (Funakoshi et al., 2009). However, this mutant already grows quite weakly at 36º C (Figure 3.2A); repeating the experiment at 33 º C, we instead observed a slight suppression when *SSA1* was deleted (Appendix B, Supplementary Figure 22B).

Overexpression of Ssa1 suppressed growth defects of CP, but not RP, assembly mutants in the presence of the amino acid analog canavanine (Figure 3.3 and Appendix B, Supplementary Notes). This suppression differed from that observed with overexpression of Ssb1, a known suppressor of CP mutants (Ohba, 1997). Here, Ssb1 suppressed both CP and RP base defects. Western blots verified that protein was expressed (Supplementary Figure 22C and not shown). Taken together, the genetic results bolster the link between Ssa1/2 and CP assembly.

If Ssa1/2 proteins have a direct role in CP assembly, one should observe assembly defects biochemically if these proteins are absent. Since Ssa1 and Ssa2 likely have a redundant role in CP assembly (see Discussion), we looked for assembly defects in an *ssa1*Δ*ssa2*Δ strain. We purified proteasomes from wild type and mutant strains, via a Flag-tag on α4, and analyzed them by native PAGE (Figure 3.4A). CP was again the major species and two faster migrating bands were observed in the WT sample; they were easier to visualize when the gel was overloaded (Figure 3.4B). We excised the indicated bands and analyzed them by LC-MS/MS. Because this experiment did not involve a depletion, bands 5 and 6 each likely contained a mixture of assembly intermediates (see Discussion). Nevertheless, the relevant result is that considerable PSMs were observed for Ssa1/2 in bands 5 and 6 but none in bands 7 and 8, corresponding to

fully assembled CP (Supplementary Figures 23 to 26). This is consistent with our previous results showing Ssa1/2 associating with assembly intermediates (Figure 3.1). Most importantly, bands 5 and 6 were greatly reduced in the *ssa1*Δ*ssa2*Δ mutant.

We also observed what appeared to be more doubly-Blm10 capped CP in the *ssa1*Δ*ssa2*Δ mutant (Figure 3.4B asterisk). Blm10 plays an undefined role in CP maturation and increased binding of Blm10 to CP can indicate a maturation defect (Marques et al., 2007). Consistent with this, we recovered peptides derived from the β2 propeptide from CP in the *ssa1*Δ*ssa2*Δ strain (band 8) but not CP in the wild type strain (band 7). The lack of β2

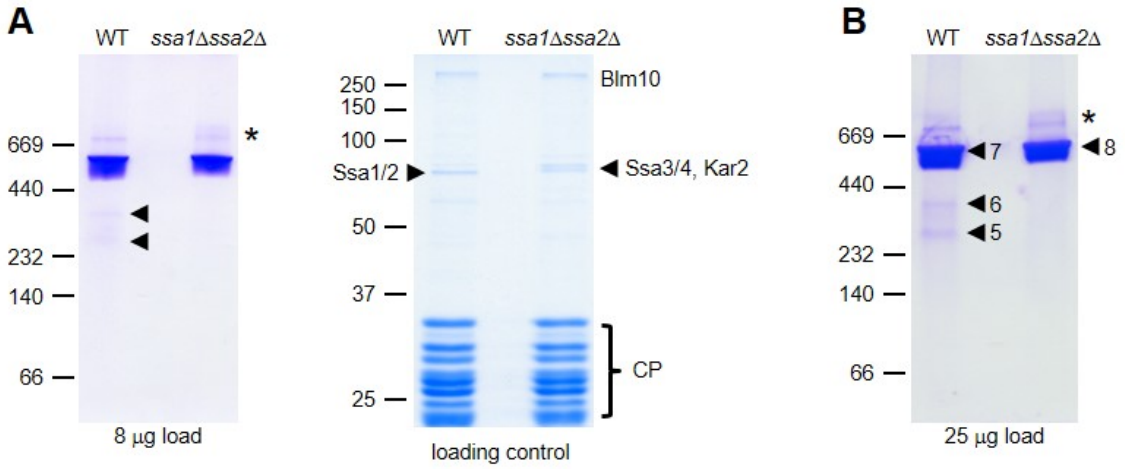

Figure 3.4 Assembly defects in a mutant lacking Ssa1 and Ssa2
(A) Equal amounts (8 µg) of Flag-purified CP material (α4-Flag) from the indicated yeast strains were analyzed by native PAGE (left). An SDS-PAGE loading control is also shown (right). (B) Same native PAGE analysis as in (A) except a larger amount of protein (25 µg) was loaded. In all gels, arrowheads denote bands of interest. Asterisk denotes migration of Blm10-bound CP (singly and doubly capped).

propeptide-derived peptides in band 7 was not due to a detection sensitivity issue; we readily recovered β2 propeptide-derived peptides from bands 5 and 6 (as expected for CP assembly intermediates) despite these two bands being much less abundant than band 7 (Appendix B Supplementary Figure 27).

Finally, the Ssa1/2 band observed by SDS-PAGE in the purified material from the wild type strain (Figure 3.4A) was replaced by a slightly slower migrating doublet in the *ssa1*Δ*ssa2*Δ mutant. LC-MS/MS analysis identified this doublet as containing Ssa3, Ssa4 and Kar2 (not shown but see Appendix B, Supplementary Notes).

3.5 Discussion

We present evidence that Ssa1/2 proteins function as CP assembly factors. First, these chaperones associate with assembly intermediates in purifications from four independent yeast strains utilizing two different Flag-tagged CP subunits (Table 3.1 and Figure 3.4B). Depletion analysis confirms association with the 13S intermediate, and a novel species we refer to as sub-13S, though Ssa1/2 likely associate with intermediates up to the half-proteasome (Appendix B, Supplementary Figures 3-5, 13, 14). Second, the physical association of Ssa1/2 with CP intermediates is corroborated by genetic association between *SSA* mutants and proteasome assembly mutants. Moreover, phenotypic suppression often indicates physical interaction, and the suppression by *SSA1* of CP (but not RP) assembly mutants is entirely consistent with a physical role for this chaperone in CP biogenesis. Third, our depletion strategy involves multiple purification steps with extensive washing. The ability of Ssa1/2 to remain bound to CP assembly intermediates throughout our depletion protocol, and their absence from bands corresponding to the PHP and fully assembled CP (Table 3.1, Appendix B, Supplementary Figures 15, 16), argues that they dissociate prior to completion of assembly; this is the very definition of an assembly factor. Finally, strains lacking Ssa1/2 have greatly reduced levels of assembly intermediates and likely exhibit a weak defect in β2 propeptide processing (Figure 3.4). Two previous observations are consistent with our findings. First, upregulation of *RPN4*, encoding the transcription factor that regulates expression of proteasome subunits (Xie & Varshavsky, 2001), has been observed in an *ssa1*Δ*ssa2*Δ double mutant (Matsumoto, Akama, Rakwal, & Iwahashi, 2005). A greater need for proteasomes would be expected if assembly is impacted by a loss of Ssa1/2. Second, the *rpn4*Δ*ssa1*Δ*ssa2*Δ triple mutant grows worse than the *ssa1*Δ*ssa2*Δ double mutant (Oling, Eisele, Kvint, & Nystrom, 2014). This is reminiscent of the synthetic sick (or lethal) phenotypes that result when deletion of *RPN4* is combined with a deletion of any CP assembly factor (Le Tallec et al., 2007).

The precise role of Ssa1/2 in CP assembly remains to be determined. They may help stabilize assembly intermediates. For instance, the 13S intermediate contains a full α-ring and three out of seven β subunits (β2, β3, β4). Recently we reported that Ssa1/2 bind to high molecular weight complexes of α4 in vivo, which are most likely rings (Hammack & Kusmierczyk, 2017). Thus, perhaps Ssa1/2 chaperone the formation of α subunit rings, or

stabilize them once formed. Also, Ssa1/2 appear to be involved in the formation (or stabilization) of a novel complex we call the sub-13S species. This complex probably contains a subset of α and β subunits (most likely α1–α4, and β2–β4) but whether or not it is a true assembly intermediate remains to be determined. On the one hand, it could be the result of a 13S intermediate falling apart during purification and/or electrophoresis. On the other hand, it could be a precursor to the 13S intermediate, suggesting the existence of an assembly pathway that does not involve an isolated α ring. We've demonstrated such α ring independent pathways for archaeal proteasomes, which serve as models for eukaryotic proteasome assembly (Panfair et al., 2015).

Regardless of the status of the sub-13S species, it is likely that CP assembly has multiple redundancies built in. There is the obvious redundancy between Ssa1 and Ssa2, as evidenced by the recovery of peptides for both Ssa1 and Ssa2 from assembly intermediates and by the similar synthetic phenotypes observed when deletion of either *SSA1* or *SSA2* is combined with assembly mutants. Consistent with this redundancy, whereas the *rpn4*Δ*ssa1*Δ*ssa2*Δ triple mutant grows worse than the *ssa1*Δ*ssa2*Δ double mutant (Oling et al., 2014), we observe no obvious phenotypes when *rpn4*Δ is combined with only *ssa1*Δ or *ssa2*Δ (Appendix B Supplementary Figure 22D). Redundancy is also seen in the *ssa1*Δ*ssa2*Δ mutant where levels of assembly intermediates (bands 5 and 6) are reduced but the overall levels of CP are not. Clearly, the subunits are still capable of coming together to form CP species, even if a small fraction of them has incompletely matured β2 subunits. Taking a broader view, the simple observation that none of the CP or RP assembly factor genes are essential (Tomko & Hochstrasser, 2013) is strongly suggestive of assembly redundancy.

Although our purification/depletion analysis did not identify additional candidates beyond Ssa1/2, the stringency of our method means that weakly/transiently bound assembly factors could have been washed away. The existence of redundancy in assembly, which implies multiple assembly pathways, makes it more likely that additional factors assisting proteasome assembly await discovery. That some of these are likely to be members of the MCN now has considerable precedent, given our results here and the proposed, though incompletely understood, role of Hsp90 in proteasome biogenesis (Imai, Maruya, Yashiroda, Yahara, & Tanaka, 2003).

CHAPTER 4. NOVEL COMPLEX: SUB-13S

4.1 Abstract

Efficient assembly of proteasomes is required for cellular homeostasis. Proteasome assembly is regarded as a regulated stepwise process. In eukaryotes, a number of assembly chaperones and assembly intermediates have been identified. The accepted model of eukaryotic proteasome biogenesis depicts a linear pathway that begins with the formation of an α ring which serves as a scaffold for the subsequent entry of β subunits. The β subunits bind in the following order β2, β3, β4, β5, β6, β1, and β7. In yeast, the earliest intermediate that can be stably isolated is the 13S, which consists of a full α ring, plus β2, β3, and β4. Here, we report evidence for an earlier intermediate we call sub-13S, consisting of α1, α2, α3, α4, β2, β3, and β4. We propose that this intermediate originates from another assembly pathway, an α ring independent pathway, that functions alongside the canonical α ring dependent pathway. Evidence of this intermediate suggests eukaryotic proteasome biogenesis can initiate through α/β subunits interactions.

4.2 Introduction

Maintaining protein homeostasis is important for maintaining proper cellular function. In eukaryotes several mechanisms contribute to homeostasis. One such mechanism is the ubiquitin-proteasome system. In this system, proteins are tagged with a modifier protein, ubiquitin, and subsequently degraded by the 26S proteasome. The 26S proteasome is comprised of two major assemblies, the 19S regulatory particle (RP) and the 20S core particle (CP). The 19S RP is made up of ~19 subunits that form two sub-complexes: the base and the lid. This structure recognizes, deubiquitinates, unfolds, and feeds substrates into the 20S CP. The 20S CP is the protease of the 26S proteasome and is comprised of seven unique α and β subunits that assemble into four stacked heptameric rings ($\alpha_{1\text{-}7}\beta_{1\text{-}7}\beta_{1\text{-}7}\alpha_{1\text{-}7}$) (Groll et al., 1997). β subunits, β1, β2, and β5, are catalytically active, and their catalytic activity is sequestered within the central hollow chamber formed by the stacked rings (Groll et al., 1997).

Many reports have described proteasome assembly as a linear pathway way containing proteasome assembly chaperones and specific intermediates (Funakoshi et al., 2009; Hirano et al., 2005; Kusmierczyk et al., 2008; Kusmierczyk et al., 2011; Le Tallec et al., 2007; Le Tallec et al., 2009; X. Li et al., 2007; Roelofs et al., 2009; Saeki et al., 2009; Yashiroda et al., 2008). The canonical pathway is considered to be an α ring dependent pathway, meaning α ring formation is required for assembly to begin (Hirano et al., 2005). While α subunits and β subunits share similar tertiary structures (Lowe et al., 1995), only α subunits independently form rings. This feature is due, in part, to a conserved α-helix (H0) in α subunits, which allows them to form stable rings, whereas β subunits lack an H0 helix and do not form stable rings on their own (Zwickl et al., 1994).

After α ring formation, the assembly process proceeds as follows. β2, β3 and β4 bind the α ring creating a 13S intermediate (Hirano et al., 2008). Next, β1, β5, and β6 assemble forming a 15S intermediate (X. Li et al., 2007; Nandi et al., 1997). Entry of the last β subunit, β7, results in a half-proteasome, which contains one full α ring and one full β ring (Hirano et al., 2008; X. Li et al., 2007). Two half-proteasomes dimerize creating the pre-holoproteasome intermediate (X. Li et al., 2007). Although this intermediate looks like the 20S CP, it is catalytically dead, due to the propeptides synthesized on β1, β2, and β5. These propeptides protect the N-terminal nucleophile threonine from being acetylated prior to assembly, which would render it inactive (Arendt & Hochstrasser, 1997; Groll et al., 1999; Jager et al., 1999). During maturation, the propeptides are autocatalytically cleaved forming the fully functional 20S CP. Several proteins have been described in assisting proteasome assembly: Pba1-Pba2, Pba3-Pba4, Ump1, and possibly Blm10 (Howell et al., 2017). Recently, we added Ssa1/2 to this growing list of assembly factors (see Chapter 3; Hammack et al. 2017). Assembly factors most likely function by preventing off-pathway interactions and promoting on-pathway interactions. While deletion of chaperone proteins results in assembly defects in yeast it does not cause lethality.

The 20S CP is conserved throughout archaea and a few bacterial lineages (De Mot et al., 1999; De Mot et al., 2007). While the overall structure and function is conserved, the archaeal and bacterial 20S CPs are far less complex than the eukaryotic 20S CPs. These proteasomes consist generally of one to two α and β type subunits (Tamura et al., 1995; Zwickl et al., 1992). Archaeal and eukaryotic proteasomes were originally thought to assemble through an α ring

dependent pathway (Groll et al., 2003; Hirano et al., 2005; Zwickl et al., 1994). By contrast, assembly of bacterial 20S CP was considered to be α ring independent, since assembly initiates through α/β subunit interactions, possibly α/β dimers (Sharon et al., 2007; Zuhl et al., 1997). Interestingly, an alternate assembly pathway was recently described for archaeal 20S CP (Panfair et al., 2015). This pathway initiates through the interaction of α and β subunits, which is reminiscent of the assembly pathway observed in bacteria.

It is widely accepted that eukaryotic proteasomes readily form through the canonical assembly pathway described above. In a previous report we identified a novel species migrating faster than the 13S by native PAGE, which we referred to as sub-13S. This species lacked a full α ring, contained β subunits, and Hsp70 proteins Ssa1/2 (Hammack et al., 2017). Here, we investigate this species as a potential 20S assembly intermediate. Since this species lacks a full α ring, it does not fit within the current model for eukaryotic assembly. We propose this species is an assembly intermediate within an α ring independent assembly pathway, that works in parallel with the canonical, α ring dependent, pathway to assemble proteasomes.

4.3 Materials and Methods

4.3.1 Yeast Strains and Manipulations

Yeast strain used are listed in Supplementary Table 4 in Appendix C. Yeast growth conditions and manipulations were carried out according to established protocols (C. Guthrie, 1991). Dilution series, purifications, depletions and electrophoresis were carried out as previously described (Hammack & Kusmierczyk, 2017; Kusmierczyk et al., 2008).

4.4 Results

A widely accepted method to study proteasome assembly involves tagging a 20S CP subunit with a given epitope (frequently Flag), using it to purify proteasomes, and analyzing the purified material via native PAGE. Species migrating faster than the 20S CP are considered assembly intermediates. This strategy has been used to identify the 13S, 15S, and half-proteasome intermediates (Frentzel, Pesold-Hurt, Seelig, & Kloetzel, 1994; Hirano et al., 2008; X. Li et al., 2007; Nandi et al., 1997; Schmidtke, Schmidt, & Kloetzel, 1997). We chose to use Flag and hexahistidine-Flag (HF) tagged α2, α4, α5, and β4 subunits in our analyses. Of course,

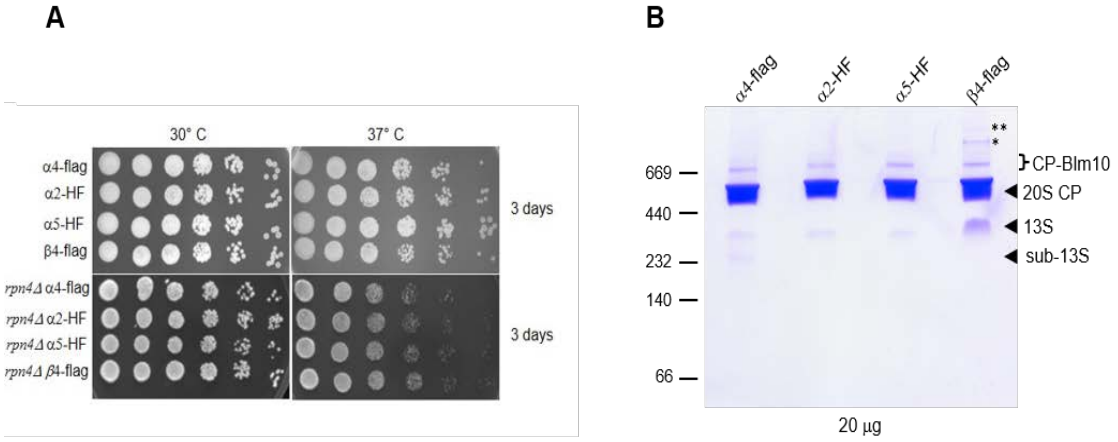

Figure 4.1 Analysis of yeast strains tagged with different subunits
(A) Dilution series of strains analyzed by native PAGE at 30° C and 37° C.
(B) Proteasomes were Flag purified using different 20S CP subunits. Equal amounts of Flag purification were analyzed by native PAGE. Species indicated are based on relative molecular weight, previous mass spectrometry analysis. Unique species (* and **) along with the other intermediate bands have been excised for mass spectrometry analysis to confirm identity. Loading control, activity assay, and another 30 µg loaded gel are in Appendix C (Supplementary Figures 28 and 29). (A) Dilution series of strains analyzed by native PAGE at 30° C and 37° C.

it is important that the tags themselves do not result in gross functional deficiencies. One way to test for a functional defect in yeast is to look for phenotypes, such as temperature sensitivity. To this end, we carried out dilution series of the indicated yeast strains (Figure 4.1A). While all the yeast strains examined grew slower under the heat stress (37 ° C), no distinguishable phenotypes were observed between α4-Flag, α2-HF, α5-HF, or β4-Flag strains (Figure 4.1A). We also tested for temperature sensitivity of strains in which the tagged subunit is combined with a deletion of the *RPN4* gene. Rpn4 is a transcription factor that regulates the levels of proteasomes in the cell through a negative feedback mechanism (Xie & Varshavsky, 2001). Therefore, one possibility for not observing temperature sensitivity in the tagged strains is that Rpn4 is able to compensate for the defects caused by the subunit tagging. When this compensation mechanism is removed, as in an *rpn4*Δ strain, even weaker perturbations in proteasome function can be revealed (Le Tallec et al., 2007). However, even in the context of an *RPN4* deletion, no growth defects were observed at 37 °C. This lack of a phenotype suggests that these tags on 20S CP subunits are not deleterious to function.

To examine 20S CP assembly in yeast, we purified proteasomes with tags on subunits α2, α4, α5, and β4, and subjected the purified material to native PAGE (Figure 4.1B). In each case,

the major species was the fully assembled 20S CP. Bands migrating immediately above the 20S CP are complexes of CP and Blm10 (Lehmann et al., 2008). Moreover, in the β4-flag purification we detected two high molecular weight bands migrating slower than the 20S-Blm10 species. Interestingly, at least one of these bands (*) has peptidase activity (Appendix C, Supplementary Figure 28). This band has been excised and will be sent off for mass spectrometry analysis to determine the protein composition. The two species migrating faster than the 20S CP in the α4-Flag sample were analyzed in a previous study (Hammack & Kusmierczyk, 2017). They were identified as the 13S intermediate and a novel species we termed the sub-13S (containing subunits α1-4 and β2-4). By contrast, the α2-HF, α5-HF, and β4-Flag stains all produced only a single species migrating faster than the 20S CP. As this species migrates at approximately the same position as the 13S intermediate in the α4-Flag sample, we presume it to be the 13S intermediate; we will confirm this by mass spectrometry analysis.

Lack of the sub-13S species in the α5-HF strain is understandable as the sub-13S species does not contain α5 and thus cannot be isolated from an α5-tagged strain. However, the sub-13S species does contain both α2 and β4, yet we do not observe sub-13S in purifications from these tagged strains. One possibility for this phenomenon is that tagging α4 with Flag, while not disruptive enough to function (as judged by the lack of phenotype in an α4-Flag *rpn4*Δ strain; Figure 4.1A), does perturb assembly sufficiently to allow novel putative assembly intermediates, such as the sub-13S, to accumulate. The simplest explanation, given the subunit composition of the sub-13S species (α1-α4 and β2-β4), argues that it is a precursor to the 13S, because it only lacks α5, α6, and α7. If this is the case, then disrupting the incorporation of one of these three missing α subunits should result in the accumulation of more sub-13S species in the α4-Flag strain. To this end, a yeast strain bearing a mutation in the *DOA5* gene, encoding the α5 subunit, was crossed into the α4-Flag strains. This α5 mutation causes an amino acid change from Gly to Asp at position 49 and is referred to as *doa5-1* (Chen & Hochstrasser, 1995). This Gly residue is normally buried within the hydrophobic core and its change to a charged Asp likely causes α5 to take longer to reach the native state. This, in turn, should slow the rate at which α5 can assemble into a nascent 20S CP. If the sub-13S species is an assembly intermediate and a precursor to the 13S intermediate, then slowing down the rate at which α5 incorporates (through the *doa5-1*

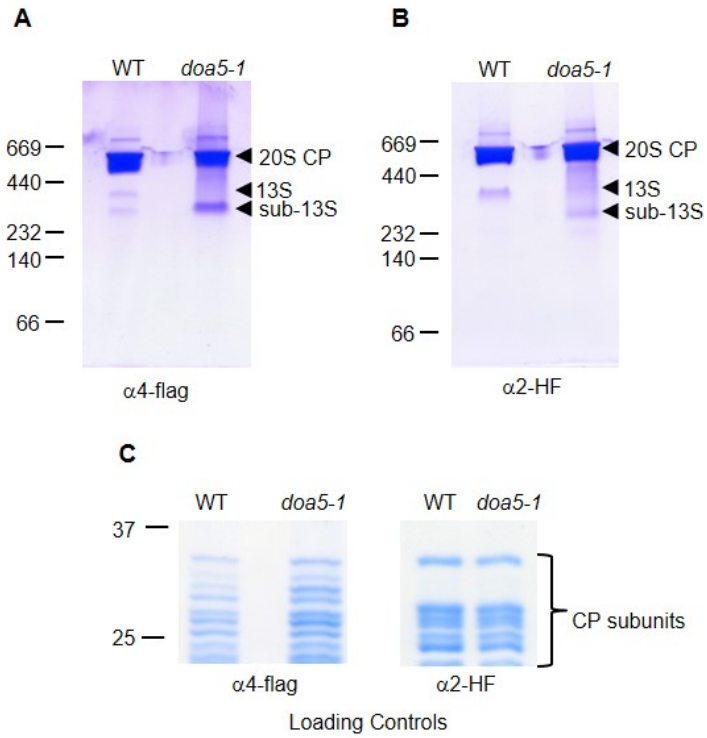

Figure 4.2 Induction of sub-13S with *doa5-1*
(A) Equal amounts (25 μg) of Flag purification (α4-Flag) were analyzed by native PAGE. Species of interest are indicated by arrow heads. (B) Equal amounts (25 μg) of Flag purification (α2-his-Flag (HF)) were analyzed by native PAGE. Species of interest are indicated by arrow heads. (C) 12% SDS-PAGE loading controls for native gels (A) and (B).

mutation) should result in the accumulation of more sub-13S species and a decrease in the 13S species. We purified proteasomes from α4-Flag and α4-Flag *doa5-1* strains and subjected them to native PAGE. As expected, the levels of 13S species decreased, while the amount of sub-13S species increased, in the presence of the *doa5-1* mutation (Figure 4.2A). The result is consistent with the sub-13S species being a precursor to the 13S intermediate, at least in the context of an α4-Flag strain. But what about the strains in which the sub-13S species is not observed?

As stated above, it is possible that the ability to observe the sub-13S species in the α4-Flag strain, but not in the α2-HF or β4-Flag strains, is due to assembly being perturbed enough in the α4-Flag strain to allow sub-13S to become visualized. If this is true, then we should be able to use the same genetic manipulation to slow down assembly in one of these two strains. The result should be that the sub-13S species would now become sufficiently populated and thus detectable. To this end, we introduced the *doa5-1* mutation into the α2-HF strain by crossing, purified 20S CP from the resulting α2-HF *doa5-1* progeny and α2-HF control, and analyzed the purified

material by native PAGE. While the α2-HF strain again failed to produce the sub-13S species, in the α2-HF *doa5-1* strain we observed a dramatic accumulation of a faster migrating species, likely the sub-13S species, and a drastic reduction in the amount of the 13S intermediate (Figure 4.2B). Again, to confirm the identities of these species, bands will be excised and their contents will be analyzed by mass spectrometry analysis. Nevertheless, the results with the α2-HF strain are entirely consistent with those observed in the α4-Flag strain, and argue that the sub-13S species is a precursor to the 13S intermediate.

Since the sub-13S looks like a 13S species lacking α5, α6, and α7, it could be argued that observing the sub-13S species is a gel artifact. The argument would be that the 13S intermediate

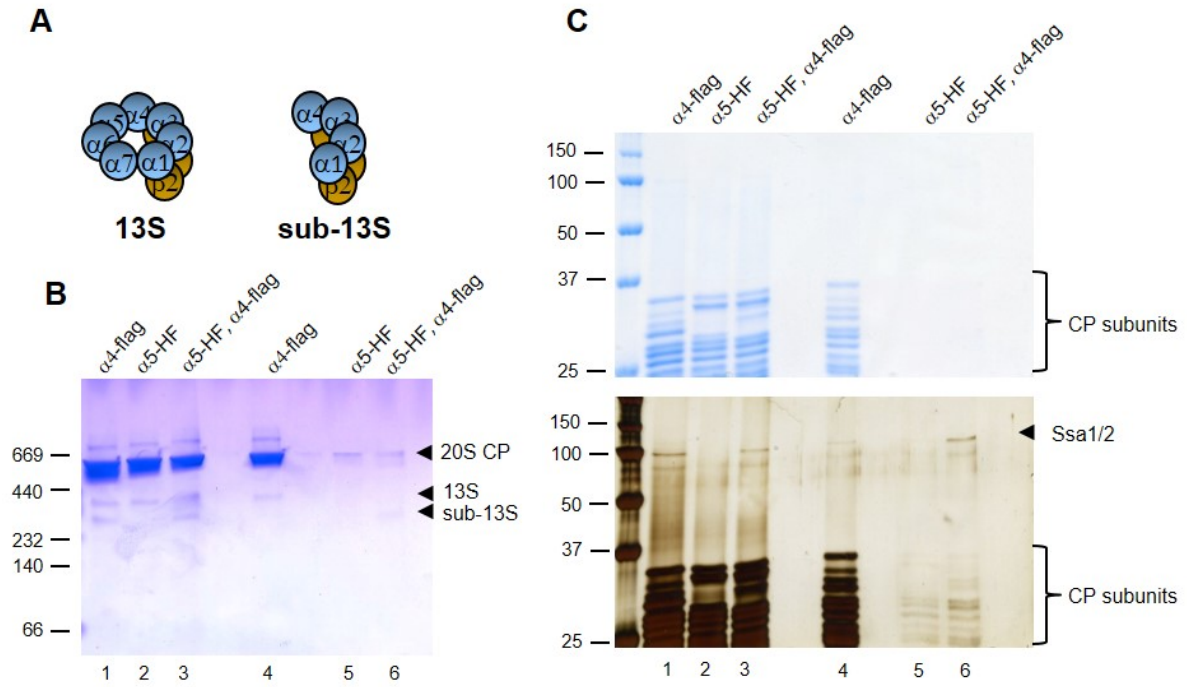

Figure 4.3 Depletion analysis to test for gel artifact
(A) Schematic of 13S and sub-13S. (B) Native PAGE analysis of Flag-purified CP (α4-Flag) from the indicated yeast strains (lanes 1 to 3). The Flag-purified material was subjected to two rounds of depletion by ICAR to remove his-tagged proteins. Aliquots of the flow through from the second ICAR round were analyzed on the same native PAGE gel (lanes 4 to 6). Arrowheads denote CP and other bands of interest. (C) Aliquots in (B) analyzed by SDS-PAGE. Gel was first stained with GelCode Blue then subsequently silver stained to better observe CP subunits and Ssa1/2 in depleted samples.

is insufficiently stable during electrophoresis and falls apart to yield the sub-13S species; inclusion of the *doa5-1* mutation only hastens this break-up because the mutation would also weaken the 13S intermediate. To address this possibility, a depletion strategy was employed to

determine if the sub-13S is the result of 13S falling apart during electrophoresis. This depletion strategy is diagramed in Appendix C, Supplementary Figure 30. In brief, the depletion strategy relies on generating an α4-Flag α5-HF strain. This strain, by virtue of the α4-Flag subunit, should contain (and does contain) both the 13S intermediate and the sub-13S species when Flag-purified material is analyzed by native PAGE (Figure 4.3A, lane 3). However, if the Flag-purified material is first subjected to a depletion via TALON resin prior to native PAGE, this will deplete all α5-containing species in the sample, including the 13S intermediate. If the sub-13S species is a gel artifact resulting from the break-up of the 13S intermediate, then the sub-13S species should not be detected in the depleted sample, since the 13S intermediate will have been removed by the TALON resin via the hexahistidine tag on α5. Nevertheless, even following depletion, we recovered small quantities of the sub-13S species (Figure 4.3B, lane 6). Moreover, in the silver stained loading control we see Ssa1/2 in the depleted sample (Figure 4.3C, lane 6) which we previously identified associating with sub-13S (Hammack et al., 2017).

4.5 Discussion and Future Work

We present evidence that the sub-13S species is an assembly intermediate and a precursor to the 13S intermediate. Its existence implies that 20S CP assembly can, at least in yeast, proceed via an alternative, α ring independent, pathway that functions in parallel with the canonical α ring dependent assembly pathway. We initially described this species in a previous report (Hammack et al., 2017). Here, we investigate the formation of the sub-13S species in additional yeast strains in which various 20S CP subunits (α2, α4, α5, β4) are epitope tagged (Figure 4.1). The tagged strains did not exhibit any growth defects on their own, or in the presence of a deletion of the *RPN4* gene, which suggests that the tags do not drastically disrupt function. Analysis of the various strains revealed the expected 13S intermediate in all of them. However, the sub-13S species was present only in the α4-Flag strain; purifications with α2-HF and β4-Flag did not produce any detectable sub-13S, even though both subunits are part of the sub-13S complex. We hypothesized that perhaps tagging the α4 subunit with Flag, while not resulting in obvious functional defects, could slow assembly enough to allow the sub-13S species to accumulate. Consistent with this, we previously reported existence of the sub-13S species from a β4-Flag strain which also contained a hexahistine tag on β5 (Hammack et al., 2017). We propose

that like the Flag tag on α4, the additional tag on β5 slows assembly down sufficiently to allow sub-13S to accumulate in a β4-Flag strain (that on its own does not accumulate it). Moreover, in this study, we showed that we could induce accumulation of the sub-13S species in the α2-HF strain by introducing a mutation, *doa5-1*, that slowed assembly further in this strain (Figure 4.2 B).

Introducing the *doa5-1* mutation also allowed us to argue that the sub-13S species is part of an assembly pathway that leads to the formation of the 13S intermediate. The sub-13S species consists of α1, α2, α3, α4, β2, β3, and β4 subunits. Consequently, α5 must be one of the next three subunits to incorporate to produce the 13S intermediate. Through the aforementioned α5 mutation, *doa5-1*, we were able to slow the rate at which α5 was incorporated. This increased the levels of sub-13S (Figure 4.2A) in both α2-HF and α4-Flag strains. More importantly, it also resulted in a reduction in the amount of 13S intermediate produced (Figure 4.2A). This coupled rise and fall in two closely related species is entirely consistent with a precursor-product relationship and strongly suggests that the sub-13S species may be a precursor to the13S intermediate.

A criticism can be raised to the relevance of the sub-13S species, based on the fact that the sub-13S species looks similar to the 13S intermediate. It could be argued that the13S intermediate is not stable and falls apart, either during lysis (or immediately after), or during electrophoresis itself, to give rise to the sub-13S species. We provide the following counter-arguments. First, we consistently observe the 13S intermediate across all purifications, but only observe the sub-13S species in some strains (Figure 4.1B and Chapter 3 Figure 3.1). If the 13S intermediate were unstable and falling apart, either prior to or during electrophoresis, it should be observed in all purifications that have the 13S intermediate. Second, we designed a depletion strategy that clearly demonstrated that the sub-13S species is not the result of dissociation during electrophoresis (Figure 4.3 and Supplementary Figure 31). Third, the ability to induce the formation of the sub-13S species with the *doa5-1* mutation (Figure 4.2) argues that species is part of an assembly pathway that feeds into the 13S intermediate. Finally, it bears mention that the manner in which protein complexes can be disassembled in vitro is often the reverse of the pathway by which they assemble (Levy, Boeri Erba, Robinson, & Teichmann, 2008). Hence even if some of the observed sub-13S species did result from the dissociation of the 13S

intermediate post lysis, this could still be consistent with sub-13S being a precursor to the 13S intermediate.

The next steps in characterizing the sub-13S species include determining if it feeds into higher intermediates and proteasomes. Since the *doa5-1* mutation produces a considerable amount of the sub-13S species, depletion strains containing *doa5-1* will be used to isolate significant amounts of this complex. It can then be incubated with yeast lysates, or with recombinantly produced 20S CP subunits. The goal is to determine if the sub-13S species can act as a precursor for higher intermediates. Lysates from different yeast strains will likely need to be tested, since it is not clear if sufficient free 20S CP subunits are present in wild type yeast lysate to observe a change in assembly. Lysate from an Rpn4 overexpression strain might be a promising candidate. Rpn4 over expression will activate transcription and translation of 20S CP subunits (Xie & Varshavsky, 2001) which should increase free subunit availability.

Demonstrating that the sub-13S species can give rise to the 13S intermediate would strongly argue that an alternate pathway of 20S CP assembly is possible. However, we are particularly interested in determining if the sub-13S can directly feed into half-proteasomes, by-passing the 13S and the other α ring dependent intermediates entirely. To test this, α ring formation will need to be disrupted in yeast. Disrupting α ring formation will force assembly to occur outside of the canonical pathway. In this noncanonical pathway, we propose assembly proceeds though the sub-13S to the half-proteasome where two half-proteasomes dimerize to form the 20S CP. In summary, we present evidence in support of a novel intermediate that participates in an alternative assembly pathway that functions along-side the canonical pathway in yeast. Upon completion of the purposed work, we will be able to elucidate the sub-13S species as a bona fide assembly intermediate. We anticipate that this work will demonstrate that proteasome assembly in eukaryotes, like archaea, occurs though more than one pathway.

CHAPTER 5. CONCLUDING REMARKS

5.1 Overview

Studies over the past two decades have supported the idea of 20S CP assembly being a linear stepwise process, initiating with the formation of an α ring (Hirano et al., 2005). Upon α ring formation, the β subunits bind in a specific order creating assembly intermediates (Hirano et al., 2008) (discussed in section 1.5) that lead to the formation of the mature 20S CP. Efficient assembly requires dedicated assembly chaperones, Ump1, Pba1-2, and Pba3-4, that promote on pathway interactions and prevent off pathway interactions (discussed in sections 1.5.1, 1.5.2, 1.5.3, and 1.5.4). Defects in proteasome function are implicated in a variety of ailments such as cancer and neurodegenerative diseases (Schmidt & Finley, 2014). Since better characterization of the proteasome assembly pathway may help in the development of future therapeutics, the overall aim of this work was to further characterize the proteasome assembly pathway. In this dissertation three major contributions to the proteasome assembly field were described: first novel high molecular weight complexes comprised of primarily α4 were identified, second Ssa1/2 were shown to function as proteasome assembly chaperones, and third a complex of α and β subunits, which may be a new assembly intermediate, was identified.

5.2 α4 Complex

While studying conditions that lead to the formation of the alternative α4-α4 proteasome in wild type cells, novel high molecular weight complexes consisting primarily of proteasome subunit α4 and Hsp70 proteins, Ssa1/2, were identified (Figure 2.3). This was the first report of such a complex forming *in vivo*. Previous reports demonstrated that human proteasome subunit α7 readily forms high molecular weight complexes when expressed recombinantly in *E.coli* (Gerards et al., 1997); however, no such complexes had been described *in vivo*, until now.

Proteasome subunits were thought to exclusively function as part of the proteasome. Identifying these non-canonical complexes *in vivo* opens the door to the idea of extra-proteasomal roles for proteasome subunits. While its function is unknown, it is hypothesized that these α4 complexes may be one of four things: (1) these complexes may have their own unique

function separate from the 20S proteasome; (2) they may serve as α4 reservoirs for efficient proteasome assembly; (3) they may act as a scaffold or template for proteasome assembly; or (4) they may be nonfunctional dead-end products. Experiments are currently underway to determine if these complexes have a unique function. One way to explore this, is by looking for phenotypes in a yeast strain where α4 complex formation is disrupted. Phenotypes can give clues to function; moreover, once a phenotype is identified a high copy suppressor screen can be implemented. Identifying which overexpressed genes suppress an α4 complex disruption phenotype will suggest which pathways, or cellular systems, this complex participates within.

Another possible way to determine function is to identify interacting proteins. Only Ssa1/2 were associated with the α4 complexes, but there could be other weakly associated proteins that may not have survived the stringent purification protocol that was implemented. To look for interacting proteins binding assays with immobilized α4 complexes and yeast lysate will be performed. Varying salt concentrations will be tested as well as binding in the presence of different nucleotides, since interacting proteins may require nucleotide for binding. Furthermore, the α4 complexes are likely comprised of rings (Figure 2.4), these rings may resemble the proteasome's α ring, which can be bound by activator proteins. It will be interesting to see if those same activators can also bind α4 complexes.

Identifying these novel high molecular weight complexes highlights that there is still much to learn about cellular homeostasis. These complexes were missed in previous studies. They were identified here by resolving SDS-PAGE gels for an extended period of time and by using engineered disulfide bonds to stabilize them on native PAGE. While the function of these α4 complexes is unclear, it is likely that they do serve a function since the levels of these complexes appear to be regulated within the cell.

5.3 Ssa1/2 Function as 20S Assembly Chaperones

This study sought to determine if any other proteins assisted in 20S CP assembly besides the previously described assembly factors, Ump1, Pba1, Pba2, Pba3, and Pba4. The findings described in this dissertation suggest that Ssa1/2 participate within 20S CP assembly. Both mature 20S CPs and intermediates were examined by native PAGE and subsequent mass spectrometry. Ssa1/2 were identified on early assembly intermediates, but not late intermediates

or the mature 20S CP (Figure 3.1 and 3.4). This argued that Ssa1/2 may function as assembly chaperones, since assembly chaperones, by definition, are only identified on assembly intermediates, and not the mature 20S CP. While the precise role of Ssa1/2 in assembly is unknown, the data suggests that they may be important for stabilizing assembly intermediates, since the levels of intermediates drastically decrease when Ssa1/2 are deleted (Figure 3.4). Moreover, this data combined with the findings outlined in Chapter 2, argue that Ssa1/2 may be important for stabilizing rings of proteasome subunits, since Ssa1/2 are observed as part of the α4 complexes, which are likely rings of α4. To better understand Ssa1/2's interaction with assembly intermediates, structural studies may provide insight into their exact role in proteasome assembly.

Ssa1/2 are part of the molecular chaperone network and have defined roles within the ubiquitin-proteasome system (Arndt et al., 2007; Huyer et al., 2004; Kettern et al., 2010; Metzger et al., 2008; Plemper et al., 1997; Shiber & Ravid, 2014). Here Ssa1/2 were added to the growing list of general chaperones that participate within the proteasome assembly network. Other chaperones that have been implicated in proteasome assembly include, Bag6 (Akahane et al., 2013) and Hsp90 (Yamano et al., 2008). Other proteins may also participate in proteasome assembly. While Ssa1/2 were the only new proteins identified interacting with assembly intermediates, there may be other weakly interacting proteins that function as 20S assembly factors, that did not survive the extensive purification protocol.

5.4 Sub-13S

A depletion strategy was implemented to purify proteasome intermediates and their potential binding partners (Figure 3.1 and 4.1B). The purified intermediates were resolved by native PAGE. While the canonical intermediates were identified, a novel species containing proteasome subunits α1-4 and β2-4 was also identified. This species migrated faster than the 13S intermediate on native PAGE, so it was referred to as the sub-13S. The sub-13S is a novel species which may be an assembly intermediate belonging to an alternative assembly pathway.

The sub-13S does not fit within the described assembly pathway for eukaryotes. Eukaryotic assembly proceeds through an α ring dependent pathway, which initiates with the formation of an α ring (Hirano et al., 2005). This is also the case in archaea, whose proteasomes

have long served as models for studying 20S CP assembly (Zwickl et al., 1994). However, a recent study uncovered an α ring independent pathway for archaeal proteasomes which initiates through the interaction of α and β subunits (Panfair et al., 2015). Since the sub-13S lacks a full α ring and contains a subset of α and β subunits, this species may be the first evidence of an α ring independent assembly pathway operating in eukaryotes.

The sub-13S resembles a 13S intermediate lacking α5, α6, and α7. Because of this similarity is was hypothesized that sub-13S may be a precursor to the 13S. Moreover, the 13S was routinely detected in proteasome purifications, while the sub-13S was only detected in a subset of purifications. This observation was attributed to disturbances in assembly caused by tagging different subunits. Tagging some subunits may perturb assembly slightly, while other tags may have no effect on the assembly process. To test the idea of a precursor product relationship between sub-13S and 13S, 13S assembly was perturbed by slowing down the rate at which α5 could incorporate by using an α5 mutant. The results were consistent with sub-13S being the immediate precursor the 13S. Slowing down assembly in strains that produced sub-13, caused more sub-13S accumulate while amount of 13S was reduced (Figure 4.2A). Furthermore, slowing down assembly with the α5 mutant induced the formation of sub-13S in strains where it was previously not detected (Figure 4.2B).

The proteasome field describes α ring formation as an essential step for proteasome assembly in eukaryotes (Hirano et al., 2005), even though no one has formally described α rings in yeast. Experiments are underway to further characterize this complex. The evidence provided in this dissertation argues for this novel sub-13S species as being an assembly intermediate that participates within an alternative assembly pathway, initiating through the interaction of α and β subunits. Perhaps, this novel intermediate is unique to yeast, but it is also possible that eukaryotes, like archaea, can use more than one assembly pathway.

5.5 Concluding Remarks

Three major contributions to the proteasome assembly field were described in this dissertation (Figure 5.1). First, novel non-canonical complexes comprised of proteasome subunit α4 and Ssa1/2 were identified. Second, a new proteasome assembly role for molecular chaperones Ssa1/2 was described. Third, a novel complex, the sub-13S, was identified and is

believed to be an assembly intermediate that participates within an alternative assembly pathway. The findings presented in this dissertation suggest that proteasome assembly likely occurs through multiple pathways using a variety of assembly factors and intermediates.

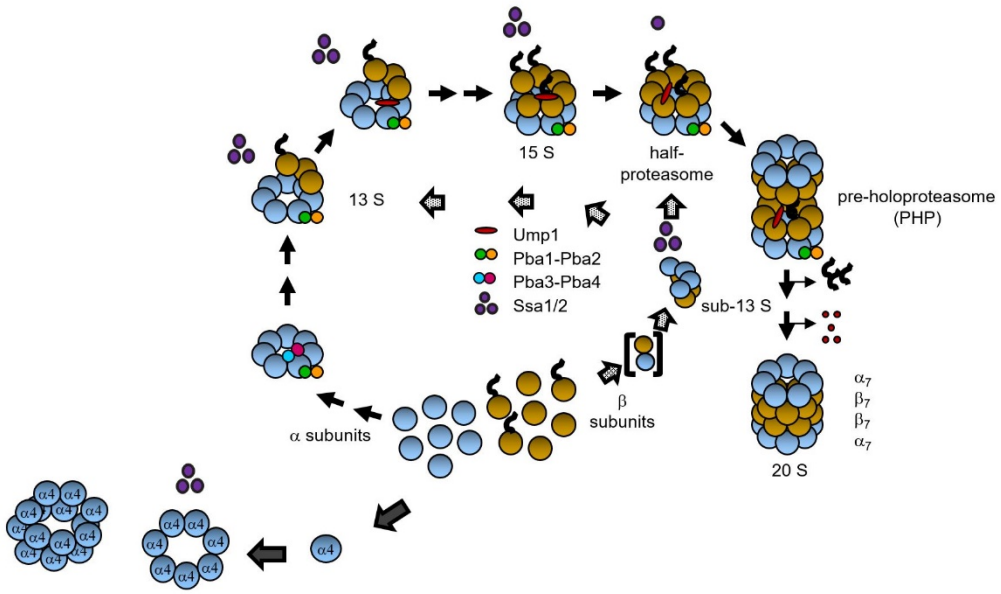

Figure 5.1 Contributions to the 20S proteasome assembly pathway
This schematic depicts the canonical 20S proteasome assembly pathway with the findings described in this dissertation

REFERENCES

Adams, J. (2004). The development of proteasome inhibitors as anticancer drugs. *Cancer Cell, 5*(5), 417-421.

Ahn, J. Y., Tanahashi, N., Akiyama, K., Hisamatsu, H., Noda, C., Tanaka, K., . . . et al. (1995). Primary structures of two homologous subunits of PA28, a gamma-interferon-inducible protein activator of the 20S proteasome. *FEBS Lett, 366*(1), 37-42.

Akahane, T., Sahara, K., Yashiroda, H., Tanaka, K., & Murata, S. (2013). Involvement of Bag6 and the TRC pathway in proteasome assembly. *Nat Commun, 4*, 2234. doi:10.1038/ncomms3234

Aki, M., Shimbara, N., Takashina, M., Akiyama, K., Kagawa, S., Tamura, T., . . . Ichihara, A. (1994). Interferon-gamma induces different subunit organizations and functional diversity of proteasomes. *J Biochem, 115*(2), 257-269.

Amm, I., Sommer, T., & Wolf, D. H. (2014). Protein quality control and elimination of protein waste: the role of the ubiquitin-proteasome system. *Biochim Biophys Acta, 1843*(1), 182-196. doi:10.1016/j.bbamcr.2013.06.031

Arendt, C. S., & Hochstrasser, M. (1997). Identification of the yeast 20S proteasome catalytic centers and subunit interactions required for active-site formation. *Proc Natl Acad Sci U S A, 94*(14), 7156-7161.

Arendt, C. S., & Hochstrasser, M. (1999). Eukaryotic 20S proteasome catalytic subunit propeptides prevent active site inactivation by N-terminal acetylation and promote particle assembly. *EMBO J, 18*(13), 3575-3585. doi:10.1093/emboj/18.13.3575

Arndt, V., Rogon, C., & Hohfeld, J. (2007). To be, or not to be--molecular chaperones in protein degradation. *Cell Mol Life Sci, 64*(19-20), 2525-2541. doi:10.1007/s00018-007-7188-6

Bai, L., Jastrab, J. B., Isasa, M., Hu, K., Yu, H., Gygi, S. P., . . . Li, H. (2017). Structural Analysis of Mycobacterium tuberculosis Homologues of the Eukaryotic Proteasome Assembly Chaperone 2 (PAC2). *J Bacteriol, 199*(9). doi:10.1128/JB.00846-16

Bai, M., Zhao, X., Sahara, K., Ohte, Y., Hirano, Y., Kaneko, T., . . . Murata, S. (2014). Assembly mechanisms of specialized core particles of the proteasome. *Biomolecules, 4*(3), 662-677. doi:10.3390/biom4030662

Barthelme, D., & Sauer, R. T. (2012). Identification of the Cdc48*20S proteasome as an ancient AAA+ proteolytic machine. *Science, 337*(6096), 843-846. doi:10.1126/science.1224352

Barton, L. F., Runnels, H. A., Schell, T. D., Cho, Y., Gibbons, R., Tevethia, S. S., . . . Monaco, J. J. (2004). Immune defects in 28-kDa proteasome activator gamma-deficient mice. *J Immunol, 172*(6), 3948-3954.

Beck, F., Unverdorben, P., Bohn, S., Schweitzer, A., Pfeifer, G., Sakata, E., . . . Forster, F. (2012). Near-atomic resolution structural model of the yeast 26S proteasome. *Proc Natl Acad Sci U S A, 109*(37), 14870-14875. doi:10.1073/pnas.1213333109

Benaroudj, N., Zwickl, P., Seemuller, E., Baumeister, W., & Goldberg, A. L. (2003). ATP hydrolysis by the proteasome regulatory complex PAN serves multiple functions in protein degradation. *Mol Cell, 11*(1), 69-78. doi:S109727650200775X [pii]

Bennett, J. A., Yarnall, J., Cadwallader, A. B., Kuennen, R., Bidey, P., Stadelmaier, B., & McCormick, J. R. (2009). Medium-dependent phenotypes of Streptomyces coelicolor with mutations in ftsI or ftsW. *J Bacteriol, 191*(2), 661-664. doi:10.1128/JB.01048-08

Bentley, S. D., Chater, K. F., Cerdeno-Tarraga, A. M., Challis, G. L., Thomson, N. R., James, K. D., . . . Hopwood, D. A. (2002). Complete genome sequence of the model actinomycete Streptomyces coelicolor A3(2). *Nature, 417*(6885), 141-147. doi:10.1038/417141a

Bibo-Verdugo, B., Jiang, Z., Caffrey, C. R., & O'Donoghue, A. J. (2017). Targeting proteasomes in infectious organisms to combat disease. *FEBS J, 284*(10), 1503-1517. doi:10.1111/febs.14029

Bishop, A., Fielding, S., Dyson, P., & Herron, P. (2004). Systematic insertional mutagenesis of a streptomycete genome: a link between osmoadaptation and antibiotic production. *Genome Res, 14*(5), 893-900. doi:10.1101/gr.1710304

Blickwedehl, J., Agarwal, M., Seong, C., Pandita, R. K., Melendy, T., Sung, P., . . . Bangia, N. (2008). Role for proteasome activator PA200 and postglutamyl proteasome activity in genomic stability. *Proc Natl Acad Sci U S A, 105*(42), 16165-16170. doi:10.1073/pnas.0803145105

Blickwedehl, J., McEvoy, S., Wong, I., Kousis, P., Clements, J., Elliott, R., . . . Bangia, N. (2007). Proteasomes and proteasome activator 200 kDa (PA200) accumulate on chromatin in response to ionizing radiation. *Radiat Res, 167*(6), 663-674. doi:10.1667/RR0690.1

Bochtler, M., Ditzel, L., Groll, M., & Huber, R. (1997). Crystal structure of heat shock locus V (HslV) from Escherichia coli. *Proc Natl Acad Sci U S A, 94*(12), 6070-6074.

Bochtler, M., Song, H. K., Hartmann, C., Ramachandran, R., & Huber, R. (2001). The quaternary arrangement of HslU and HslV in a cocrystal: a response to Wang, Yale. *J Struct Biol, 135*(3), 281-293. doi:10.1006/jsbi.2001.4413

Bolten, M., Delley, C. L., Leibundgut, M., Boehringer, D., Ban, N., & Weber-Ban, E. (2016). Structural Analysis of the Bacterial Proteasome Activator Bpa in Complex with the 20S Proteasome. *Structure, 24*(12), 2138-2151. doi:10.1016/j.str.2016.10.008

Boubakri, H., Seghezzi, N., Duchateau, M., Gominet, M., Kofronova, O., Benada, O., . . . Pernodet, J. L. (2015). The Absence of Pupylation (Prokaryotic Ubiquitin-Like Protein Modification) Affects Morphological and Physiological Differentiation in Streptomyces coelicolor. *J Bacteriol, 197*(21), 3388-3399. doi:10.1128/JB.00591-15

Burns, K. E., Cerda-Maira, F. A., Wang, T., Li, H., Bishai, W. R., & Darwin, K. H. (2010). "Depupylation" of prokaryotic ubiquitin-like protein from mycobacterial proteasome substrates. *Mol Cell, 39*(5), 821-827. doi:10.1016/j.molcel.2010.07.019

Burri, L., Hockendorff, J., Boehm, U., Klamp, T., Dohmen, R. J., & Levy, F. (2000). Identification and characterization of a mammalian protein interacting with 20S proteasome precursors. *Proc Natl Acad Sci U S A, 97*(19), 10348-10353. doi:10.1073/pnas.190268597

C. Guthrie, G. R. F. (1991). *Guide to Yeast Genetics and Molecular Biology*: Academic Press.

Carr, S., Aebersold, R., Baldwin, M., Burlingame, A., Clauser, K., Nesvizhskii, A., . . . Protein Identification, D. (2004). The need for guidelines in publication of peptide and protein identification data: Working Group on Publication Guidelines for Peptide and Protein Identification Data. *Mol Cell Proteomics, 3*(6), 531-533. doi:10.1074/mcp.T400006-MCP200

Cascio, P. (2014). PA28alphabeta: the enigmatic magic ring of the proteasome? *Biomolecules, 4*(2), 566-584. doi:10.3390/biom4020566

Cascio, P., Call, M., Petre, B. M., Walz, T., & Goldberg, A. L. (2002). Properties of the hybrid form of the 26S proteasome containing both 19S and PA28 complexes. *EMBO J, 21*(11), 2636-2645. doi:10.1093/emboj/21.11.2636

Cascio, P., Hilton, C., Kisselev, A. F., Rock, K. L., & Goldberg, A. L. (2001). 26S proteasomes and immunoproteasomes produce mainly N-extended versions of an antigenic peptide. *EMBO J, 20*(10), 2357-2366. doi:10.1093/emboj/20.10.2357

Chater, K. F., Biro, S., Lee, K. J., Palmer, T., & Schrempf, H. (2010). The complex extracellular biology of Streptomyces. *FEMS Microbiol Rev, 34*(2), 171-198. doi:10.1111/j.1574-6976.2009.00206.x

Chater, K. F., & Chandra, G. (2008). The use of the rare UUA codon to define "expression space" for genes involved in secondary metabolism, development and environmental adaptation in streptomyces. *J Microbiol, 46*(1), 1-11. doi:10.1007/s12275-007-0233-1

Chau, V., Tobias, J. W., Bachmair, A., Marriott, D., Ecker, D. J., Gonda, D. K., & Varshavsky, A. (1989). A multiubiquitin chain is confined to specific lysine in a targeted short-lived protein. *Science, 243*(4898), 1576-1583.

Chen, P., & Hochstrasser, M. (1995). Biogenesis, structure and function of the yeast 20S proteasome. *EMBO J, 14*(11), 2620-2630.

Chen, P., & Hochstrasser, M. (1996). Autocatalytic subunit processing couples active site formation in the 20S proteasome to completion of assembly. *Cell, 86*(6), 961-972. doi:S0092-8674(00)80171-3 [pii]

Choi, H. S., Rai, P. R., Chu, H. W., Cool, C., & Chan, E. D. (2002). Analysis of nitric oxide synthase and nitrotyrosine expression in human pulmonary tuberculosis. *Am J Respir Crit Care Med, 166*(2), 178-186.

Chuang, S. E., Burland, V., Plunkett, G., 3rd, Daniels, D. L., & Blattner, F. R. (1993). Sequence analysis of four new heat-shock genes constituting the hslTS/ibpAB and hslVU operons in Escherichia coli. *Gene, 134*(1), 1-6.

Compton, C. L., Fernandopulle, M. S., Nagari, R. T., & Sello, J. K. (2015). Genetic and Proteomic Analyses of Pupylation in Streptomyces coelicolor. *J Bacteriol, 197*(17), 2747-2753. doi:10.1128/JB.00302-15

Cusack, J. C., Jr., Liu, R., Houston, M., Abendroth, K., Elliott, P. J., Adams, J., & Baldwin, A. S., Jr. (2001). Enhanced chemosensitivity to CPT-11 with proteasome inhibitor PS-341: implications for systemic nuclear factor-kappaB inhibition. *Cancer Res, 61*(9), 3535-3540.

da Fonseca, P. C., He, J., & Morris, E. P. (2012). Molecular model of the human 26S proteasome. *Mol Cell, 46*(1), 54-66. doi:S1097-2765(12)00263-8 [pii]10.1016/j.molcel.2012.03.026

Dange, T., Smith, D., Noy, T., Rommel, P. C., Jurzitza, L., Cordero, R. J., . . . Schmidt, M. (2011). Blm10 protein promotes proteasomal substrate turnover by an active gating mechanism. *J Biol Chem, 286*(50), 42830-42839. doi:10.1074/jbc.M111.300178M111.300178 [pii]

Darwin, K. H., Ehrt, S., Gutierrez-Ramos, J. C., Weich, N., & Nathan, C. F. (2003). The proteasome of Mycobacterium tuberculosis is required for resistance to nitric oxide. *Science, 302*(5652), 1963-1966. doi:10.1126/science.1091176302/5652/1963 [pii]

Darwin, K. H., Lin, G., Chen, Z., Li, H., & Nathan, C. F. (2005). Characterization of a Mycobacterium tuberculosis proteasomal ATPase homologue. *Mol Microbiol, 55*(2), 561-571. doi:10.1111/j.1365-2958.2004.04403.x

De Mot, R., Nagy, I., Walz, J., & Baumeister, W. (1999). Proteasomes and other self-compartmentalizing proteases in prokaryotes. *Trends Microbiol, 7*(2), 88-92.

De Mot, R., Schoofs, G., & Nagy, I. (2007). Proteome analysis of Streptomyces coelicolor mutants affected in the proteasome system reveals changes in stress-responsive proteins. *Arch Microbiol, 188*(3), 257-271. doi:10.1007/s00203-007-0243-8

Delley, C. L., Laederach, J., Ziemski, M., Bolten, M., Boehringer, D., & Weber-Ban, E. (2014). Bacterial proteasome activator bpa (rv3780) is a novel ring-shaped interactor of the mycobacterial proteasome. *PLoS One, 9*(12), e114348. doi:10.1371/journal.pone.0114348

DeMartino, G. N., & Slaughter, C. A. (1999). The proteasome, a novel protease regulated by multiple mechanisms. *J Biol Chem, 274*(32), 22123-22126.

Demo, S. D., Kirk, C. J., Aujay, M. A., Buchholz, T. J., Dajee, M., Ho, M. N., . . . Bennett, M. K. (2007). Antitumor activity of PR-171, a novel irreversible inhibitor of the proteasome. *Cancer Res, 67*(13), 6383-6391. doi:10.1158/0008-5472.CAN-06-4086

Dietrich, C., Bartsch, T., Schanz, F., Oesch, F., & Wieser, R. J. (1996). p53-dependent cell cycle arrest induced by N-acetyl-L-leucinyl-L-leucinyl-L-norleucinal in platelet-derived growth factor-stimulated human fibroblasts. *Proc Natl Acad Sci U S A, 93*(20), 10815-10819.

Djuranovic, S., Rockel, B., Lupas, A. N., & Martin, J. (2006). Characterization of AMA, a new AAA protein from Archaeoglobus and methanogenic archaea. *J Struct Biol, 156*(1), 130-138. doi:10.1016/j.jsb.2006.03.010

Doherty, K. M., Pride, L. D., Lukose, J., Snydsman, B. E., Charles, R., Pramanik, A., . . . Moore, C. W. (2012). Loss of a 20S proteasome activator in Saccharomyces cerevisiae downregulates genes important for genomic integrity, increases DNA damage, and selectively sensitizes cells to agents with diverse mechanisms of action. *G3 (Bethesda), 2*(8), 943-959. doi:10.1534/g3.112.003376

Dubiel, W., Pratt, G., Ferrell, K., & Rechsteiner, M. (1992). Purification of an 11 S regulator of the multicatalytic protease. *J Biol Chem, 267*(31), 22369-22377.

Elsasser, S., Gali, R. R., Schwickart, M., Larsen, C. N., Leggett, D. S., Muller, B., . . . Finley, D. (2002). Proteasome subunit Rpn1 binds ubiquitin-like protein domains. *Nat Cell Biol, 4*(9), 725-730. doi:10.1038/ncb845

Firestone, K., Awonusi, D., Panfair, D., Roland, D., Ramamurthy, A., & Kusmierczyk, A. R. (2016). YPL260W, a high-copy suppressor of a copper-sensitive phenotype in yeast, is linked to DNA repair and proteasome function. *Plant Gene, 5*, 38-48. doi:10.1016/j.plgene.2015.11.002

Flardh, K., & Buttner, M. J. (2009). Streptomyces morphogenetics: dissecting differentiation in a filamentous bacterium. *Nat Rev Microbiol, 7*(1), 36-49. doi:10.1038/nrmicro1968

Forouzan, D., Ammelburg, M., Hobel, C. F., Stroh, L. J., Sessler, N., Martin, J., & Lupas, A. N. (2012). The archaeal proteasome is regulated by a network of AAA ATPases. *J Biol Chem, 287*(46), 39254-39262. doi:10.1074/jbc.M112.386458

Fort, P., Kajava, A. V., Delsuc, F., & Coux, O. (2015). Evolution of proteasome regulators in eukaryotes. *Genome Biol Evol, 7*(5), 1363-1379. doi:10.1093/gbe/evv068

Frankenberg, R. J., Hsu, T. S., Yakota, H., Kim, R., & Clark, D. S. (2001). Chemical denaturation and elevated folding temperatures are required for wild-type activity and stability of recombinant Methanococcus jannaschii 20S proteasome. *Protein Sci, 10*(9), 1887-1896. doi:10.1110/ps.ps.05801

Frentzel, S., Pesold-Hurt, B., Seelig, A., & Kloetzel, P. M. (1994). 20 S proteasomes are assembled via distinct precursor complexes. Processing of LMP2 and LMP7 proproteins takes place in 13-16 S preproteasome complexes. *J Mol Biol, 236*(4), 975-981.

Fricke, B., Heink, S., Steffen, J., Kloetzel, P. M., & Kruger, E. (2007). The proteasome maturation protein POMP facilitates major steps of 20S proteasome formation at the endoplasmic reticulum. *EMBO Rep, 8*(12), 1170-1175. doi:10.1038/sj.embor.7401091

Fu, H., Doelling, J. H., Arendt, C. S., Hochstrasser, M., & Vierstra, R. D. (1998). Molecular organization of the 20S proteasome gene family from Arabidopsis thaliana. *Genetics, 149*(2), 677-692.

Fuchs, A. C. D., Alva, V., Maldoner, L., Albrecht, R., Hartmann, M. D., & Martin, J. (2017). The Architecture of the Anbu Complex Reflects an Evolutionary Intermediate at the Origin of the Proteasome System. *Structure, 25*(6), 834-845 e835. doi:10.1016/j.str.2017.04.005

Funakoshi, M., Li, X., Velichutina, I., Hochstrasser, M., & Kobayashi, H. (2004). Sem1, the yeast ortholog of a human BRCA2-binding protein, is a component of the proteasome regulatory particle that enhances proteasome stability. *J Cell Sci, 117*(Pt 26), 6447-6454. doi:jcs.01575 [pii]10.1242/jcs.01575

Funakoshi, M., Tomko, R. J., Jr., Kobayashi, H., & Hochstrasser, M. (2009). Multiple assembly chaperones govern biogenesis of the proteasome regulatory particle base. *Cell, 137*(5), 887-899. doi:S0092-8674(09)00526-1 [pii]10.1016/j.cell.2009.04.061

Gaczynska, M., Rock, K. L., & Goldberg, A. L. (1993). Role of proteasomes in antigen presentation. *Enzyme Protein, 47*(4-6), 354-369.

Gerards, W. L., de Jong, W. W., Bloemendal, H., & Boelens, W. (1998). The human proteasomal subunit HsC8 induces ring formation of other alpha-type subunits. *J Mol Biol, 275*(1), 113-121. doi:10.1006/jmbi.1997.1429

Gerards, W. L., Enzlin, J., Haner, M., Hendriks, I. L., Aebi, U., Bloemendal, H., & Boelens, W. (1997). The human alpha-type proteasomal subunit HsC8 forms a double ringlike structure, but does not assemble into proteasome-like particles with the beta-type subunits HsDelta or HsBPROS26. *J Biol Chem, 272*(15), 10080-10086.

Gille, C., Goede, A., Schloetelburg, C., Preissner, R., Kloetzel, P. M., Gobel, U. B., & Frommel, C. (2003). A comprehensive view on proteasomal sequences: implications for the evolution of the proteasome. *J Mol Biol, 326*(5), 1437-1448. doi:S0022283602014705 [pii]

Glickman, M. H., Rubin, D. M., Coux, O., Wefes, I., Pfeifer, G., Cjeka, Z., . . . Finley, D. (1998). A subcomplex of the proteasome regulatory particle required for ubiquitin-conjugate degradation and related to the COP9-signalosome and eIF3. *Cell, 94*(5), 615-623. doi:S0092-8674(00)81603-7 [pii]

Global Tuberculosis Report. (2016). Retrieved from http://apps.who.int/iris/bitstream/10665/250441/1/9789241565394-eng.pdf?ua=1:

Gong, Y., Kakihara, Y., Krogan, N., Greenblatt, J., Emili, A., Zhang, Z., & Houry, W. A. (2009). An atlas of chaperone-protein interactions in Saccharomyces cerevisiae: implications to protein folding pathways in the cell. *Mol Syst Biol, 5*, 275. doi:10.1038/msb.2009.26

Grana, M., Bellinzoni, M., Miras, I., Fiez-Vandal, C., Haouz, A., Shepard, W., . . . Alzari, P. M. (2009). Structure of Mycobacterium tuberculosis Rv2714, a representative of a duplicated gene family in Actinobacteria. *Acta Crystallogr Sect F Struct Biol Cryst Commun, 65*(Pt 10), 972-977. doi:10.1107/S1744309109035027

Griffin, T. A., Nandi, D., Cruz, M., Fehling, H. J., Kaer, L. V., Monaco, J. J., & Colbert, R. A. (1998). Immunoproteasome assembly: cooperative incorporation of interferon gamma (IFN-gamma)-inducible subunits. *J Exp Med, 187*(1), 97-104.

Groettrup, M., Soza, A., Eggers, M., Kuehn, L., Dick, T. P., Schild, H., . . . Kloetzel, P. M. (1996). A role for the proteasome regulator PA28alpha in antigen presentation. *Nature, 381*(6578), 166-168. doi:10.1038/381166a0

Groettrup, M., Standera, S., Stohwasser, R., & Kloetzel, P. M. (1997). The subunits MECL-1 and LMP2 are mutually required for incorporation into the 20S proteasome. *Proc Natl Acad Sci U S A, 94*(17), 8970-8975.

Groll, M., Bajorek, M., Kohler, A., Moroder, L., Rubin, D. M., Huber, R., . . . Finley, D. (2000). A gated channel into the proteasome core particle. *Nat Struct Biol, 7*(11), 1062-1067. doi:10.1038/80992

Groll, M., Brandstetter, H., Bartunik, H., Bourenkow, G., & Huber, R. (2003). Investigations on the maturation and regulation of archaebacterial proteasomes. *J Mol Biol, 327*(1), 75-83.

Groll, M., Ditzel, L., Lowe, J., Stock, D., Bochtler, M., Bartunik, H. D., & Huber, R. (1997). Structure of 20S proteasome from yeast at 2.4 A resolution. *Nature, 386*(6624), 463-471. doi:10.1038/386463a0

Groll, M., Heinemeyer, W., Jager, S., Ullrich, T., Bochtler, M., Wolf, D. H., & Huber, R. (1999). The catalytic sites of 20S proteasomes and their role in subunit maturation: a mutational and crystallographic study. *Proc Natl Acad Sci U S A, 96*(20), 10976-10983.

Groll, M., Koguchi, Y., Huber, R., & Kohno, J. (2001). Crystal structure of the 20 S proteasome:TMC-95A complex: a non-covalent proteasome inhibitor. *J Mol Biol, 311*(3), 543-548. doi:10.1006/jmbi.2001.4869

Guerrero, C., Milenkovic, T., Przulj, N., Kaiser, P., & Huang, L. (2008). Characterization of the proteasome interaction network using a QTAX-based tag-team strategy and protein interaction network analysis. *Proc Natl Acad Sci U S A, 105*(36), 13333-13338. doi:0801870105 [pii]10.1073/pnas.0801870105

Guerrero, C., Tagwerker, C., Kaiser, P., & Huang, L. (2006). An integrated mass spectrometry-based proteomic approach: quantitative analysis of tandem affinity-purified in vivo cross-linked protein complexes (QTAX) to decipher the 26 S proteasome-interacting network. *Mol Cell Proteomics, 5*(2), 366-378. doi:10.1074/mcp.M500303-MCP200

Guillaume, B., Chapiro, J., Stroobant, V., Colau, D., Van Holle, B., Parvizi, G., . . . Van den Eynde, B. J. (2010). Two abundant proteasome subtypes that uniquely process some antigens presented by HLA class I molecules. *Proc Natl Acad Sci U S A, 107*(43), 18599-18604. doi:10.1073/pnas.1009778107

Guth, E., Thommen, M., & Weber-Ban, E. (2011). Mycobacterial ubiquitin-like protein ligase PafA follows a two-step reaction pathway with a phosphorylated pup intermediate. *J Biol Chem, 286*(6), 4412-4419. doi:10.1074/jbc.M110.189282

Hammack, L., & Kusmierczyk, A. R. (2016). Data on the identity of non-canonical complexes formed from proteasome subunits in vivo. *Data Brief, Submitted*.

Hammack, L. J., Firestone, K., Chang, W., & Kusmierczyk, A. R. (2017). Molecular chaperones of the Hsp70 family assist in the assembly of 20S proteasomes. *Biochem Biophys Res Commun, 486*(2), 438-443. doi:10.1016/j.bbrc.2017.03.059

Hammack, L. J., & Kusmierczyk, A. R. (2016). Data on the identity of non-canonical complexes formed from proteasome subunits in vivo. *Data Brief, 9*, 1130-1137. doi:10.1016/j.dib.2016.11.048

Hammack, L. J., & Kusmierczyk, A. R. (2017). Assembly of proteasome subunits into non-canonical complexes in vivo. *Biochem Biophys Res Commun, 482*(1), 164-169. doi:10.1016/j.bbrc.2016.11.024

Hari, P. N., Shain, K. H., Voorhees, P. M., Gabrail, N., Abidi, M. H., Zonder, J., . . . Paba Prada, C. (2014). Oprozomib and Dexamethasone in Patients with Relapsed and/or Refractory Multiple Myeloma: Initial Results from the Dose Escalation Portion of a Phase 1b/2, Multicenter, Open-Label Study. *Blood, 124*(21), 3453-3453.

Harshbarger, W., Miller, C., Diedrich, C., & Sacchettini, J. (2015). Crystal structure of the human 20S proteasome in complex with carfilzomib. *Structure, 23*(2), 418-424. doi:10.1016/j.str.2014.11.017

Hatanaka, A., Chen, B., Sun, J. Q., Mano, Y., Funakoshi, M., Kobayashi, H., . . . Oki, M. (2011). Fub1p, a novel protein isolated by boundary screening, binds the proteasome complex. *Genes Genet Syst, 86*(5), 305-314.

Heinemeyer, W., Fischer, M., Krimmer, T., Stachon, U., & Wolf, D. H. (1997). The active sites of the eukaryotic 20 S proteasome and their involvement in subunit precursor processing. *J Biol Chem, 272*(40), 25200-25209.

Heink, S., Ludwig, D., Kloetzel, P. M., & Kruger, E. (2005). IFN-gamma-induced immune adaptation of the proteasome system is an accelerated and transient response. *Proc Natl Acad Sci U S A, 102*(26), 9241-9246. doi:0501711102 [pii]10.1073/pnas.0501711102

Hendil, K. B., Khan, S., & Tanaka, K. (1998). Simultaneous binding of PA28 and PA700 activators to 20 S proteasomes. *Biochem J, 332 (Pt 3)*, 749-754.

Hepowit, N. L., Uthandi, S., Miranda, H. V., Toniutti, M., Prunetti, L., Olivarez, O., . . . Maupin-Furlow, J. A. (2012). Archaeal JAB1/MPN/MOV34 metalloenzyme (HvJAMM1) cleaves ubiquitin-like small archaeal modifier proteins (SAMPs) from protein-conjugates. *Mol Microbiol, 86*(4), 971-987. doi:10.1111/mmi.12038

Hershko, A., & Ciechanover, A. (1998). The ubiquitin system. *Annu Rev Biochem, 67*, 425-479. doi:10.1146/annurev.biochem.67.1.425

Hideshima, T., Richardson, P., Chauhan, D., Palombella, V. J., Elliott, P. J., Adams, J., & Anderson, K. C. (2001). The proteasome inhibitor PS-341 inhibits growth, induces apoptosis, and overcomes drug resistance in human multiple myeloma cells. *Cancer Res, 61*(7), 3071-3076.

Hirano, Y., Hayashi, H., Iemura, S., Hendil, K. B., Niwa, S., Kishimoto, T., . . . Murata, S. (2006). Cooperation of multiple chaperones required for the assembly of mammalian 20S proteasomes. *Mol Cell, 24*(6), 977-984. doi:S1097-2765(06)00786-6 [pii]10.1016/j.molcel.2006.11.015

Hirano, Y., Hendil, K. B., Yashiroda, H., Iemura, S., Nagane, R., Hioki, Y., . . . Murata, S. (2005). A heterodimeric complex that promotes the assembly of mammalian 20S proteasomes. *Nature, 437*(7063), 1381-1385. doi:nature04106 [pii]10.1038/nature04106

Hirano, Y., Kaneko, T., Okamoto, K., Bai, M., Yashiroda, H., Furuyama, K., . . . Murata, S. (2008). Dissecting beta-ring assembly pathway of the mammalian 20S proteasome. *EMBO J, 27*(16), 2204-2213. doi:emboj2008148 [pii]10.1038/emboj.2008.148

Hochstrasser, M. (1996). Ubiquitin-dependent protein degradation. *Annu Rev Genet, 30*, 405-439. doi:10.1146/annurev.genet.30.1.405

Holkova, B., & Grant, S. (2012). Proteasome inhibitors in mantle cell lymphoma. *Best Pract Res Clin Haematol, 25*(2), 133-141. doi:10.1016/j.beha.2012.04.007

Houry, W. A. (2014). The Molecular Chaperones Interaction Networks in Protein Folding and Degradation. New York: Springer-Verlag.

Howell, L. A., Tomko, R. J., & Kusmierczyk, A. R. (2017). Putting it all together: intrinsic and extrinsic mechanisms governing proteasome biogenesis. *Frontiers in Biology, 12*(1), 19-48. doi:10.1007/s11515-017-1439-1

Hu, G., Lin, G., Wang, M., Dick, L., Xu, R. M., Nathan, C., & Li, H. (2006). Structure of the Mycobacterium tuberculosis proteasome and mechanism of inhibition by a peptidyl boronate. *Mol Microbiol, 59*(5), 1417-1428. doi:10.1111/j.1365-2958.2005.05036.x

Hua, S., To, W. Y., Nguyen, T. T., Wong, M. L., & Wang, C. C. (1996). Purification and characterization of proteasomes from Trypanosoma brucei. *Mol Biochem Parasitol, 78*(1-2), 33-46.

Huang, L., Haratake, K., Miyahara, H., & Chiba, T. (2016). Proteasome activators, PA28gamma and PA200, play indispensable roles in male fertility. *Sci Rep, 6*, 23171. doi:10.1038/srep23171

Huang, X., Luan, B., Wu, J., & Shi, Y. (2016a). An atomic structure of the human 26S proteasome. *Nat Struct Mol Biol*. doi:10.1038/nsmb.3273

Huang, X., Luan, B., Wu, J., & Shi, Y. (2016b). An atomic structure of the human 26S proteasome. *Nat Struct Mol Biol, 23*(9), 778-785. doi:10.1038/nsmb.3273

Huber, E. M., & Groll, M. (2017). The Mammalian Proteasome Activator PA28 Forms an Asymmetric alpha4beta3 Complex. *Structure*. doi:10.1016/j.str.2017.07.013

Huber, E. M., Heinemeyer, W., Li, X., Arendt, C. S., Hochstrasser, M., & Groll, M. (2016). A unified mechanism for proteolysis and autocatalytic activation in the 20S proteasome. *Nat Commun, 7*, 10900. doi:10.1038/ncomms10900

Humbard, M. A., Miranda, H. V., Lim, J. M., Krause, D. J., Pritz, J. R., Zhou, G., . . . Maupin-Furlow, J. A. (2010). Ubiquitin-like small archaeal modifier proteins (SAMPs) in Haloferax volcanii. *Nature, 463*(7277), 54-60. doi:10.1038/nature08659

Husnjak, K., Elsasser, S., Zhang, N., Chen, X., Randles, L., Shi, Y., . . . Dikic, I. (2008). Proteasome subunit Rpn13 is a novel ubiquitin receptor. *Nature, 453*(7194), 481-488. doi:nature06926 [pii]10.1038/nature06926

Huyer, G., Piluek, W. F., Fansler, Z., Kreft, S. G., Hochstrasser, M., Brodsky, J. L., & Michaelis, S. (2004). Distinct machinery is required in Saccharomyces cerevisiae for the endoplasmic reticulum-associated degradation of a multispanning membrane protein and a soluble luminal protein. *J Biol Chem, 279*(37), 38369-38378. doi:10.1074/jbc.M402468200

Imai, J., Maruya, M., Yashiroda, H., Yahara, I., & Tanaka, K. (2003). The molecular chaperone Hsp90 plays a role in the assembly and maintenance of the 26S proteasome. *EMBO J, 22*(14), 3557-3567. doi:10.1093/emboj/cdg349

Imkamp, F., Striebel, F., Sutter, M., Ozcelik, D., Zimmermann, N., Sander, P., & Weber-Ban, E. (2010). Dop functions as a depupylase in the prokaryotic ubiquitin-like modification pathway. *EMBO Rep, 11*(10), 791-797. doi:10.1038/embor.2010.119

Imkamp, F., Ziemski, M., & Weber-Ban, E. (2015). Pupylation-dependent and -independent proteasomal degradation in mycobacteria. *Biomol Concepts, 6*(4), 285-301. doi:10.1515/bmc-2015-0017

Ishii, K., Noda, M., Yagi, H., Thammaporn, R., Seetaha, S., Satoh, T., . . . Uchiyama, S. (2015). Disassembly of the self-assembled, double-ring structure of proteasome alpha7 homo-tetradecamer by alpha6. *Sci Rep, 5*, 18167. doi:10.1038/srep18167

Iwai, H., & Pluckthun, A. (1999). Circular beta-lactamase: stability enhancement by cyclizing the backbone. *FEBS Lett, 459*(2), 166-172.

Iyer, L. M., Burroughs, A. M., & Aravind, L. (2008). Unraveling the biochemistry and provenance of pupylation: a prokaryotic analog of ubiquitination. *Biol Direct, 3*, 45. doi:10.1186/1745-6150-3-45

Jager, S., Groll, M., Huber, R., Wolf, D. H., & Heinemeyer, W. (1999). Proteasome beta-type subunits: unequal roles of propeptides in core particle maturation and a hierarchy of active site function. *J Mol Biol, 291*(4), 997-1013. doi:10.1006/jmbi.1999.2995S0022-2836(99)92995-9 [pii]

Jastrab, J. B., Wang, T., Murphy, J. P., Bai, L., Hu, K., Merkx, R., . . . Darwin, K. H. (2015). An adenosine triphosphate-independent proteasome activator contributes to the virulence of Mycobacterium tuberculosis. *Proc Natl Acad Sci U S A, 112*(14), E1763-1772. doi:10.1073/pnas.1423319112

Jayarapu, K., & Griffin, T. A. (2004). Protein-protein interactions among human 20S proteasome subunits and proteassemblin. *Biochem Biophys Res Commun, 314*(2), 523-528.

Jentsch, S. (1992). The ubiquitin-conjugation system. *Annu Rev Genet, 26*, 179-207. doi:10.1146/annurev.ge.26.120192.001143

Kane, R. C., Bross, P. F., Farrell, A. T., & Pazdur, R. (2003). Velcade: U.S. FDA approval for the treatment of multiple myeloma progressing on prior therapy. *Oncologist, 8*(6), 508-513.

Kettern, N., Dreiseidler, M., Tawo, R., & Hohfeld, J. (2010). Chaperone-assisted degradation: multiple paths to destruction. *Biol Chem, 391*(5), 481-489. doi:10.1515/BC.2010.058

Khor, B., Bredemeyer, A. L., Huang, C. Y., Turnbull, I. R., Evans, R., Maggi, L. B., Jr., . . . Sleckman, B. P. (2006). Proteasome activator PA200 is required for normal spermatogenesis. *Mol Cell Biol, 26*(8), 2999-3007. doi:10.1128/MCB.26.8.2999-3007.2006

Kim, Y. E., Cho, N., Cheon, S., & Kim, K. K. (2017). Bortezomib, a proteasome inhibitor, alleviates atopic dermatitis by increasing claudin 1 protein expression. *Biochem Biophys Res Commun*. doi:10.1016/j.bbrc.2017.08.120

Kincaid, E. Z., Che, J. W., York, I., Escobar, H., Reyes-Vargas, E., Delgado, J. C., . . . Rock, K. L. (2011). Mice completely lacking immunoproteasomes show major changes in antigen presentation. *Nat Immunol, 13*(2), 129-135. doi:10.1038/ni.2203

Klare, N., Seeger, M., Janek, K., Jungblut, P. R., & Dahlmann, B. (2007). Intermediate-type 20 S proteasomes in HeLa cells: "asymmetric" subunit composition, diversity and adaptation. *J Mol Biol, 373*(1), 1-10. doi:10.1016/j.jmb.2007.07.038

Knowlton, J. R., Johnston, S. C., Whitby, F. G., Realini, C., Zhang, Z., Rechsteiner, M., & Hill, C. P. (1997). Structure of the proteasome activator REGalpha (PA28alpha). *Nature, 390*(6660), 639-643. doi:10.1038/37670

Kock, M., Nunes, M. M., Hemann, M., Kube, S., Dohmen, R. J., Herzog, F., . . . Wendler, P. (2015). Proteasome assembly from 15S precursors involves major conformational changes and recycling of the Pba1-Pba2 chaperone. *Nat Commun, 6*, 6123. doi:10.1038/ncomms7123

Kubiczkova, L., Pour, L., Sedlarikova, L., Hajek, R., & Sevcikova, S. (2014). Proteasome inhibitors - molecular basis and current perspectives in multiple myeloma. *J Cell Mol Med, 18*(6), 947-961. doi:10.1111/jcmm.12279

Kuhn, D. J., Chen, Q., Voorhees, P. M., Strader, J. S., Shenk, K. D., Sun, C. M., . . . Orlowski, R. Z. (2007). Potent activity of carfilzomib, a novel, irreversible inhibitor of the ubiquitin-proteasome pathway, against preclinical models of multiple myeloma. *Blood, 110*(9), 3281-3290. doi:10.1182/blood-2007-01-065888

Kumoi, K., Satoh, T., Murata, K., Hiromoto, T., Mizushima, T., Kamiya, Y., . . . Kato, K. (2013). An archaeal homolog of proteasome assembly factor functions as a proteasome activator. *PLoS One, 8*(3), e60294. doi:10.1371/journal.pone.0060294

Kunjappu, M. J., & Hochstrasser, M. (2014). Assembly of the 20S proteasome. *Biochim Biophys Acta, 1843*(1), 2-12. doi:10.1016/j.bbamcr.2013.03.008

Kusmierczyk, A. R., & Hochstrasser, M. (2008). Some assembly required: dedicated chaperones in eukaryotic proteasome biogenesis. *Biol Chem, 389*(9), 1143-1151. doi:10.1515/bc.2008.130

Kusmierczyk, A. R., Kunjappu, M. J., Funakoshi, M., & Hochstrasser, M. (2008). A multimeric assembly factor controls the formation of alternative 20S proteasomes. *Nat Struct Mol Biol, 15*(3), 237-244. doi:nsmb.1389 [pii]10.1038/nsmb.1389

Kusmierczyk, A. R., Kunjappu, M. J., Kim, R. Y., & Hochstrasser, M. (2011). A conserved 20S proteasome assembly factor requires a C-terminal HbYX motif for proteasomal precursor binding. *Nat Struct Mol Biol, 18*(5), 622-629. doi:10.1038/nsmb.2027

Kwon, Y. D., Nagy, I., Adams, P. D., Baumeister, W., & Jap, B. K. (2004). Crystal structures of the Rhodococcus proteasome with and without its pro-peptides: implications for the role of the pro-peptide in proteasome assembly. *J Mol Biol, 335*(1), 233-245.

Lander, G. C., Estrin, E., Matyskiela, M. E., Bashore, C., Nogales, E., & Martin, A. (2012). Complete subunit architecture of the proteasome regulatory particle. *Nature, 482*(7384), 186-191. doi:nature10774 [pii]10.1038/nature10774

Le Tallec, B., Barrault, M. B., Courbeyrette, R., Guerois, R., Marsolier-Kergoat, M. C., & Peyroche, A. (2007). 20S proteasome assembly is orchestrated by two distinct pairs of chaperones in yeast and in mammals. *Mol Cell, 27*(4), 660-674. doi:S1097-2765(07)00415-7 [pii]10.1016/j.molcel.2007.06.025

Le Tallec, B., Barrault, M. B., Guerois, R., Carre, T., & Peyroche, A. (2009). Hsm3/S5b participates in the assembly pathway of the 19S regulatory particle of the proteasome. *Mol Cell, 33*(3), 389-399. doi:10.1016/j.molcel.2009.01.010

Lee do, H., Sherman, M. Y., & Goldberg, A. L. (2016). The requirements of yeast Hsp70 of SSA family for the ubiquitin-dependent degradation of short-lived and abnormal proteins. *Biochem Biophys Res Commun, 475*(1), 100-106. doi:10.1016/j.bbrc.2016.05.046

Lehmann, A., Jechow, K., & Enenkel, C. (2008). Blm10 binds to pre-activated proteasome core particles with open gate conformation. *EMBO Rep, 9*(12), 1237-1243. doi:embor2008190 [pii]10.1038/embor.2008.190

Levy, E. D., Boeri Erba, E., Robinson, C. V., & Teichmann, S. A. (2008). Assembly reflects evolution of protein complexes. *Nature, 453*(7199), 1262-1265. doi:10.1038/nature06942

Li, D., Li, H., Wang, T., Pan, H., Lin, G., & Li, H. (2010). Structural basis for the assembly and gate closure mechanisms of the Mycobacterium tuberculosis 20S proteasome. *EMBO J, 29*(12), 2037-2047. doi:10.1038/emboj.2010.95

Li, J., & Rechsteiner, M. (2001). Molecular dissection of the 11S REG (PA28) proteasome activators. *Biochimie, 83*(3-4), 373-383.

Li, X., Kusmierczyk, A. R., Wong, P., Emili, A., & Hochstrasser, M. (2007). beta-Subunit appendages promote 20S proteasome assembly by overcoming an Ump1-dependent checkpoint. *EMBO J, 26*(9), 2339-2349. doi:10.1038/sj.emboj.7601681

Li, X., Li, Y., Arendt, C. S., & Hochstrasser, M. (2016). Distinct Elements in the Proteasomal beta5 Subunit Propeptide Required for Autocatalytic Processing and Proteasome Assembly. *J Biol Chem, 291*(4), 1991-2003. doi:10.1074/jbc.M115.677047

Liu, G., Chater, K. F., Chandra, G., Niu, G., & Tan, H. (2013). Molecular regulation of antibiotic biosynthesis in streptomyces. *Microbiol Mol Biol Rev, 77*(1), 112-143. doi:10.1128/MMBR.00054-12

Lowe, J., Stock, D., Jap, B., Zwickl, P., Baumeister, W., & Huber, R. (1995). Crystal structure of the 20S proteasome from the archaeon T. acidophilum at 3.4 A resolution. *Science, 268*(5210), 533-539.

Lu, Y., Lee, B. H., King, R. W., Finley, D., & Kirschner, M. W. (2015). Substrate degradation by the proteasome: a single-molecule kinetic analysis. *Science, 348*(6231), 1250834. doi:10.1126/science.1250834

Luan, B., Huang, X., Wu, J., Mei, Z., Wang, Y., Xue, X., . . . Wang, F. (2016). Structure of an endogenous yeast 26S proteasome reveals two major conformational states. *Proc Natl Acad Sci U S A, 113*(10), 2642-2647. doi:10.1073/pnas.1601561113

Luders, J., Demand, J., & Hohfeld, J. (2000). The ubiquitin-related BAG-1 provides a link between the molecular chaperones Hsc70/Hsp70 and the proteasome. *J Biol Chem, 275*(7), 4613-4617.

Lupas, A., Zuhl, F., Tamura, T., Wolf, S., Nagy, I., De Mot, R., & Baumeister, W. (1997). Eubacterial proteasomes. *Mol Biol Rep, 24*(1-2), 125-131.

Ma, C. P., Slaughter, C. A., & DeMartino, G. N. (1992). Identification, purification, and characterization of a protein activator (PA28) of the 20 S proteasome (macropain). *J Biol Chem, 267*(15), 10515-10523.

Manasanch, E. E., & Orlowski, R. Z. (2017). Proteasome inhibitors in cancer therapy. *Nat Rev Clin Oncol, 14*(7), 417-433. doi:10.1038/nrclinonc.2016.206

Mao, X. M., Ren, N. N., Sun, N., Wang, F., Zhou, R. C., Tang, Y., & Li, Y. Q. (2014). Proteasome involvement in a complex cascade mediating SigT degradation during differentiation of Streptomyces coelicolor. *FEBS Lett, 588*(4), 608-613. doi:10.1016/j.febslet.2013.12.029

Marques, A. J., Glanemann, C., Ramos, P. C., & Dohmen, R. J. (2007). The C-terminal extension of the beta7 subunit and activator complexes stabilize nascent 20 S proteasomes and promote their maturation. *J Biol Chem, 282*(48), 34869-34876. doi:M705836200 [pii]10.1074/jbc.M705836200

Masson, P., Andersson, O., Petersen, U. M., & Young, P. (2001). Identification and characterization of a Drosophila nuclear proteasome regulator. A homolog of human 11 S REGgamma (PA28gamma). *J Biol Chem, 276*(2), 1383-1390. doi:10.1074/jbc.M007379200M007379200 [pii]

Masters, E. I., Pratt, G., Forster, A., & Hill, C. P. (2005). Purification and analysis of recombinant 11S activators of the 20S proteasome: Trypanosoma brucei PA26 and human PA28 alpha, PA28 beta, and PA28 gamma. *Methods Enzymol, 398*, 306-321. doi:10.1016/S0076-6879(05)98025-7

Matsumoto, R., Akama, K., Rakwal, R., & Iwahashi, H. (2005). The stress response against denatured proteins in the deletion of cytosolic chaperones SSA1/2 is different from heat-shock response in Saccharomyces cerevisiae. *BMC Genomics, 6*, 141. doi:10.1186/1471-2164-6-141

Maupin-Furlow, J. A. (2013). Ubiquitin-like proteins and their roles in archaea. *Trends Microbiol, 21*(1), 31-38. doi:10.1016/j.tim.2012.09.006

Mellacheruvu, D., Wright, Z., Couzens, A. L., Lambert, J. P., St-Denis, N. A., Li, T., . . . Nesvizhskii, A. I. (2013). The CRAPome: a contaminant repository for affinity purification-mass spectrometry data. *Nat Methods, 10*(8), 730-736. doi:10.1038/nmeth.2557

Metzger, M. B., Maurer, M. J., Dancy, B. M., & Michaelis, S. (2008). Degradation of a cytosolic protein requires endoplasmic reticulum-associated degradation machinery. *J Biol Chem, 283*(47), 32302-32316. doi:10.1074/jbc.M806424200

Meyer, H. J., & Rape, M. (2014). Enhanced protein degradation by branched ubiquitin chains. *Cell, 157*(4), 910-921. doi:10.1016/j.cell.2014.03.037

Miranda, H. V., Antelmann, H., Hepowit, N., Chavarria, N. E., Krause, D. J., Pritz, J. R., . . . Maupin-Furlow, J. A. (2014). Archaeal ubiquitin-like SAMP3 is isopeptide-linked to proteins via a UbaA-dependent mechanism. *Mol Cell Proteomics, 13*(1), 220-239. doi:10.1074/mcp.M113.029652

Miranda, H. V., Nembhard, N., Su, D., Hepowit, N., Krause, D. J., Pritz, J. R., . . . Maupin-Furlow, J. A. (2011). E1- and ubiquitin-like proteins provide a direct link between protein conjugation and sulfur transfer in archaea. *Proc Natl Acad Sci U S A, 108*(11), 4417-4422. doi:10.1073/pnas.1018151108

Moreau, P., Masszi, T., Grzasko, N., Bahlis, N. J., Hansson, M., Pour, L., . . . Group, T.-M. S. (2016). Oral Ixazomib, Lenalidomide, and Dexamethasone for Multiple Myeloma. *N Engl J Med, 374*(17), 1621-1634. doi:10.1056/NEJMoa1516282

Mumberg, D., Muller, R., & Funk, M. (1995). Yeast vectors for the controlled expression of heterologous proteins in different genetic backgrounds. *Gene, 156*(1), 119-122.

Murata, S., Kawahara, H., Tohma, S., Yamamoto, K., Kasahara, M., Nabeshima, Y., . . . Chiba, T. (1999). Growth retardation in mice lacking the proteasome activator PA28gamma. *J Biol Chem, 274*(53), 38211-38215.

Murata, S., Sasaki, K., Kishimoto, T., Niwa, S., Hayashi, H., Takahama, Y., & Tanaka, K. (2007). Regulation of CD8+ T cell development by thymus-specific proteasomes. *Science, 316*(5829), 1349-1353. doi:316/5829/1349 [pii]10.1126/science.1141915

Murata, S., Udono, H., Tanahashi, N., Hamada, N., Watanabe, K., Adachi, K., . . . Chiba, T. (2001). Immunoproteasome assembly and antigen presentation in mice lacking both PA28alpha and PA28beta. *EMBO J, 20*(21), 5898-5907. doi:10.1093/emboj/20.21.5898

Nandi, D., Woodward, E., Ginsburg, D. B., & Monaco, J. J. (1997). Intermediates in the formation of mouse 20S proteasomes: implications for the assembly of precursor beta subunits. *EMBO J, 16*(17), 5363-5375. doi:10.1093/emboj/16.17.5363

Nelson, R. J., Heschl, M. F., & Craig, E. A. (1992). Isolation and characterization of extragenic suppressors of mutations in the SSA hsp70 genes of Saccharomyces cerevisiae. *Genetics, 131*(2), 277-285.

Nicholson, S., Bonecini-Almeida Mda, G., Lapa e Silva, J. R., Nathan, C., Xie, Q. W., Mumford, R., . . . Ho, J. L. (1996). Inducible nitric oxide synthase in pulmonary alveolar macrophages from patients with tuberculosis. *J Exp Med, 183*(5), 2293-2302.

Nitta, T., Kochi, Y., Muro, R., Tomofuji, Y., Okamura, T., Murata, S., . . . Takayanagi, H. (2017). Human thymoproteasome variations influence CD8 T cell selection. *Sci Immunol, 2*(12). doi:10.1126/sciimmunol.aan5165

Ohba, M. (1994). A 70-kDa heat shock cognate protein suppresses the defects caused by a proteasome mutation in Saccharomyces cerevisiae. *FEBS Lett, 351*(2), 263-266.

Ohba, M. (1997). Modulation of intracellular protein degradation by SSB1-SIS1 chaperon system in yeast S. cerevisiae. *FEBS Lett, 409*(2), 307-311.

Oling, D., Eisele, F., Kvint, K., & Nystrom, T. (2014). Opposing roles of Ubp3-dependent deubiquitination regulate replicative life span and heat resistance. *EMBO J, 33*(7), 747-761. doi:10.1002/embj.201386822

Padmanabhan, A., Vuong, S. A., & Hochstrasser, M. (2016). Assembly of an Evolutionarily Conserved Alternative Proteasome Isoform in Human Cells. *Cell Rep, 14*(12), 2962-2974. doi:10.1016/j.celrep.2016.02.068

Panfair, D., Ramamurthy, A., & Kusmierczyk, A. R. (2015). Alpha-ring independent assembly of the 20S proteasome. *Sci Rep, 5*, 13130. doi:10.1038/srep13130

Pearce, M. J., Mintseris, J., Ferreyra, J., Gygi, S. P., & Darwin, K. H. (2008). Ubiquitin-like protein involved in the proteasome pathway of Mycobacterium tuberculosis. *Science, 322*(5904), 1104-1107. doi:10.1126/science.1163885

Pfund, C., Huang, P., Lopez-Hoyo, N., & Craig, E. A. (2001). Divergent functional properties of the ribosome-associated molecular chaperone Ssb compared with other Hsp70s. *Mol Biol Cell, 12*(12), 3773-3782.

Pickering, A. M., & Davies, K. J. (2012). Differential roles of proteasome and immunoproteasome regulators Pa28alphabeta, Pa28gamma and Pa200 in the degradation of oxidized proteins. *Arch Biochem Biophys, 523*(2), 181-190. doi:10.1016/j.abb.2012.04.018

Plemper, R. K., Bohmler, S., Bordallo, J., Sommer, T., & Wolf, D. H. (1997). Mutant analysis links the translocon and BiP to retrograde protein transport for ER degradation. *Nature, 388*(6645), 891-895. doi:10.1038/42276

Preckel, T., Fung-Leung, W. P., Cai, Z., Vitiello, A., Salter-Cid, L., Winqvist, O., . . . Yang, Y. (1999). Impaired immunoproteasome assembly and immune responses in PA28-/- mice. *Science, 286*(5447), 2162-2165. doi:8078 [pii]

Qian, M. X., Pang, Y., Liu, C. H., Haratake, K., Du, B. Y., Ji, D. Y., . . . Qiu, X. B. (2013). Acetylation-mediated proteasomal degradation of core histones during DNA repair and spermatogenesis. *Cell, 153*(5), 1012-1024. doi:10.1016/j.cell.2013.04.032S0092-8674(13)00508-4 [pii]

Rabl, J., Smith, D. M., Yu, Y., Chang, S. C., Goldberg, A. L., & Cheng, Y. (2008). Mechanism of gate opening in the 20S proteasome by the proteasomal ATPases. *Mol Cell, 30*(3), 360-368. doi:S1097-2765(08)00175-5 [pii]10.1016/j.molcel.2008.03.004

Raedler, L. (2015). Velcade (Bortezomib) Receives 2 New FDA Indications: For Retreatment of Patients with Multiple Myeloma and for First-Line Treatment of Patients with Mantle-Cell Lymphoma. *Am Health Drug Benefits, 8*(Spec Feature), 135-140.

Raedler, L. A. (2016). Ninlaro (Ixazomib): First Oral Proteasome Inhibitor Approved for the Treatment of Patients with Relapsed or Refractory Multiple Myeloma. *Am Health Drug Benefits, 9*(Spec Feature), 102-105.

Ramos, P. C., Hockendorff, J., Johnson, E. S., Varshavsky, A., & Dohmen, R. J. (1998). Ump1p is required for proper maturation of the 20S proteasome and becomes its substrate upon completion of the assembly. *Cell, 92*(4), 489-499. doi:S0092-8674(00)80942-3 [pii]

Ramos, P. C., Marques, A. J., London, M. K., & Dohmen, R. J. (2004). Role of C-terminal extensions of subunits beta2 and beta7 in assembly and activity of eukaryotic proteasomes. *J Biol Chem, 279*(14), 14323-14330. doi:10.1074/jbc.M308757200

Raule, M., Cerruti, F., & Cascio, P. (2014). Enhanced rate of degradation of basic proteins by 26S immunoproteasomes. *Biochim Biophys Acta, 1843*(9), 1942-1947. doi:10.1016/j.bbamcr.2014.05.005

Realini, C., Dubiel, W., Pratt, G., Ferrell, K., & Rechsteiner, M. (1994). Molecular cloning and expression of a gamma-interferon-inducible activator of the multicatalytic protease. *J Biol Chem, 269*(32), 20727-20732.

Rechsteiner, M., Realini, C., & Ustrell, V. (2000). The proteasome activator 11 S REG (PA28) and class I antigen presentation. *Biochem J, 345 Pt 1*, 1-15. reference, T. i. a. p.

Reuter, C. J., Kaczowka, S. J., & Maupin-Furlow, J. A. (2004). Differential regulation of the PanA and PanB proteasome-activating nucleotidase and 20S proteasomal proteins of the haloarchaeon Haloferax volcanii. *J Bacteriol, 186*(22), 7763-7772. doi:10.1128/JB.186.22.7763-7772.2004

Richardson, P. G., & Anderson, K. C. (2003). Bortezomib: a novel therapy approved for multiple myeloma. *Clin Adv Hematol Oncol, 1*(10), 596-600.

Rock, K. L., & Goldberg, A. L. (1999). Degradation of cell proteins and the generation of MHC class I-presented peptides. *Annu Rev Immunol, 17*, 739-779. doi:10.1146/annurev.immunol.17.1.739

Roelofs, J., Park, S., Haas, W., Tian, G., McAllister, F. E., Huo, Y., . . . Finley, D. (2009). Chaperone-mediated pathway of proteasome regulatory particle assembly. *Nature, 459*(7248), 861-865. doi:10.1038/nature08063

Sa-Moura, B., Funakoshi, M., Tomko, R. J., Jr., Dohmen, R. J., Wu, Z., Peng, J., & Hochstrasser, M. (2013). A conserved protein with AN1 zinc finger and ubiquitin-like domains modulates Cdc48 (p97) function in the ubiquitin-proteasome pathway. *J Biol Chem, 288*(47), 33682-33696. doi:10.1074/jbc.M113.521088

Sa-Moura, B., Simoes, A. M., Fraga, J., Fernandes, H., Abreu, I. A., Botelho, H. M., . . . Macedo-Ribeiro, S. (2013). Biochemical and biophysical characterization of recombinant yeast proteasome maturation factor ump1. *Comput Struct Biotechnol J, 7*, e201304006. doi:10.5936/csbj.201304006

Sadre-Bazzaz, K., Whitby, F. G., Robinson, H., Formosa, T., & Hill, C. P. (2010). Structure of a Blm10 complex reveals common mechanisms for proteasome binding and gate opening. *Mol Cell, 37*(5), 728-735. doi:10.1016/j.molcel.2010.02.002

Saeki, Y., Sone, T., Toh-e, A., & Yokosawa, H. (2002). Identification of ubiquitin-like protein-binding subunits of the 26S proteasome. *Biochem Biophys Res Commun, 296*(4), 813-819.

Saeki, Y., & Tanaka, K. (2007). Unlocking the proteasome door. *Mol Cell, 27*(6), 865-867. doi:S1097-2765(07)00585-0 [pii]10.1016/j.molcel.2007.09.001

Saeki, Y., Toh, E. A., Kudo, T., Kawamura, H., & Tanaka, K. (2009). Multiple proteasome-interacting proteins assist the assembly of the yeast 19S regulatory particle. *Cell, 137*(5), 900-913. doi:S0092-8674(09)00528-5 [pii]10.1016/j.cell.2009.05.005

Samanovic, M. I., & Darwin, K. H. (2016). Game of 'Somes: Protein Destruction for Mycobacterium tuberculosis Pathogenesis. *Trends Microbiol, 24*(1), 26-34. doi:10.1016/j.tim.2015.10.001

Sasaki, K., Hamazaki, J., Koike, M., Hirano, Y., Komatsu, M., Uchiyama, Y., . . . Murata, S. (2010). PAC1 gene knockout reveals an essential role of chaperone-mediated 20S proteasome biogenesis and latent 20S proteasomes in cellular homeostasis. *Mol Cell Biol, 30*(15), 3864-3874. doi:MCB.00216-10 [pii]10.1128/MCB.00216-10

Schmidt, M., & Finley, D. (2014). Regulation of proteasome activity in health and disease. *Biochim Biophys Acta, 1843*(1), 13-25. doi:10.1016/j.bbamcr.2013.08.012

Schmidt, M., Haas, W., Crosas, B., Santamaria, P. G., Gygi, S. P., Walz, T., & Finley, D. (2005). The HEAT repeat protein Blm10 regulates the yeast proteasome by capping the core particle. *Nat Struct Mol Biol, 12*(4), 294-303. doi:10.1038/nsmb914

Schmidtke, G., Schmidt, M., & Kloetzel, P. M. (1997). Maturation of mammalian 20 S proteasome: purification and characterization of 13 S and 16 S proteasome precursor complexes. *J Mol Biol, 268*(1), 95-106. doi:10.1006/jmbi.1997.0947

Schweitzer, A., Aufderheide, A., Rudack, T., Beck, F., Pfeifer, G., Plitzko, J. M., . . . Baumeister, W. (2016). Structure of the human 26S proteasome at a resolution of 3.9 A. *Proc Natl Acad Sci U S A, 113*(28), 7816-7821. doi:10.1073/pnas.1608050113

Shah, J., Niesvizky, R., Stadtmauer, E., Rifkin, R. M., Berenson, J., Berdeja, J. G., . . . Usmani, S. (2015). Oprozomib, Pomalidomide, and Dexamethasone (OPomd) in Patients (Pts) with Relapsed and/or Refractory Multiple Myeloma (RRMM): Initial Results of a Phase 1b Study (NCT01999335). *Blood, 126*(23), 378-378.

Shah, S. A., Potter, M. W., McDade, T. P., Ricciardi, R., Perugini, R. A., Elliott, P. J., . . . Callery, M. P. (2001). 26S proteasome inhibition induces apoptosis and limits growth of human pancreatic cancer. *J Cell Biochem, 82*(1), 110-122.

Sharon, M., Witt, S., Glasmacher, E., Baumeister, W., & Robinson, C. V. (2007). Mass spectrometry reveals the missing links in the assembly pathway of the bacterial 20 S proteasome. *J Biol Chem, 282*(25), 18448-18457. doi:10.1074/jbc.M701534200

Shiber, A., Breuer, W., Brandeis, M., & Ravid, T. (2013). Ubiquitin conjugation triggers misfolded protein sequestration into quality control foci when Hsp70 chaperone levels are limiting. *Mol Biol Cell, 24*(13), 2076-2087. doi:10.1091/mbc.E13-01-0010

Shiber, A., & Ravid, T. (2014). Chaperoning proteins for destruction: diverse roles of Hsp70 chaperones and their co-chaperones in targeting misfolded proteins to the proteasome. *Biomolecules, 4*(3), 704-724. doi:10.3390/biom4030704

Shimizu, N., Ueno, K., Kurita, E., Shin, S. W., Nishihara, T., Amano, T., . . . Matsumoto, K. (2014). Possible role of ZPAC, zygote-specific proteasome assembly chaperone, during spermatogenesis in the mouse. *J Reprod Dev, 60*(3), 179-186.

Shin, S. W., Shimizu, N., Tokoro, M., Nishikawa, S., Hatanaka, Y., Anzai, M., . . . Matsumoto, K. (2013). Mouse zygote-specific proteasome assembly chaperone important for maternal-to-zygotic transition. *Biol Open, 2*(2), 170-182. doi:10.1242/bio.20123020

Siegel, D. (2012). Initial success, frequent recurrence: tomorrow's multiple myeloma treatments and the value of subtype analysis. Interview with David Siegel. *Am J Manag Care, 18*(5 Spec No.), SP226-227, cover.

Sikdar, A., Satoh, T., Kawasaki, M., & Kato, K. (2014). Crystal structure of archaeal homolog of proteasome-assembly chaperone PbaA. *Biochem Biophys Res Commun, 453*(3), 493-497. doi:10.1016/j.bbrc.2014.09.114

Smith, D. M., Chang, S. C., Park, S., Finley, D., Cheng, Y., & Goldberg, A. L. (2007). Docking of the proteasomal ATPases' carboxyl termini in the 20S proteasome's alpha ring opens the gate for substrate entry. *Mol Cell, 27*(5), 731-744. doi:S1097-2765(07)00445-5 [pii]10.1016/j.molcel.2007.06.033

Smith, D. M., Kafri, G., Cheng, Y., Ng, D., Walz, T., & Goldberg, A. L. (2005). ATP binding to PAN or the 26S ATPases causes association with the 20S proteasome, gate opening, and translocation of unfolded proteins. *Mol Cell, 20*(5), 687-698. doi:10.1016/j.molcel.2005.10.019

Stadtmueller, B. M., Kish-Trier, E., Ferrell, K., Petersen, C. N., Robinson, H., Myszka, D. G., . . . Hill, C. P. (2012). Structure of a proteasome Pba1-Pba2 complex: implications for proteasome assembly, activation, and biological function. *J Biol Chem, 287*(44), 37371-37382. doi:10.1074/jbc.M112.367003

Striebel, F., Hunkeler, M., Summer, H., & Weber-Ban, E. (2010). The mycobacterial Mpa-proteasome unfolds and degrades pupylated substrates by engaging Pup's N-terminus. *EMBO J, 29*(7), 1262-1271. doi:10.1038/emboj.2010.23

Striebel, F., Imkamp, F., Sutter, M., Steiner, M., Mamedov, A., & Weber-Ban, E. (2009). Bacterial ubiquitin-like modifier Pup is deamidated and conjugated to substrates by distinct but homologous enzymes. *Nat Struct Mol Biol, 16*(6), 647-651. doi:10.1038/nsmb.1597

Su, H., Yang, J. R., Xu, T., Huang, J., Xu, L., Yuan, Y., & Zhuang, S. M. (2009). MicroRNA-101, down-regulated in hepatocellular carcinoma, promotes apoptosis and suppresses tumorigenicity. *Cancer Res, 69*(3), 1135-1142. doi:10.1158/0008-5472.CAN-08-2886

Summer, H., Bruderer, R., & Weber-Ban, E. (2006). Characterization of a new AAA+ protein from archaea. *J Struct Biol, 156*(1), 120-129. doi:10.1016/j.jsb.2006.01.010

Sun, G., & Anderson, V. E. (2004). Prevention of artifactual protein oxidation generated during sodium dodecyl sulfate-gel electrophoresis. *Electrophoresis, 25*(7-8), 959-965. doi:10.1002/elps.200305800

Takagi, K., Saeki, Y., Yashiroda, H., Yagi, H., Kaiho, A., Murata, S., . . . Kato, K. (2014). Pba3-Pba4 heterodimer acts as a molecular matchmaker in proteasome alpha-ring formation. *Biochem Biophys Res Commun, 450*(2), 1110-1114. doi:10.1016/j.bbrc.2014.06.119

Tamura, T., Nagy, I., Lupas, A., Lottspeich, F., Cejka, Z., Schoofs, G., . . . Baumeister, W. (1995). The first characterization of a eubacterial proteasome: the 20S complex of Rhodococcus. *Curr Biol, 5*(7), 766-774. doi:S0960-9822(95)00153-9 [pii]

Tanahashi, N., Murakami, Y., Minami, Y., Shimbara, N., Hendil, K. B., & Tanaka, K. (2000). Hybrid proteasomes. Induction by interferon-gamma and contribution to ATP-dependent proteolysis. *J Biol Chem, 275*(19), 14336-14345.

Tanaka, K. (1994). Role of proteasomes modified by interferon-gamma in antigen processing. *J Leukoc Biol, 56*(5), 571-575.

Thompson, J. L. (2013). Carfilzomib: a second-generation proteasome inhibitor for the treatment of relapsed and refractory multiple myeloma. *Ann Pharmacother, 47*(1), 56-62. doi:10.1345/aph.1R561

Tian, G., Park, S., Lee, M. J., Huck, B., McAllister, F., Hill, C. P., . . . Finley, D. (2011). An asymmetric interface between the regulatory and core particles of the proteasome. *Nat Struct Mol Biol, 18*(11), 1259-1267. doi:10.1038/nsmb.2147nsmb.2147 [pii]

To, W. Y., & Wang, C. C. (1997). Identification and characterization of an activated 20S proteasome in Trypanosoma brucei. *FEBS Lett, 404*(2-3), 253-262.

Tomko, R. J., Jr., Funakoshi, M., Schneider, K., Wang, J., & Hochstrasser, M. (2010). Heterohexameric ring arrangement of the eukaryotic proteasomal ATPases: implications for proteasome structure and assembly. *Mol Cell, 38*(3), 393-403. doi:10.1016/j.molcel.2010.02.035

Tomko, R. J., Jr., & Hochstrasser, M. (2011). Incorporation of the Rpn12 subunit couples completion of proteasome regulatory particle lid assembly to lid-base joining. *Mol Cell, 44*(6), 907-917. doi:10.1016/j.molcel.2011.11.020

Tomko, R. J., Jr., & Hochstrasser, M. (2013). Molecular architecture and assembly of the eukaryotic proteasome. *Annu Rev Biochem, 82*, 415-445. doi:10.1146/annurev-biochem-060410-150257

Uechi, H., Hamazaki, J., & Murata, S. (2014). Characterization of the testis-specific proteasome subunit alpha4s in mammals. *J Biol Chem, 289*(18), 12365-12374. doi:10.1074/jbc.M114.558866

Uekusa, Y., Okawa, K., Yagi-Utsumi, M., Serve, O., Nakagawa, Y., Mizushima, T., . . . Kato, K. (2013). Backbone H, C, and N assignments of yeast Ump1, an intrinsically disordered protein that functions as a proteasome assembly chaperone. *Biomol NMR Assign*. doi:10.1007/s12104-013-9523-1

Ustrell, V., Hoffman, L., Pratt, G., & Rechsteiner, M. (2002). PA200, a nuclear proteasome activator involved in DNA repair. *EMBO J, 21*(13), 3516-3525. doi:10.1093/emboj/cdf333

Valas, R. E., & Bourne, P. E. (2008). Rethinking proteasome evolution: two novel bacterial proteasomes. *J Mol Evol, 66*(5), 494-504. doi:10.1007/s00239-008-9075-7

Varambally, S., Cao, Q., Mani, R. S., Shankar, S., Wang, X., Ateeq, B., . . . Chinnaiyan, A. M. (2008). Genomic loss of microRNA-101 leads to overexpression of histone methyltransferase EZH2 in cancer. *Science, 322*(5908), 1695-1699. doi:10.1126/science.1165395

Velichutina, I., Connerly, P. L., Arendt, C. S., Li, X., & Hochstrasser, M. (2004). Plasticity in eucaryotic 20S proteasome ring assembly revealed by a subunit deletion in yeast. *EMBO J, 23*(3), 500-510. doi:10.1038/sj.emboj.76000597600059 [pii]

Verma, R., Aravind, L., Oania, R., McDonald, W. H., Yates, J. R., 3rd, Koonin, E. V., & Deshaies, R. J. (2002). Role of Rpn11 metalloprotease in deubiquitination and degradation by the 26S proteasome. *Science, 298*(5593), 611-615. doi:10.1126/science.1075898

Verma, R., Chen, S., Feldman, R., Schieltz, D., Yates, J., Dohmen, J., & Deshaies, R. J. (2000). Proteasomal proteomics: identification of nucleotide-sensitive proteasome-interacting proteins by mass spectrometric analysis of affinity-purified proteasomes. *Mol Biol Cell, 11*(10), 3425-3439.

Voges, D., Zwickl, P., & Baumeister, W. (1999). The 26S proteasome: a molecular machine designed for controlled proteolysis. *Annu Rev Biochem, 68*, 1015-1068. doi:10.1146/annurev.biochem.68.1.1015

Volker, C., & Lupas, A. N. (2002). Molecular evolution of proteasomes. *Curr Top Microbiol Immunol, 268*, 1-22.

Wang, C. H., Liu, C. Y., Lin, H. C., Yu, C. T., Chung, K. F., & Kuo, H. P. (1998). Increased exhaled nitric oxide in active pulmonary tuberculosis due to inducible NO synthase upregulation in alveolar macrophages. *Eur Respir J, 11*(4), 809-815.

Wani, P. S., Rowland, M. A., Ondracek, A., Deeds, E. J., & Roelofs, J. (2015). Maturation of the proteasome core particle induces an affinity switch that controls regulatory particle association. *Nat Commun, 6*, 6384. doi:10.1038/ncomms7384

Wilk, S., Chen, W. E., & Magnusson, R. P. (2000). Properties of the beta subunit of the proteasome activator PA28 (11S REG). *Arch Biochem Biophys, 384*(1), 174-180. doi:10.1006/abbi.2000.2112

Wilson, H. L., Ou, M. S., Aldrich, H. C., & Maupin-Furlow, J. (2000). Biochemical and physical properties of the Methanococcus jannaschii 20S proteasome and PAN, a homolog of the ATPase (Rpt) subunits of the eucaryal 26S proteasome. *J Bacteriol, 182*(6), 1680-1692.

Witt, E., Zantopf, D., Schmidt, M., Kraft, R., Kloetzel, P. M., & Kruger, E. (2000). Characterisation of the newly identified human Ump1 homologue POMP and analysis of LMP7(beta 5i) incorporation into 20 S proteasomes. *J Mol Biol, 301*(1), 1-9. doi:10.1006/jmbi.2000.3959

Wolf, S., Nagy, I., Lupas, A., Pfeifer, G., Cejka, Z., Muller, S. A., . . . Baumeister, W. (1998). Characterization of ARC, a divergent member of the AAA ATPase family from Rhodococcus erythropolis. *J Mol Biol, 277*(1), 13-25. doi:10.1006/jmbi.1997.1589

Xie, Y., & Varshavsky, A. (2001). RPN4 is a ligand, substrate, and transcriptional regulator of the 26S proteasome: a negative feedback circuit. *Proc Natl Acad Sci U S A, 98*(6), 3056-3061. doi:10.1073/pnas.07102229898/6/3056 [pii]

Xu, P., Duong, D. M., Seyfried, N. T., Cheng, D., Xie, Y., Robert, J., . . . Peng, J. (2009). Quantitative proteomics reveals the function of unconventional ubiquitin chains in proteasomal degradation. *Cell, 137*(1), 133-145. doi:S0092-8674(09)00089-0 [pii]10.1016/j.cell.2009.01.041

Yamano, T., Mizukami, S., Murata, S., Chiba, T., Tanaka, K., & Udono, H. (2008). Hsp90-mediated assembly of the 26 S proteasome is involved in major histocompatibility complex class I antigen processing. *J Biol Chem, 283*(42), 28060-28065. doi:10.1074/jbc.M803077200

Yao, T., & Cohen, R. E. (2002). A cryptic protease couples deubiquitination and degradation by the proteasome. *Nature, 419*(6905), 403-407. doi:10.1038/nature01071

Yao, Y., Huang, L., Krutchinsky, A., Wong, M. L., Standing, K. G., Burlingame, A. L., & Wang, C. C. (1999). Structural and functional characterizations of the proteasome-activating protein PA26 from Trypanosoma brucei. *J Biol Chem, 274*(48), 33921-33930.

Yao, Y., Toth, C. R., Huang, L., Wong, M. L., Dias, P., Burlingame, A. L., . . . Wang, C. C. (1999). alpha5 subunit in Trypanosoma brucei proteasome can self-assemble to form a cylinder of four stacked heptamer rings. *Biochem J, 344 Pt 2*, 349-358.

Yashiroda, H., Mizushima, T., Okamoto, K., Kameyama, T., Hayashi, H., Kishimoto, T., . . . Tanaka, K. (2008). Crystal structure of a chaperone complex that contributes to the assembly of yeast 20S proteasomes. *Nat Struct Mol Biol, 15*(3), 228-236. doi:nsmb.1386 [pii]10.1038/nsmb.1386

Yashiroda, H., Toda, Y., Otsu, S., Takagi, K., Mizushima, T., & Murata, S. (2015). N-terminal alpha7 deletion of the proteasome 20S core particle substitutes for yeast PI31 function. *Mol Cell Biol, 35*(1), 141-152. doi:10.1128/MCB.00582-14

Yu, Y., Smith, D. M., Kim, H. M., Rodriguez, V., Goldberg, A. L., & Cheng, Y. (2010). Interactions of PAN's C-termini with archaeal 20S proteasome and implications for the eukaryotic proteasome-ATPase interactions. *EMBO J, 29*(3), 692-702. doi:10.1038/emboj.2009.382

Zhang, H., Xu, X., Gajewiak, J., Tsukahara, R., Fujiwara, Y., Liu, J., . . . Prestwich, G. D. (2009). Dual activity lysophosphatidic acid receptor pan-antagonist/autotaxin inhibitor reduces breast cancer cell migration in vitro and causes tumor regression in vivo. *Cancer Res, 69*(13), 5441-5449. doi:10.1158/0008-5472.CAN-09-0302

Zhang, X., Schulz, R., Edmunds, S., Kruger, E., Markert, E., Gaedcke, J., . . . Dobbelstein, M. (2015). MicroRNA-101 Suppresses Tumor Cell Proliferation by Acting as an Endogenous Proteasome Inhibitor via Targeting the Proteasome Assembly Factor POMP. *Mol Cell, 59*(2), 243-257. doi:10.1016/j.molcel.2015.05.036

Zhang, Z., Krutchinsky, A., Endicott, S., Realini, C., Rechsteiner, M., & Standing, K. G. (1999). Proteasome activator 11S REG or PA28: recombinant REG alpha/REG beta hetero-oligomers are heptamers. *Biochemistry, 38*(17), 5651-5658. doi:10.1021/bi990056+

Zhang, Z., & Zhang, R. (2008). Proteasome activator PA28 gamma regulates p53 by enhancing its MDM2-mediated degradation. *EMBO J, 27*(6), 852-864. doi:10.1038/emboj.2008.25

Zhong, L., & Belote, J. M. (2007). The testis-specific proteasome subunit Prosalpha6T of D. melanogaster is required for individualization and nuclear maturation during spermatogenesis. *Development, 134*(19), 3517-3525. doi:dev.004770 [pii]10.1242/dev.004770

Zuhl, F., Seemuller, E., Golbik, R., & Baumeister, W. (1997). Dissecting the assembly pathway of the 20S proteasome. *FEBS Lett, 418*(1-2), 189-194. doi:S0014-5793(97)01370-7 [pii]

Zwickl, P., Grziwa, A., Puhler, G., Dahlmann, B., Lottspeich, F., & Baumeister, W. (1992). Primary structure of the Thermoplasma proteasome and its implications for the structure, function, and evolution of the multicatalytic proteinase. *Biochemistry, 31*(4), 964-972.

Zwickl, P., Kleinz, J., & Baumeister, W. (1994). Critical elements in proteasome assembly. *Nat Struct Biol, 1*(11), 765-770.

Zwickl, P., Ng, D., Woo, K. M., Klenk, H. P., & Goldberg, A. L. (1999). An archaebacterial ATPase, homologous to ATPases in the eukaryotic 26 S proteasome, activates protein breakdown by 20 S proteasomes. *J Biol Chem, 274*(37), 26008-26014.

Zwickl, P., Voges, D., & Baumeister, W. (1999). The proteasome: a macromolecular assembly designed for controlled proteolysis. *Philos Trans R Soc Lond B Biol Sci, 354*(1389), 1501-1511. doi:10.1098/rstb.1999.0494

APPENDIX A. SUPPLEMENTARY FOR CHAPTER 2

Supplementary Note

In the Discussion section of the main-text, we argue that α4 HMWCs may not be as stable on native PAGE as other CP-related species, requiring the presence of α4CC to visualize them (Figure 3 and Supplementary Figure 8). It deserves mention that although $CuCl_2$-induced crosslinking was used to observe the α4 HMWCs by non-reducing SDS-PAGE in Figure 1B, it was not used prior to analysis of the same samples by native PAGE (Figure 2A). The primary reason for this is that following $CuCl_2$ treatment, the species migrating faster than the CP appear as a uniform smear on native PAGE (not shown). This treatment is too oxidizing for the multi-protein species to resolve into distinct bands on the native gel and would have resulted in us not being able to identify the α4 HMWCs.

However, we have shown before that experimental conditions during lysis, especially protracted periods of purification, are sufficiently oxidizing to enable (some) crosslinking to occur (Panfair et al., 2015). This is clearly seen in Figure 4A, whereby the his flow through samples following the lengthy depletion analysis exhibited essentially complete crosslinking of α4CC, even in the absence of $CuCl_2$. Contrast this with Figure 1B, which shows the sample after a much shorter protocol (Flag purification only, no depletion) and requires $CuCl_2$ for visualization of the slow migrating α4 species. Finally, the process of electrophoresis is itself oxidizing to proteins ((Sun & Anderson, 2004) and references therein), and the native PAGE here is carried out over a period of 10 hours. This also should provide considerable time for (some) crosslinking to occur. Therefore, even if the efficiency of crosslinking does not approach 100% in the absence of exogenously added $CuCl_2$ (as may be the case following Flag purification only), enough crosslinking is likely taking place during electrophoresis that a homomeric ring (such as the α4 HMWC) can be stabilized and thus survive native PAGE.

Supplementary Table 1: Yeast Strains used in Chapter 2

Name	Genotype
AKY889	MATa *his3-*Δ*200 leu2-3,112 ura3-52 lys2-801 trp1-1 pre6Δ*::HIS3 [pRS315 pre6-Flag]
AKY892	MATα *his3-*Δ*200 leu2-3,112 ura3-52 lys2-801 trp1-1 pre9*Δ::HIS3 pre6Δ::HIS3 [pRS315 pre6N79C,I155C-Flag]
AKY893	MATa *his3-*Δ*200 leu2-3,112 ura3-52 lys2-801 trp1-1 pre6*Δ::HIS3 [pRS315 pre6N79C,I155C-Flag]
AKY1145	MATa *his3-*Δ*200 leu2-3,112 ura3-52 lys2-801 trp1-1 pre9Δ*::HIS3 pre6Δ::HIS3 [pRS315 pre6N79C,I155C-Flag]
AKY1066	MATa *his3-*Δ*200 leu2-3,112 ura3-52 lys2-801 trp1-1 pre8*-HF(URA)
AKY1100	MATa *his3-*Δ*200 leu2-3,112 ura3-52 lys2-801 trp1-1 pre8*-HF(URA) *pre9Δ*::HIS3 *pre6Δ*::HIS3 [pRS315 pre6N79C,I155C-Flag]
AKY1168	MATa *his3-*Δ*200 leu2-3,112 ura3-52 lys2-801 trp1-1 pre9Δ*::HIS3 *pre6Δ*::HIS3 [pRS315 pre6-Flag]

All strains generated in this study.

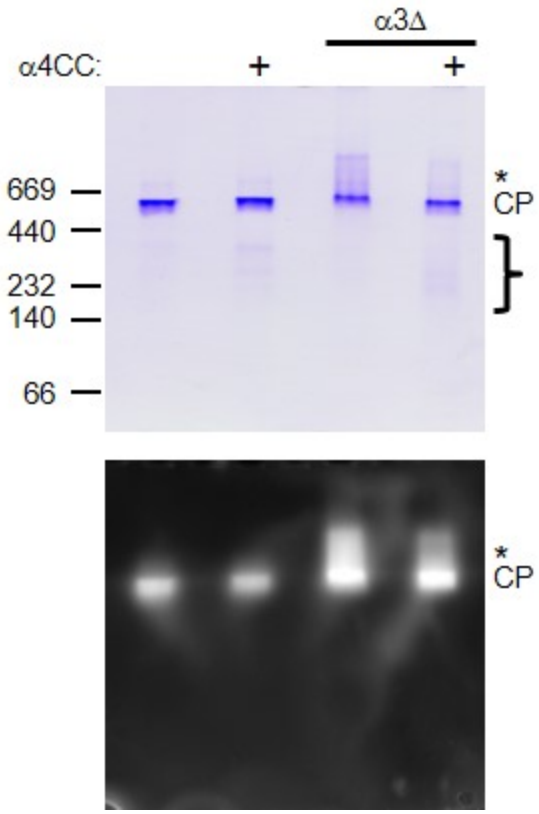

Supplementary Figure 1. Yeast lysates from the indicated strains were bound to Flag resin
The Flag-purified CP was subjected to native PAGE and substrate overlay assay. The gel was stained with Gelcode blue and the migration of molecular size standards is indicated at left. CP denotes migration of the core particle. Asterisk denotes migration of CP-Blm10 complexes. Faster migrating species, likely containing CP assembly intermediates, is denoted by the bracket. This figure demonstrates the requirement for loading of excess protein onto native PAGE in order to better visualize the faster migrating species of interest.

α/β-subunits	# Peptides	# PSMs	% Coverage	Other proteins	# Peptides	# PSMs	% Coverage
α1	22	**78**	88	**PBA1**	12	**54**	62
α2	12	**65**	52	**PBA2**	9	**27**	32
α3	19	**58**	74	**UMP1**	3	**22**	23
α4	16	**135**	79	**EMC29**	5	**5**	4
α5	17	**34**	60	**RKR1**	5	**5**	10
α6	19	**60**	84	**BLM10**	6	**8**	5
α7	16	**49**	61	**HSP60**	3	**4**	7
β1	6	**7**	35	**PFK26**	9	**9**	14
β2	9	**69**	32	**TDH2**	3	**4**	21
β3	8	**38**	47				
β4	10	**20**	47				
β5	8	**9**	33				
β6	5	**12**	35				

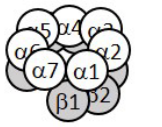

15S intermediate

Supplementary Figure 2. Composition of Band 1 from Figure 2.2
Results of LC-MS/MS analysis (left) and the identity of the likely CP intermediate and/or CP-subunit-derived species present (right).

α/β-subunits	# Peptides	# PSMs	% Coverage	Other proteins	# Peptides	# PSMs	% Coverage
α1	19	**57**	83	**UMP1**	2	**8**	16
α2	11	**40**	37	**RPN3**	5	**6**	15
α3	18	**43**	77	**RPN8**	4	**7**	17
α4	13	**143**	78	**RPN9**	3	**4**	14
α5	6	**6**	29	**BLM10**	11	**13**	6
β1	6	**8**	36	**SSC1**	6	**8**	13
β2	7	**41**	31	**ERG6**	6	**8**	24
β3	8	**27**	47	**ACS2**	4	**8**	9
β4	7	**15**	46	**ENO**	6	**7**	21
				ALO1	5	**5**	11
				ADH1	4	**5**	16
				PDC1	6	**11**	21
				PFK26	12	**13**	19
				EFT2	4	**5**	8

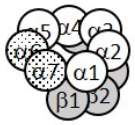

13S-like intermediate

Supplementary Figure 3. Composition of Band 2 from Figure 2.2
Results of LC-MS/MS analysis (left) and the identity of the likely CP intermediate and/or CP-subunit-derived species present (right).

α/β-subunits	# Peptides	# PSMs	% Coverage	Other proteins	# Peptides	# PSMs	% Coverage
α1	22	**75**	90	**PBA1**	11	**19**	57
α2	11	**48**	52	**PBA2**	7	**10**	31
α3	18	**34**	77	**PBA3**	3	**4**	36
α4	16	**448**	68	**PBA4**	3	**5**	36
α5	13	**15**	44	**UMP1**	5	**20**	42
α6	14	**37**	78	**BLM10**	4	**4**	3
α7	9	**27**	52	**HSP60**	6	**6**	15
β1	8	**12**	65	**PFK26**	10	**10**	17
β2	7	**47**	47				
β3	9	**29**	42				
β4	8	**14**	47				
β5	6	**10**	25				
β6	6	**11**	36				

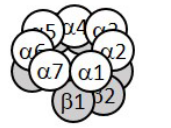

15S intermediate

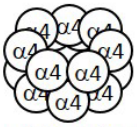

α4 Complex
Double Ring?

Supplementary Figure 4. Composition of Band 3 from Figure 2.2
Results of LC-MS/MS analysis (left) and the identity of the likely CP intermediate and/or CP-subunit-derived species present (right).

α/β-subunits	# Peptides	# PSMs	% Coverage	Other proteins	# Peptides	# PSMs	% Coverage
α1	30	**198**	93	**PBA1**	11	**28**	57
α2	12	**70**	52	**PBA2**	6	**13**	28
α3	22	**84**	91	**PBA4**	5	**10**	37
α4	17	**506**	67	**UMP1**	5	**51**	46
α5	17	**25**	62	**BLM10**	13	**17**	8
α6	17	**57**	83	**RKR1**	6	**8**	5
α7	14	**72**	63	**SSA1**	10	**12**	24
β2	13	**85**	59	**SSA2**	11	**13**	28
β3	8	**49**	43	**GRP78**	4	**4**	8
β4	9	**48**	44	**TDH3**	6	**11**	34
β5	5	**5**	25	**PFK26**	10	**10**	17
β6	2	**6**	18				

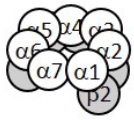

15S-like intermediate

α4 Complex
Single Ring?

Supplementary Figure 5. Composition of Band 4 from Figure 2.2
Results of LC-MS/MS analysis (left) and the identity of the likely CP intermediate and/or CP-subunit-derived species present (right).

α/β-subunits	# Peptides	# PSMs	% Coverage	Other proteins	# Peptides	# PSMs	% Coverage
α1	17	**47**	79	**PBA1**	3	**6**	12
α2	7	**10**	44	**UBI4**	3	**5**	54
α4	19	**957**	70	**SSA1**	14	**24**	31
α5	14	**20**	58	**SSA2**	16	**26**	35
α6	10	**12**	61	**KAR2**	6	**8**	11
α7	6	**10**	31	**THI20**	12	**27**	32
β1	8	**11**	40				
β2	3	**10**	2				
β3	10	**24**	52				
β4	10	**27**	47				
β5	4	**6**	25				
β6	5	**14**	32				

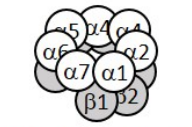

15S intermediate

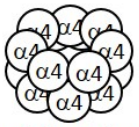

α4 Complex
Double Ring?

Supplementary Figure 6. Composition of Band 5 from Figure 2.2
Results of LC-MS/MS analysis (left) and the identity of the likely CP intermediate and/or CP-subunit-derived species present (right).

α/β-subunits	# Peptides	# PSMs	% Coverage	Other proteins	# Peptides	# PSMs	% Coverage
α1	20	**63**	79	**PBA1**	8	**19**	46
α2	8	**13**	44	**PBA3**	4	**5**	45
α4	21	**1120**	74	**UBI4**	3	**4**	54
α5	14	**26**	57	**SSA1**	34	**61**	59
α6	10	**16**	63	**SSA2**	32	**58**	55
α7	6	**10**	31	**GRP78**	15	**22**	30
β1	8	**10**	59	**THI20**	21	**30**	51
β2	7	**13**	37	**ENO**	5	**6**	16
β3	8	**31**	47	**PDC1**	2	**3**	9
β4	9	**49**	47	**TDH3**	3	**6**	17
β5	5	**6**	25				
β6	6	**18**	40				

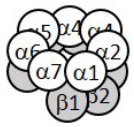

15S intermediate

α4 Complex
Single Ring?

Supplementary Figure 7. Composition of Band 6 from Figure 2.2
Results of LC-MS/MS analysis (left) and the identity of the likely CP intermediate and/or CP-subunit-derived species present (right).

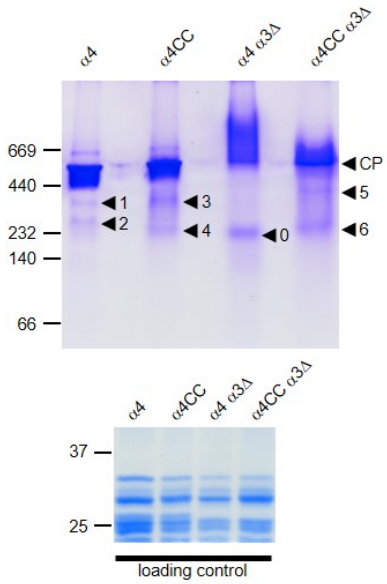

	band1		band 2		band 3		band 4		band 5		band 6		band 0	
	peptides	PSM	peptides	PSM	peptides	PSM	peptides	PSM	peptides	PSM	peptides	PSM	peptides	PSM
α1	23	123	23	134	24	186	12	37	21	76	22	113	12	40
α2	11	46	10	49	11	70	8	13	9	22	14	47	10	20
α3	19	64	17	64	20	83	16	41	3*	4*	-	-	-	-
α4	18	268	19	160	15	760	16	604	15	787	15	867	16	446
α5	17	49	7	9	17	36	9	12	14	26	17	39	14	19
α6	17	55	-	-	16	57	5	6	13	31	10	15	4	15
α7	12	45	3	5	13	89	3	3	8	29	7	13	-	-
β1	10	17	-	-	4	5	-	-	12	22	14	26	8	10
β2	11	67	10	53	12	124	6	13	18	31	10	61	5	13
β3	8	41	9	46	10	50	6	9	9	39	12	71	12	79
β4	8	24	9	30	9	39	7	17	8	24	14	106	11	104
β5	9	23	3	4	7	10	-	-	6	17	9	23	4	4
β6	7	26	3	9	5	17	3	13	10	46	12	54	4	19
β7	7	51	-	-	5	21	4	7	8	67	6	41	3	9

Supplementary Figure 8. Analysis of putative α4-containing HMWCs by native PAGE
This is essentially a repeat of the experiment described in Figure 2.2, except one additional sample (α4 α3Δ) was included. Flag-purified CP from the indicated yeast strains was subjected to native PAGE on 4–15% gels followed by staining with Imperial Stain (top panel). To verify equal loading of proteins, aliquots of the material analyzed by native PAGE were withdrawn and subjected to SDS-PAGE on 12% gels, followed by staining with GelCode blue (middle panel). The position of molecular size standards for each gel is indicated on the left. Arrowheads denote migration of CP and of CP assembly intermediates. Bands 1 to 6 on this gel are equivalent to bands 1 to 6 on the native gel in Figure 2. To demonstrate this equivalence, the contents of the indicated bands was analyzed by LC-MS/MS following their excision from the gel, and the α and β subunit contents of the bands is shown (bottom panel). Red denotes the excess in PSMs for the α4 subunit, as observed in Figure 2. Bands 5, 6, and 0 are derived from α3Δ strains, and while bands 6 and 0 do not exhibit peptides derived from α3 (as expected), there are a few α3 peptides in band 5 (asterisk). However, the low number of PSMs for α3, compared to the other CP subunits in this sample, argues that this is likely an experimental artifact.

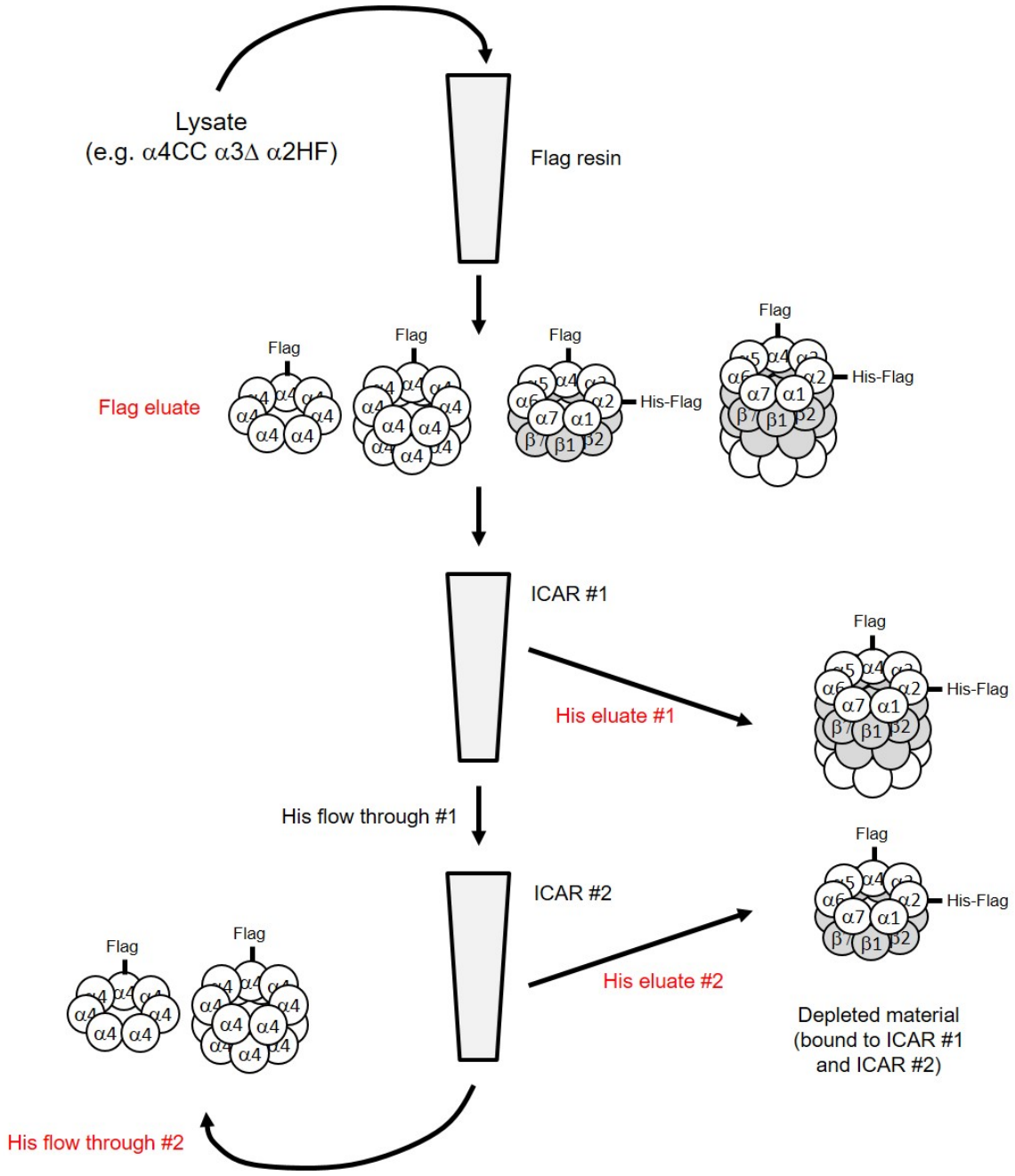

Supplementary Figure 9. Depletion strategy
Flag tag on subunits α4 and α2 enables the isolation of all CP and CP intermediates, as well as α4 HMWCs. Subjecting the Flag eluates to two rounds of ICAR binding depletes α2-containing species (CP and CP intermediates) because α2 also contains a His tag. For simplicity, the tags are shown on only one subunit at a time. Red denotes samples loaded on various gels in this study.

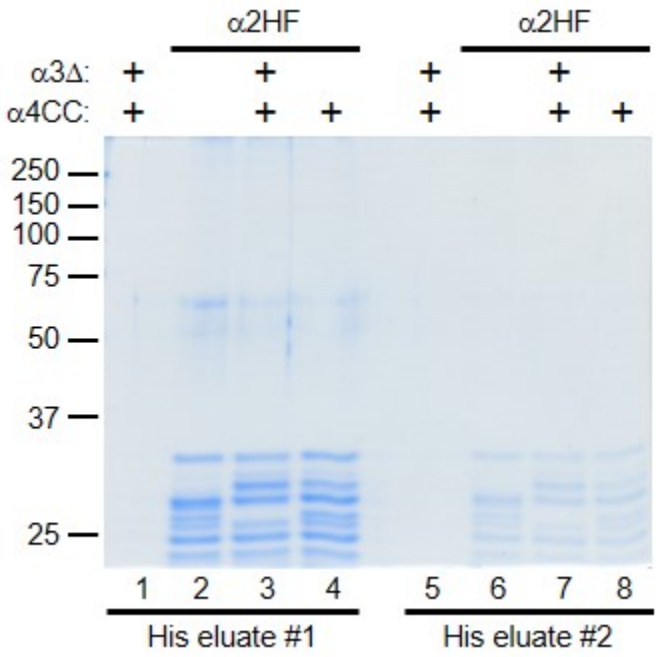

Supplementary Figure 10. Depletion requires more than one round of ICAR binding
The Flag eluates from Figure 2.3C were subjected to depletion of his-tagged proteins by binding to ICAR. The bound material was eluted and subjected to SDS-PAGE (lanes 1-4). The unbound material (i.e. flow-through #1) was bound a second time to ICAR using fresh resin. This twice-depleted material was eluted and subjected to SDS-PAGE (lanes 5-8). The gel was stained with Gelcode blue and the migration of molecular size standards is indicated at left.

APPENDIX B. SUPPLEMENTARY FOR CHAPTER 3

Supplementary Notes

On the recovery of Hsp70 proteins in previous high-throughput approaches versus this study.

As stated in the main text, previous high-throughput studies demonstrating physical association between Hsp70 proteins and the proteasome did not attempt to distinguish binding between fully assembled proteasomes and proteasome assembly intermediates (Gong et al., 2009; Guerrero et al., 2008; Guerrero, Tagwerker, Kaiser, & Huang, 2006; Verma et al., 2000). Here, we clearly demonstrate the association of Ssa1/2 with CP assembly intermediates but not with fully assembled CP. However, not finding Ssa1/2 associated with fully assembled CP in this study does not imply that additional interactions between Ssa1/2 and the CP do not occur. Such interactions could simply be weak/transient enough to not survive our purification scheme (especially the rigorous depletion protocol) and/or electrophoresis on native PAGE. Also, in order to focus on the CP, our purifications omitted ATP which means that our biochemical analysis would not detect Hsp70 interactions with RP components. Hsp70 proteins like Ssa1/2 likely play several roles in UPS function, including: enhancing ubiquitination; temporary triage of ubiquitinated substrates into soluble inclusions; substrate delivery to the proteasome; and this newly discovered role in CP assembly (Lee do, Sherman, & Goldberg, 2016; Luders, Demand, & Hohfeld, 2000; Shiber, Breuer, Brandeis, & Ravid, 2013).

On suppression of CP mutants by high-copy Hsp70.

We observed suppression of CP assembly defects by overexpression of both *SSA1* and *SSB1* (Figure 3). Suppression of CP mutants by *SSB1* had been observed previously, but the author failed to detect suppression by *SSA1* (Ohba, 1994, 1997). We believe the discrepancy between our studies with regards to observing suppression with *SSA1* might be attributed to protein levels. The earlier work relied on expression of *SSA1* and *SSB1* from their endogenous promoters (Ohba, 1997). Here, we express *SSA1* and *SSB1* from a strong heterologous promoter (*TEF*) that drives expression to higher levels (Mumberg, Muller, & Funk, 1995).

On the recovery of CP-bound Ssa3/4 in *ssa1*Δ*ssa2*Δ strains.

In the main text, Flag-purified CP from a wild type strain (α4-Flag) clearly shows a band corresponding to Ssa1/2 on SDS-PAGE (Figure 3.4A). By contrast, when CP is purified from an

*ssa1*Δ*ssa2*Δ strain, the Ssa1/2 band is replaced by a doublet from which we recovered peptides corresponding to Kar2 and Ssa3/4. Kar2 is an ER-resident Hsp70; its recovery is likely an artifact of the lysis scheme (bead beating) which disrupts cellular membranes. By contrast, the cytoplasmic Ssa3 and Ssa4 proteins are normally repressed but become induced under stress conditions, or when both Ssa1 and Ssa2 are absent (Nelson, Heschl, & Craig, 1992). The recovery of Ssa3/4 in Flag-purified CP material in the absence of Ssa1/2 suggests that Ssa3/4 may provide some redundancy in CP function/assembly. However, with respect to assembly, any redundancy provided by Ssa3/4 must be partial (at best). This is because levels of CP assembly intermediates are dramatically decreased in the *ssa1*Δ*ssa2*Δ mutant, despite the induction of Ssa3/4. Clearly, Ssa3/4 cannot fully replace Ssa1/2 in CP assembly.

Supplementary Table 2: Yeast Strains used in Chapter 3

Name	Alias	Genotype	Source
AKY600	MHY500	*MAT***a** *his3-Δ200 leu2-3,112 ura3-52 lys2-801 trp1-1 gal2*	(Chen & Hochstrasser, 1995)
AKY601	MHY501	*MATα his3-Δ200 leu2-3,112 ura3-52 lys2-801 trp1-1 gal2*	(Chen & Hochstrasser, 1995)
AKY783		*MAT***a** *his3-Δ200 leu2-3,112 ura3-52 lys2-801 trp1-1 gal2*	(Firestone et al., 2016)
AKY784		*MATα his3-Δ200 leu2-3,112 ura3-52 lys2-801 trp1-1 gal2*	(Firestone et al., 2016)
AKY207	MHY4299	*MATα pba4Δ::hphMX*	(Kusmierczyk et al., 2008)
AKY408		*MATα pre9Δ::hphMX*	(Firestone et al., 2016)
AKY417		*MAT***a** *rpn4Δ::hphMX*	
AKY604	MHY1069	*MATα pre9Δ::HIS3*	(Fu, Doelling, Arendt, Hochstrasser, & Vierstra, 1998)
AKY678	MHY4786	*MATα sem1Δ::HIS3*	(Tomko & Hochstrasser, 2011)
AKY698	MHY5279	*MAT***a** *nas2Δ::kanMX nas6Δ::HIS3 rpn14Δ::HIS3*	(Funakoshi et al., 2009)
AKY699	MHY5749	*MATα rpn12-234Δ::hphMX*	(Tomko & Hochstrasser, 2011)
AKY709	MHY6952	*MAT***a** *PRE1-6xgly-3xFlag:kanMX4*	(Sa-Moura, Simoes, et al., 2013)
AKY789		*MATα pre9Δ::HIS3*	
AKY808		*MAT***a** *pre3Δ::HIS3 pup1Δ::leu2::HIS3 doa3Δ::HIS3 PRE1-6xgly-3xFlag:kanMX4* [Ycplac22 *pre3*(T1A), pRS317 *pup1*(T1A), pRS315 *DOA3-6xhis*]	
AKY889		*MAT***a** *pre6Δ::HIS3* [pRS315 *PRE6-Flag*]	(Hammack & Kusmierczyk, 2017)
AKY924		*MATα ssa1Δ::hphMX4*	
AKY925		*MAT***a** *ssa1Δ::hphMX4*	
AKY926		*MATα ssb1Δ::hphMX4*	
AKY927		*MAT***a** *ssb1Δ::hphMX4*	
AKY942		*MAT***a** *pre3Δ::HIS3 pup1Δ::leu2::HIS3 doa3Δ::HIS3 PRE1-6xgly-3xFlag:kanMX4* [Ycplac22 *PRE3*, pRS317 *PUP1*, pRS315 *DOA3-6xhis*]	
AKY985		*MAT***a** *pre9Δ::HIS3 PRE1-6xgly-3xFlag:kanMX4*	
AKY1011		*MATα pre9Δ::HIS3 ssa1Δ::hphMX4*	
AKY1013		*MATα sem1Δ::HIS3 ssa1Δ::hphMX4*	
AKY1015		*MATα nas2Δ::kanMX nas6Δ::HIS3 rpn14Δ::HIS3 ssa1Δ::hphMX4*	
AKY1017		*MATα pre9Δ::HIS3 ssb1Δ::hphMX4*	
AKY1019		*MATα sem1Δ::HIS3 ssb1Δ::hphMX4*	
AKY1021		*MATα nas2Δ::kanMX nas6Δ::HIS3 rpn14Δ::HIS3 ssb1Δ::hphMX4*	
AKY1068		*MAT***a** *ssa2Δ::hphMX*	
AKY1109		*MAT***a** *pre9Δ::HIS3 ssa2Δ::hphMX*	
AKY1113		*MAT***a** *pre9Δ::HIS3 ssa2Δ::hphMX PRE1-6xgly-3xFlag:kanMX4*	
AKY1116		*MAT***a** *rpn12-234Δ::hphMX ssa2Δ::hphMX*	
AKY1129		*MAT***a** *rpn4Δ::hphMX ssa2Δ::hphMX*	
AKY1132		*MAT***a** *rpn4Δ::hphMX ssa1Δ::hphMX*	
AKY1143		*MAT***a** *pre3Δ::HIS3 pup1Δ::leu2::HIS3 doa3Δ::HIS3 PRE1-6xgly-3xFlag:kanMX4* [Ycplac22 *PRE3*, pRS317 *PUP1*, pRS315 *doa3*(T1A) *DOA3-6xhis*]	
AKY1293		*MAT***a** *pre6Δ::HIS3 ssa1Δ::natMX4 ssa2Δ::kanMX4* [pRS315 *PRE6-Flag*]	

AKY600, AKY601, AKY783 and AKY784 are wild type strains and remaining strains are congenic with these four. All strains are from this study, except as noted in the table.

Supplementary Table 3: Plasmids used in Chapter 3

Name	Genotype/Alias	Description	Source
AKB323	p416TEF	Empty vector	(Mumberg et al., 1995; Pfund, Huang, Lopez-Hoyo, & Craig, 2001)
AKB324	p416TEF His-*SSA1*	Construct for overexpression of *SSA1* from TEF promoter	(Pfund et al., 2001)
AKB325	p416TEF His-*SSB1*	Construct for overexpression of *SSB1* from TEF promoter	(Pfund et al., 2001)

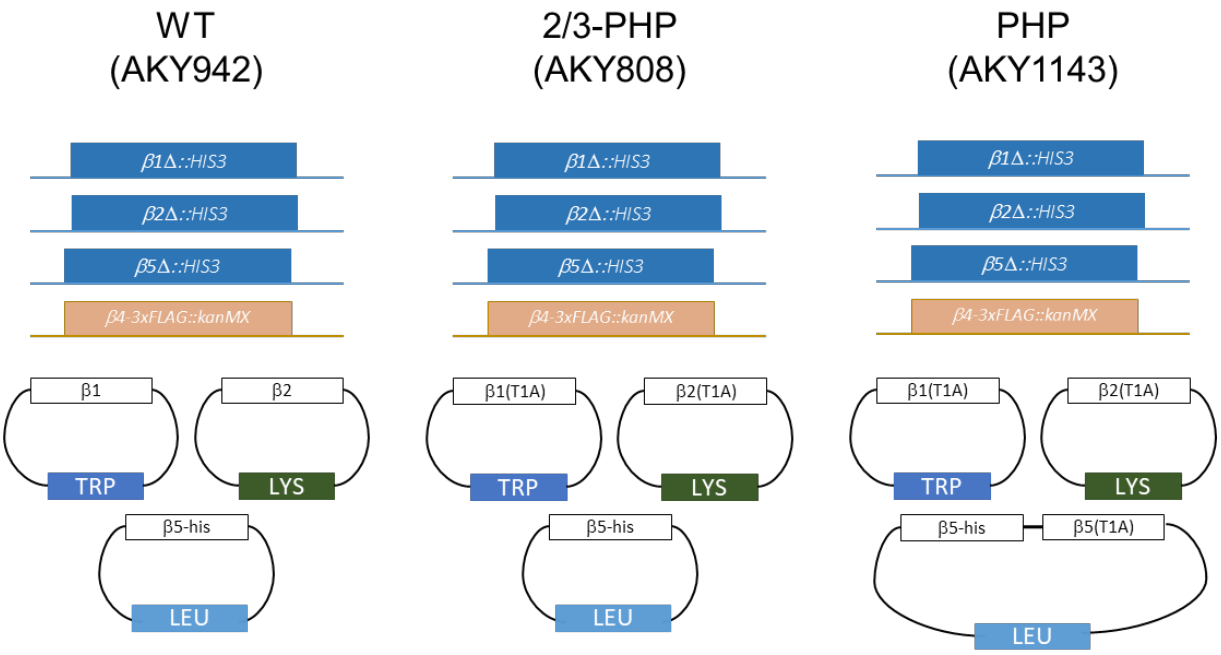

Supplementary Figure 11. The genotypes of all three depleted strains are shown
The PHP is normally a short-lived species. To enrich its formation, we employed β subunit mutants that were incapable of maturation due to substitution of their active site threonines with alanine (T1A mutants). Yeast tolerate β1 (T1A) and β2 (T1A) mutations well (Arendt & Hochstrasser, 1997) and the PHP strain contained both of these mutations as the only copies of b1 and b2 in the cell. However, since β5 activity is essential (Chen & Hochstrasser, 1996), we had to engineer the PHP strain to retain functional β5 while also allowing expression of a β5 (T1A) variant. To this end we generated a centromeric plasmid containing both wild type β5 and β5 (T1A) mutant, each expressed from its endogenous promoter and containing its endogenous terminator regions. This should help ensure more equitable expression of these two variants. The 2/3-PHP was similar to the PHP strain except only a wild type copy of β5 was present. We refer to it as the “two-thirds preholoproteasome” because it looks like a PHP in which two out of three active sites are incapable of full maturation. The wild type strain only contains wild type versions of all β subunits. In all cases, the wild type β5 allele encodes a C-terminal hexahistidine tag (his-tag) to enable depletion analysis.

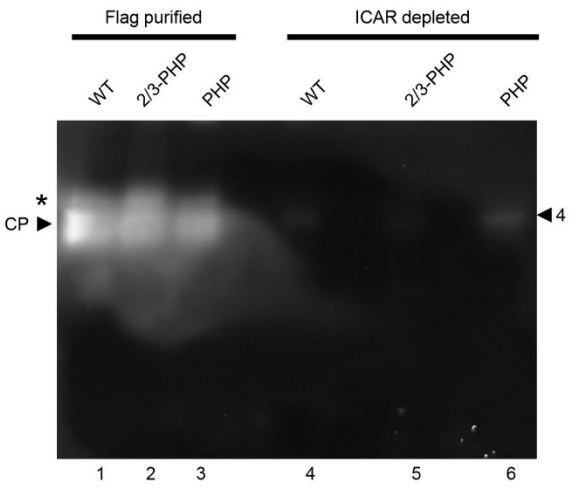

Supplementary Figure 12. Depletion analysis activity assay
The native gel in Figure 1A of the main text was subjected to a substrate overlay assay using the fluorogenic peptide substrate Suc-LLVY-AMC prior to staining with Imperial stain. CP denotes migration of the core particle. Asterisk denotes migration of CP-Blm10 complexes. Migration of band 4 in the PHP sample (see main text) is indicated.

α/β-subunits	# Peptides	# PSMs	% Coverage	Other proteins	# Peptides	# PSMs	% Coverage
α1	24	**109**	86	**Pba1**	5	**7**	25
α2	11	**36**	41	**Ump1**	7	**30**	59
α3	17	**59**	74	**Ssa1/2**	16	**29**	36
α4	16	**98**	76	**Ssc1**	3	**4**	7
α5	8	**8**	33	**Eno**	5	**7**	17
α6	6	**6**	32				
α7	5	**7**	22				
β2	9	**58**	51				
β3	8	**37**	48				
β4	8	**26**	36				

sub-13S intermediate

Supplementary Figure 13. Composition of PHP band 1 from Figure 3.1
Results of LC-MS/MS analysis (left) and the identity of the likely CP intermediate (right).

α/β-subunits	# Peptides	# PSMs	% Coverage	Other proteins	# Peptides	# PSMs	% Coverage
α1	21	**95**	86	**Pba1**	13	**25**	70
α2	10	**39**	37	**Pba2**	4	**11**	20
α3	17	**57**	85	**Ump1**	4	**7**	49
α4	14	**72**	69	**Ssa1/2**	25	**63**	46
α5	15	**26**	60				
α6	13	**54**	78				
α7	10	**37**	50				
β1	3	**4**	17				
β2	7	**49**	43				
β3	8	**31**	47				
β4	9	**20**	40				
β5	4	**6**	22				
β7	2	**10**	15				

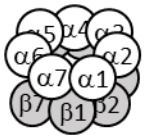

13S/15S intermediate

Supplementary Figure 14. Composition of PHP band 2 from Figure 3.1
Results of LC-MS/MS analysis (left) and the identity of the likely CP intermediate (right).

α/β-subunits	# Peptides	# PSMs	% Coverage	Other proteins	# Peptides	# PSMs	% Coverage
α1	16	**66**	79	**Pba1**	10	**19**	58
α2	11	**28**	37	**Pba2**	3	**4**	17
α3	17	**42**	74	**Ump1**	2	**5**	20
α4	16	**35**	76	**Rpn3**	2	**7**	6
α5	12	**20**	40	**Ssa1**	4	**6**	9
α6	13	**40**	79	**Hsp60**	6	**9**	16
α7	8	**21**	43				
β1	9	**13**	54				
β2	5	**42**	31				
β3	9	**24**	52				
β4	7	**17**	39				
β5	11	**47**	46				
β6	5	**28**	37				
β7	7	**74**	50				

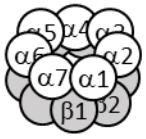

½ proteasome intermediate

Supplementary Figure 15. Composition of PHP band 3 from Figure 3.1
Results of LC-MS/MS analysis (left) and the identity of the likely CP intermediate (right).

α/β-subunits	# Peptides	# PSMs	% Coverage	Other proteins	# Peptides	# PSMs	% Coverage
α1	28	**328**	86	**Pba1**	16	**78**	75
α2	16	**124**	68	**Pba2**	8	**38**	38
α3	23	**170**	86	**Ump1**	9	**80**	71
α4	17	**507**	75	**Hsp60**	3	**4**	6
α5	20	**124**	87				
α6	22	**222**	88				
α7	14	**85**	64				
β1	25	**109**	97				
β2	11	**157**	60				
β3	12	**62**	65				
β4	11	**53**	58				
β5	18	**253**	81				
β6	13	**222**	86				
β7	13	**277**	61				

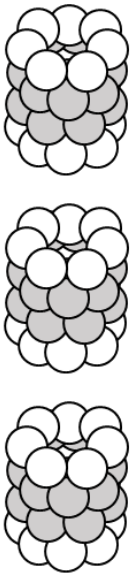

2/3 PHP (all β5-his)

Mixed Species β5-his β5T1A

PHP (all β5T1A)

Supplementary Figure 16. Composition of PHP band 4 from Figure 3.1
Results of LC-MS/MS analysis (left) and the identity of the likely CP intermediates (right).

α/β-subunits	# Peptides	# PSMs	% Coverage	Other proteins	# Peptides	# PSMs	% Coverage
α1	25	**134**	81	**Pba1**	8	**9**	47
α2	12	**60**	56	**Ump1**	8	**31**	71
α3	19	**74**	85	**Rpn2**	3	**3**	11
α4	16	**131**	76	**Blm10**	3	**5**	3
α5	11	**13**	47	**Rkr1**	3	**4**	8
α6	9	**12**	64	**Ssa1**	11	**16**	28
α7	7	**19**	38	**Ssc1**	5	**5**	12
β2	11	**94**	62	**Eno2**	4	**5**	17
β3	9	**54**	47	**Thi20**	4	**5**	11
β4	8	**35**	36	**Adh1**	7	**10**	32
				Eft1	5	**5**	9

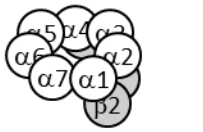

sub-13S intermediate

Supplementary Figure 17. Composition of 2/3-PHP band 1 from Figure 3.1
Results of LC-MS/MS analysis (left) and the identity of the likely CP intermediate (right).

α/β-subunits	# Peptides	# PSMs	% Coverage	Other proteins	# Peptides	# PSMs	% Coverage
α1	22	**112**	81	**Pba1**	13	**34**	66
α2	10	**58**	37	**Pba2**	8	**17**	41
α3	20	**85**	85	**Ump1**	8	**36**	67
α4	19	**118**	81	**Ssa1/2**	24	**56**	49
α5	15	**34**	60	**Eft1**	7	**8**	12
α6	16	**56**	87				
α7	10	**50**	50				
β2	9	**75**	51				
β3	9	**44**	52				
β4	9	**33**	40				
β5	4	**5**	21				

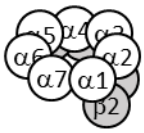

13S intermediate

Supplementary Figure 18. Composition of 2/3-PHP band 2 from Figure 3.1
Results of LC-MS/MS analysis (left) and the identity of the likely CP intermediate (right).

α/β-subunits	# Peptides	# PSMs	% Coverage	Other proteins	# Peptides	# PSMs	% Coverage
α1	27	**195**	86	**Pba1**	6	**9**	36
α2	12	**78**	56	**Ump1**	9	**54**	74
α3	23	**104**	80	**Rkr1**	7	**9**	7
α4	19	**194**	81	**Ssa1**	8	**11**	18
α5	11	**15**	52	**Eno2**	4	**4**	17
α6	4	**5**	33	**Pfk26**	5	**6**	9
α7	7	**11**	31	**Thi20**	3	**3**	9
β1	4	**5**	29				
β2	13	**125**	65				
β3	10	**51**	52				
β4	8	**39**	36				
β5	3	**6**	17				

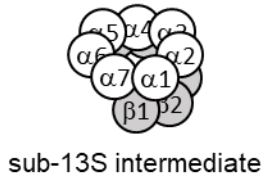

sub-13S intermediate

Supplementary Figure 19. Composition of WT band 1 from Figure 3.1.
Results of LC-MS/MS analysis (left) and the identity of the likely CP intermediate (right).

α/β-subunits	# Peptides	# PSMs	% Coverage	Other proteins	# Peptides	# PSMs	% Coverage
α1	26	**201**	86	**Pba1**	17	**114**	79
α2	13	**72**	63	**Pba2**	8	**44**	38
α3	22	**110**	86	**Ump1**	7	**34**	61
α4	20	**558**	81	**Ssa1/2**	19	**40**	43
α5	18	**64**	73	**Eft1**	8	**9**	15
α6	22	**132**	88				
α7	12	**74**	59				
β2	12	**99**	58				
β3	11	**57**	62				
β4	10	**35**	40				
β5	5	**7**	27				

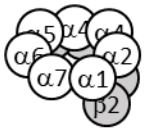

13S intermediate

Supplementary Figure 20. Composition of WT band 2 from Figure 3.1
Results of LC-MS/MS analysis (left) and the identity of the likely CP intermediate (right).

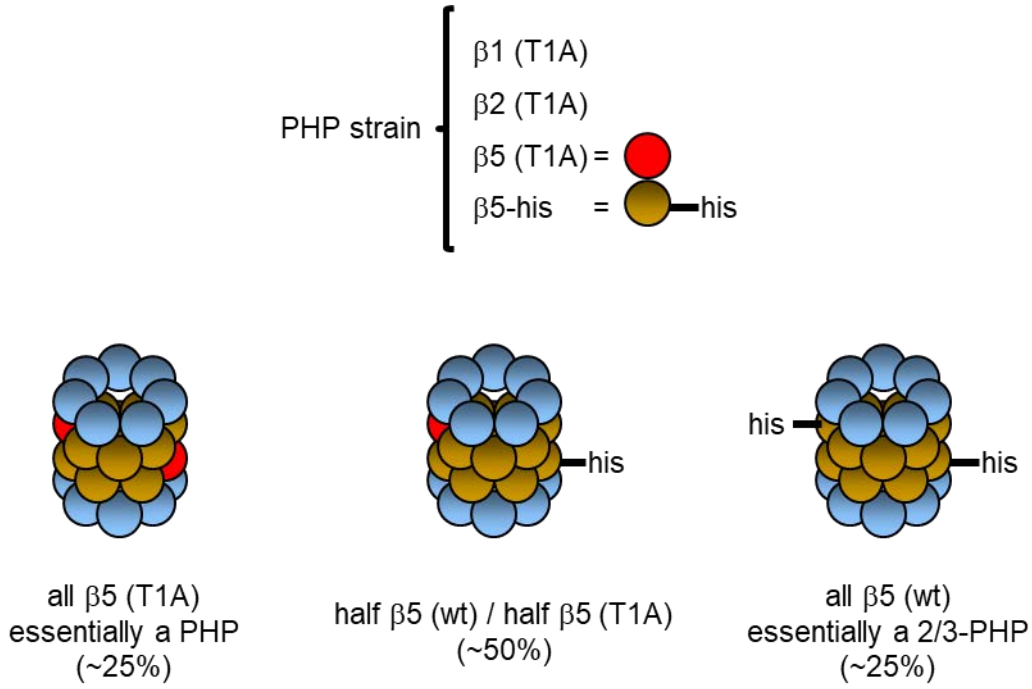

Supplementary Figure 21. Likely composition of PHP band 4
The PHP strain contains mutant (T1A) versions of all three catalytic b subunits, plus a wild type copy of the β5 subunit that is also his-tagged. Assuming β5 (T1A) and β5-his incorporate with equal efficiency during assembly, equal amounts of two types of half-proteasome will be produced, one containing β5 (T1A) and one containing β5-his. Assuming also that there is no difference in how these two half-proteasomes dimerize, three possible CP species will be produced in the idealized ratios shown above. Of course, the two species containing β5-his should be depleted during ICAR, but we have observed that the depletion is not complete (see main text Figure). So it is likely that some of each of the two β5-his containing species will persist in the second ICAR flow-through. This is confirmed by the residual activity of the PHP band 4 (Supplementary Figure 12). This could help account for the presence of three bands in observed in band 4.

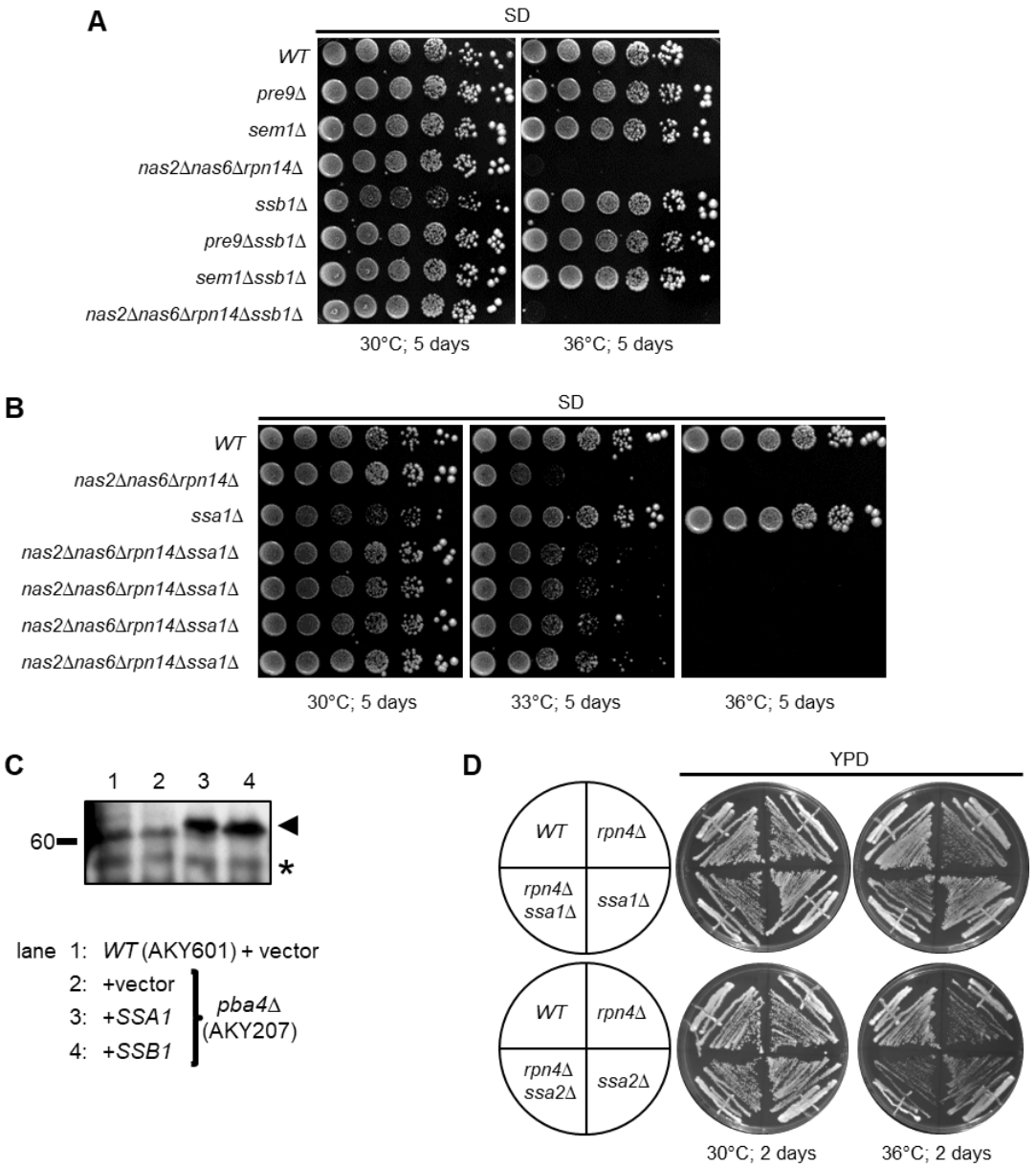

Supplementary Figure 22. Genetic analysis of Hsp70 mutants
(A) Dilution series showing no genetic interactions between mutations that affect proteasome assembly and deletion of the Hsp70 gene, *SSB1*. (B) Dilution series showing a genetic interaction between an assembly mutant of the RP base and deletion of *SSA1*. Four separate quadruple mutants, each from a different spore following tetrad dissection, are shown. (C) Representative Western blot with anti-Express antibody for the suppression experiments in main text Figure 3 to verify expression of plasmid-encoded Hsp70 proteins (arrowhead). A non-specific band serves as an internal loading control (asterisk). (D) Indicated yeast strains were struck out onto YPD plates and incubated as shown. No obvious genetic interaction is observed between deletion of *SSA1* alone, or *SSA2* alone, and deletion of *RPN4*.

α/β-subunits	# Peptides	# PSMs	% Coverage	Other proteins	# Peptides	# PSMs	% Coverage
α1	26	**332**	90	**Pba1**	9	**12**	48
α2	21	**202**	73	**Pba2**	4	**6**	21
α3	23	**313**	91	**Pba3**	4	**6**	36
α4	22	**294**	84	**Pba4**	4	**6**	35
α5	14	**82**	61	**Ump1**	11	**54**	74
α6	17	**54**	79	**Blm10**	64	**115**	34
α7	13	**47**	52	**Rpn3**	6	**6**	12
β1	11	**51**	72	**Rpn5**	6	**8**	16
β2	14	**97**	64	**Rpn6**	4	**5**	11
β3	10	**153**	58	**Rpn7**	6	**9**	12
β4	14	**107**	66	**Rpn8**	7	**12**	37
β5	11	**54**	51	**Rpn9**	9	**12**	24
β6	9	**111**	43	**Rpn11**	3	**3**	11
β7	8	**40**	62	**Ecm29**	42	**65**	27
				Ssa1/2	52	**138**	73
				Ssc1	15	**35**	42
				Sse1	4	**6**	8
				Kar2	30	**48**	41

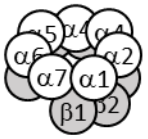

13S/15S intermediate

Supplementary Figure 23. Composition of WT band 5 from Figure 3.4
Results of LC-MS/MS analysis (left) and the identity of the species (right). For simplicity, only proteasome-related proteins and Hsp70 family members are shown. Ssa1/2 are highlighted.

α/β-subunits	# Peptides	# PSMs	% Coverage	Other proteins	# Peptides	# PSMs	% Coverage
α1	23	**481**	87	**Pba1**	12	**39**	69
α2	20	**211**	87	**Pba2**	8	**32**	35
α3	20	**530**	87	**Pba3**	5	**6**	53
α4	16	**258**	75	**Pba4**	6	**10**	42
α5	16	**244**	77	**Ump1**	9	**28**	74
α6	17	**278**	75	**Blm10**	47	**82**	25
α7	14	**110**	58	**Ecm29**	32	**46**	22
β1	11	**164**	67	**Rpn5**	11	**18**	24
β2	12	**250**	64	**Rpn6**	8	**8**	24
β3	9	**219**	58	**Rpn7**	3	**5**	8
β4	11	**112**	73	**Rpn8**	10	**15**	47
β5	14	**199**	69	**Rpn9**	11	**14**	31
β6	10	**287**	53	**Rpn11**	8	**11**	32
β7	7	**121**	58	**Ssa1/2**	37	**63**	62
				Ssc1	3	**5**	7.
				Kar2	10	**15**	19

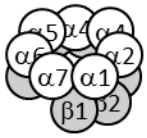

15S intermediate

Supplementary Figure 24. Composition of WT band 6 from Figure 3.4
Results of LC-MS/MS analysis (left) and the identity of the species (right). For simplicity, only proteasome-related proteins and Hsp70 family members are shown. Ssa1/2 are highlighted.

α/β-subunits	# Peptides	# PSMs	% Coverage	Other proteins	# Peptides	# PSMs	% Coverage
α1	26	**929**	91	**Blm10**	11	**19**	8
α2	21	**312**	85	**Fub1**	2	**7**	12
α3	22	**704**	90				
α4	16	**512**	75				
α5	17	**516**	80				
α6	18	**667**	82				
α7	19	**231**	69				
β1	15	**558**	78				
β2	9	**414**	53				
β3	9	**419**	58				
β4	12	**191**	74				
β5	14	**804**	66				
β6	16	**355**	60				
β7	11	**450**	65				

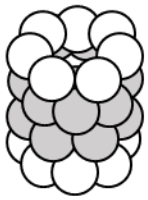
20S CP

Supplementary Figure 25. Composition of WT band 7 from Figure 3.4
Results of LC-MS/MS analysis (left) and the identity of the likely species (right).

α/β-subunits	# Peptides	# PSMs	% Coverage	Other proteins	# Peptides	# PSMs	% Coverage
α1	24	**981**	88	**Blm10**	4	**5**	2
α2	22	**336**	88	**Fub1**	5	**26**	30
α3	20	**759**	87	**Hsp60**	3	**4**	7
α4	18	**485**	80				
α5	17	**565**	82				
α6	18	**681**	79				
α7	15	**228**	60				
β1	15	**620**	78				
β2	11	**481**	59				
β3	10	**420**	58				
β4	11	**218**	71				
β5	17	**855**	68				
β6	17	**371**	65				
β7	12	**460**	67				

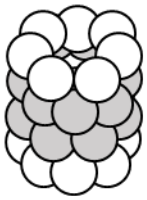

20S CP

Supplementary Figure 26. Composition of *ssa1*Δ*ssa2*Δ band 8 from Figure 3.4
Results of LC-MS/MS analysis (left) and the identity of the likely species (right).

Band 5 (Assembly intermediate(s), from WT)

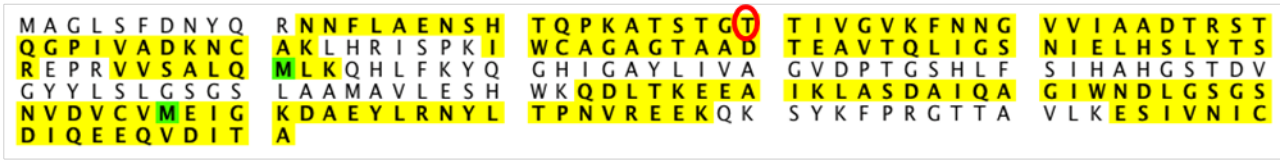

Band 6 (Assembly intermediate(s), from WT)

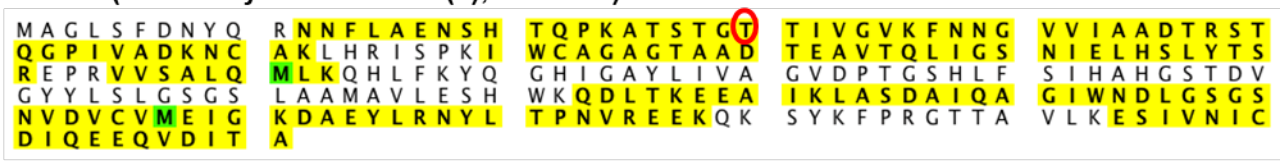

Band 7 (CP from WT)

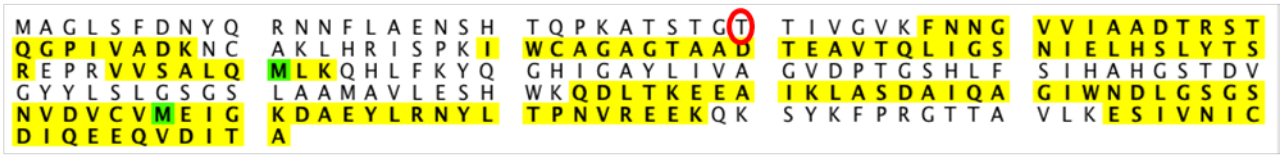

Band 8 (CP from *ssa1Δssa2Δ*)

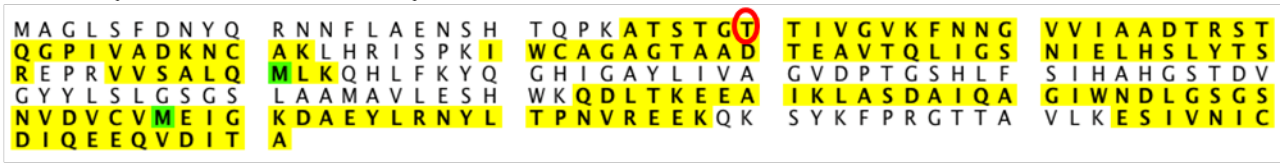

β2 propeptide-derived peptide	Band 5	Band 6	Band 7	Band 8
(R)NNFLAENSHTQPK(A)	12	9	0	0
(K)ATSTGTTIVGVK(F)	9	5	0	2
(K)ATSTGTTIVGVKFNNGVVIAADTR(S)	2	0	0	0

Supplementary Figure 27. Likely β2 propeptide processing defect in *ssa1Δssa2Δ* cells
(Top) Peptide coverage maps for the β2 subunits in each of the 4 bands from Figure 3.4 analyzed by LC-MS/MS. Maps were prepared with the program Scaffold. Red ovals denote the N-terminal threonine nucleophile (Thr1) which becomes exposed following removal of the propeptide. Propeptide sequences recovered in the LC-MS/MS analysis are those highlighted in yellow and to the left of Thr1. Green denotes oxidized methionines identified by LC-MS/MS..
(Bottom) Number of peptide spectral matches (PSMs) for the various β2 propeptide-derived peptides recovered from each of the 4 bands referenced above. Thr1 is shown in red.

APPENDIX C. SUPPLEMENTARY FOR CHAPTER 4

Supplementary Table 4: Yeast Strains used in Chapter 4

Name	Genotype	Source
AKY709	MATa *his3-Δ200 leu2-3,112 ura3-52 lys2-801 trp1-1 PRE1*-6XGLY-3XFlag::kanMX6	(Sa-Moura, Funakoshi, et al., 2013)
AKY889	MATa *his3-Δ200 leu2-3,112 ura3-52 lys2-801 trp1-1 pre6Δ*::HIS3 [pRS315 pre6-Flag]	(Hammack & Kusmierczyk, 2017)
AKY1066	MATa *his3-Δ200 leu2-3,112 ura3-52 lys2-801 trp1-1 pre8*-HF(URA)	(Hammack & Kusmierczyk, 2017)
AKY1368	MATa *his3-Δ200 leu2-3,112 ura3-52 lys2-801 trp1- pre6Δ*::HIS3 *rpn4Δ::hphMX6* [pRS315 pre6-Flag]	
AKY1346	MATa *his3-Δ200 leu2-3,112 ura3-52 lys2-801 trp1-1 pre6Δ*::HIS3 *DOA5*-HF::hphMX6 [pRS315 pre6-Flag]	
AKY1347	MATa *his3-Δ200 leu2-3,112 ura3-52 lys2-801 trp1-1 pre6Δ*::HIS3 *doa5Δ*::HIS3 [pRS315 pre6-Flag] [Ycplac22 doa5-1]	
AKY1375	MATa *his3-Δ200 leu2-3,112 ura3-52 lys2-801 trp1-1 pre8*-HF(URA) *rpn4Δ::hphMX6*	
AKY1377	MATa *his3-Δ200 leu2-3,112 ura3-52 lys2-801 trp1-1 DOA5*-HF::hphMX6 *rpn4Δ::hphMX6 pre6Δ*::HIS3	
AKY1379	MATa *his3-Δ200 leu2-3,112 ura3-52 lys2-801 trp1-1 DOA5*-HF::hphMX6 *PRE1*-6XGLY-3XFlag::kanMX6	
AKY1402	MATa *his3-Δ200 leu2-3,112 ura3-52 lys2-801 trp1-1 pre8*-HF(URA) *doa5Δ*::HIS3 [Ycplac22 doa5-1]	

Unless otherwise indicated strains were generated in this study.

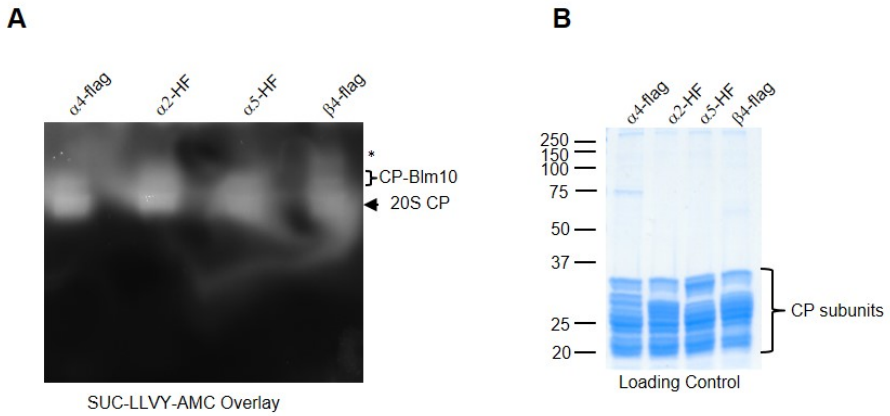

Supplementary Figure 28. Substrate overlay and loading control for Figure 4.1
(A) SUC-LLVY-AMC substrate overlay of native gel (20 μg load) prior to staining.
(B) 12% SDS-PAGE loading control for native PAGE.

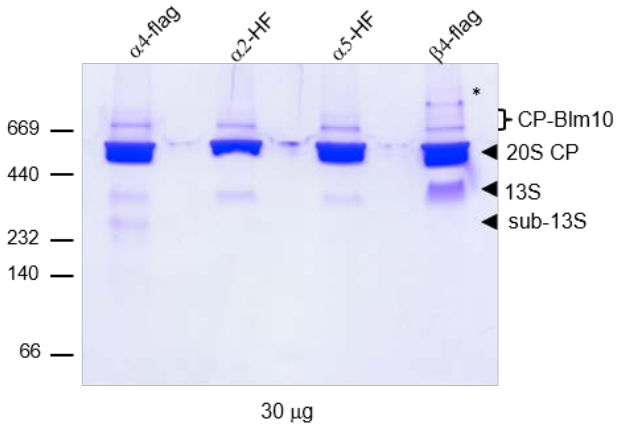

Supplementary Figure 29. Native PAGE heavy load of Figure 4.1
To better visualize intermediates and high molecular weight species in β4-Flag lane (*) 30 µg of purified protein was analyzed via native PAGE.

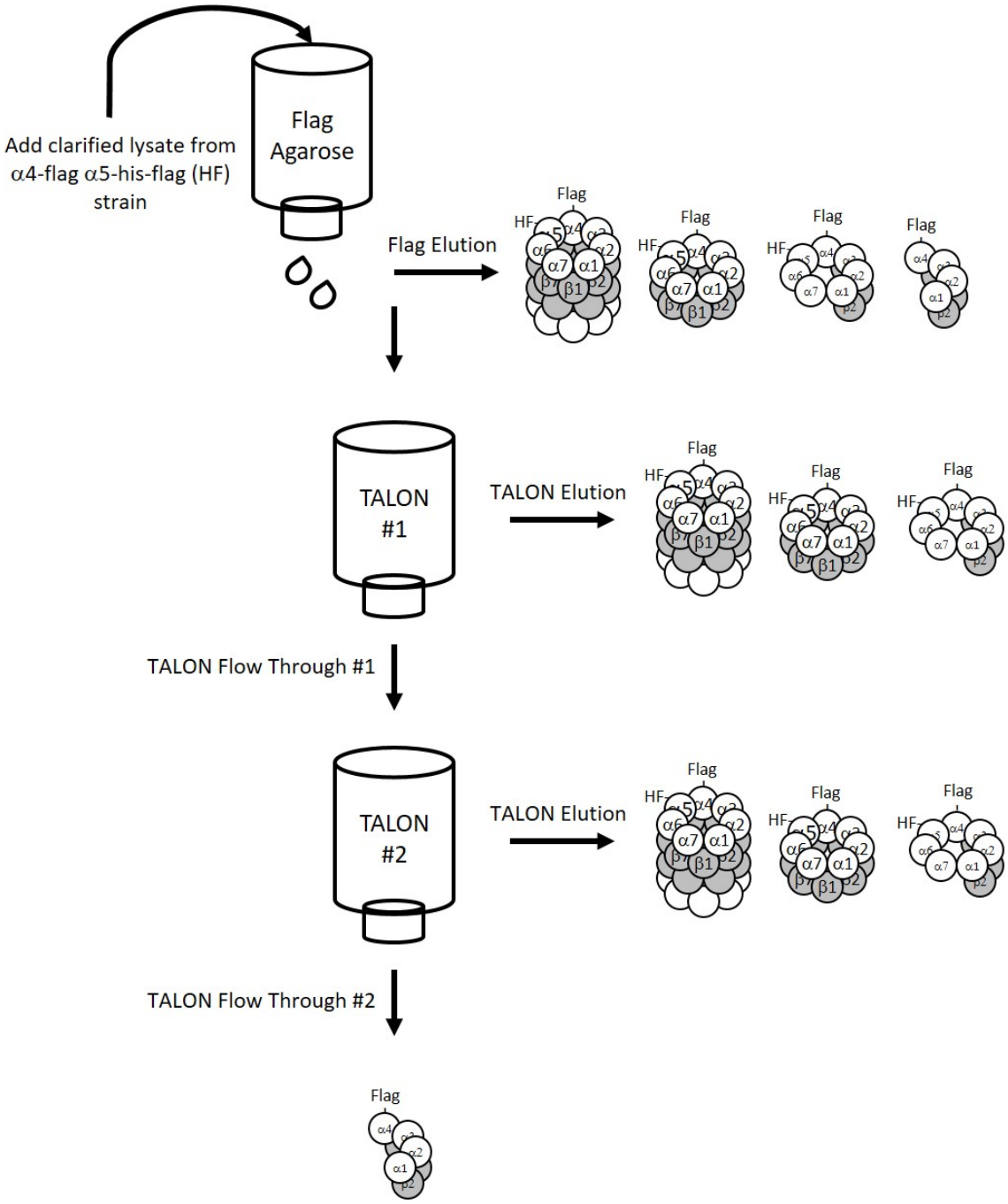

Supplementary Figure 30. Depletion strategy for isolating sub-13S
First yeast lysate is Flag-purified. The Flag purification is followed by two rounds of ICAR. If sub-13S is a gel artifact, the sub-13S species will be absent from the depletion strain. Results for this strategy are depicted in Figure 4.2.